The mathematical formulation of QDAS, Q-par Dichroic Array Software

Q-par/FSS/TRFSS2/1.1

Q-par Angus Ltd

IDEAS ENGINEERED

Cover + viii + 76 pages

April 2003

Technical Report

Barons Cross Laboratories,
Leominster, Herefordshire, HR6 8RS, UK.
Tel: +44 (0) 1568 612138 Fax: +44 (0) 1568 616373
Web: www.q-par.com E-mail: sales@q-par.com

ADS
Advancing UK Aerospace Defence and Security Industries

Q-par Angus Ltd.
Barons Cross Lodge, Leominster,
Herefordshire, HR6 8RS, UK.

Author Dr Andrew J. Mackay

Date April 2003

Issued by Q-par Angus Ltd.
Barons Cross Lodge
Leominster
Herefordshire HR6 HRS
UK.

Document changes record

Issue	Date	Change summary
Issue 1.0	August 2002	New document
Issue 1.1	April 2003	Added formulation for equivalent impedances
Issue 1.2	March 2005	Note added on scattering matrix issues

Abstract

This report provides a detailed mathematical formulation of the important elements of the Frequency Selective Surface analysis used in QDAS (Q-par Dichroic Array Software). The QDAS software is a general purpose Floquet modal boundary element method featuring triangular Wilton-Glisson-Rao style basis functions and an efficient coupling scheme for multiple FSS composites.

List of contents

List of figures

1 Introduction and fundamentals

1.1 Version and formulation

The description of the formulation is appropriate to QDAS Version 01.00.012 August 2002. It is expected that future modification to the software may require minor changes and/or additions to the formulation.

The document provides a detailed description of the more important elements of the mathematical formulation. It should be of use to anyone seeking to write their own software and demonstrates the underlying capabilities of QDAS. The coupling schemes are, to the best of our knowledge, original. For use of the software, the user guide [1] should be consulted.

1.2 A brief description of the QDAS analysis

Dichroic surfaces, more commonly referred to as Frequency Selective Surfaces (FSS), have been established in military and civil applications for many years. Early radar applications were mostly classified, though some technical papers appeared in the open literature (e.g. by Pelton & Munk [2]) and much work has been performed in classified research programmes. The author, amongst others, was significantly involved in the analysis and application of such structures in the UK. However, the use of FSS for civil applications is becoming more important and the theory and analysis is now quite well established in the open literature. Indeed, text books have recently appeared on the subject [3].

A basic understanding of electromagnetics and Maxwell's equations is assumed in this volume. A familiarity with FSS methods, e.g. as propounded by Chen [4] for single surfaces and Cwik and Mittra [5] for couplings would also be helpful.

A single FSS is often defined as a two dimensionally periodic array of slots or elements of arbitrary shape on a flat surface. An FSS is characterised by a unit cell which is often of the order of a wavelength in size and designed to resonate at certain frequencies. One consequence is that such surfaces may exhibit pass-band and stop-band filter characteristics which allow the selective propagation of electromagnetic waves at certain frequencies. Composite structures can be designed which are composed of multiple FSS, separated by one or several layers of dielectric.

There are a large number of possible methods that may be used to analyse FSS. These range from the essentially empirical, using equivalent circuit formulations, to a rigorous solution using boundary or finite element methods. It is the aim of the QDAS (Q-par Dichroic Array Software) software to provide a general purpose multi-layer tool that finds a compromise between accuracy, numerical efficiency (i.e. computational complexity) and flexibility. It should be capable of accurately predicting the performance of quite general composite FSS structures with no *a-priori* information concerning their electromagnetic characteristics. This must be done with the minimum of computer resources.

Predictive accuracy requires a rigorous solution and QDAS employs a Floquet modal boundary element method using some special techniques. There are a number of such methods described in the literature. Some are very efficient, but restrictive on the geometrical description of the FSS. For example, regular grid methods can use FFT conjugate gradient algorithms for very rapid computation of (at least single layer) FSS structures. However, such methods are not well suited to the modeling of curved geometries, such as circular rings, or strips which do not lie parallel to a unit cell. In order to avoid 'stair-casing' discretisation errors in such problems, a very fine mesh is required which works against the inherent efficiency of the method.

We decided at the outset not to follow the FFT approach, preferring the use of an unstructured mesh and a more general solution technique. This has the advantage of greater freedom of representation and, from previous experience, is known to work well for a wide class of FSS geometries. Moreover, in a composite structure containing closely coupled FSS, it is not clear whether FFT conjugate gradient methods can significantly reduce the numerical complexity of the problem. Nevertheless, it is possible to make computational savings by recognising that *parts* of an FSS can be represented by a regular mesh and QDAS takes advantage of this.

QDAS will adopt a cascade analysis, similar in concept to that described by Cwik and Mittra [5]. This allows a general FSS composite to be analysed 'one FSS at a time', with couplings between FSS described explicitly by Floquet modes. This results in a matrix cascade. An alternative method is to construct a Greens function for the entire composite and consider each element of each FSS as part of a single global entity. If each FSS is represented by N_i basis function, and there are T FSS, then there is a requirement to solve a moment method system of equations with $\sum_{i=1}^{T} N_i$ unknowns. This approach is efficient for a large number of very tightly bound FSS, but takes no account of the small size of many of the interactions in a weakly bound system. Furthermore, there is no possibility of simple analysis of periodically incommensurate[1] weakly bound FSS using this approach.

Dielectric layers are assumed to be isotropic and represented by a complex electric relative permittivity ϵ_r and a complex magnetic relative permeability μ_r. FSS geometry is modeled by two classes of structures termed *slots* (or *apertures*) and *elements*. An element FSS is characterised by modeling the (possibly partially) conducting pattern with an unknown electric current. In this case the conducting elements are represented by basis functions and the conducting pattern is appropriately meshed. A slot FSS is characterised by modeling the gaps in a perfect conductor by an unknown electric field, where the gaps may be assigned a non-zero surface conductivity. In this case the gaps are represented by basis functions and appropriately meshed. Any representation may be used for any FSS, but it is efficient to use the element description when the fraction of conductor per unit cell is small and to use the slot description when the fraction of conductor per unit cell is large. In either case,

[1] FSS are said to be periodically incommensurate (or simply incommensurate) if (1) each FSS is periodic and defined by a unit cell and (2) where there is no finite Global Unit Cell defined on the composite as a whole.

a tensor-valued surface conductivity or resistivity is permitted those regions which are not defined to be perfect conductor.

1.3 Floquet modes and basic principles

Slots or elements are represented by a finite number of discrete basis functions, of the sort required in any finite boundary element analysis. However, in addition, the FSS is represented by a finite number of Floquet modes; an approximation which is unique to periodic structures. Mathematically, no closed form expression exists for the Greens function of a general FSS; such a function is represented by an infinite two-dimensional sum, e.g. over Floquet modes. In QDAS, the sums are represented only to a finite number of terms in the spectral domain, described by the integers P and Q. Floquet mode indices p, $-P \leq p \leq P$, and q, $-Q \leq q \leq Q$ are used within the computation.[2] Physically, a finite number of Floquet modes imposes a spatial resolution limit to the unit cell. It is as if the sharp edges of the slots or elements are slightly blurred. Since the basis functions themselves only approximately represent the true electric and magnetic fields this resolution limit is not a serious problem. This is discussed further in section 4.6.

Each Floquet mode may be represented by a plane wave, usually evanescent, described by a unique pair of indices p and q together with a third unique index r which describes the polarisation of the mode. QDAS uses the convention $r = 1$ for transverse electric (TE) modes and $r = 2$ for transverse magnetic (TM) modes. A TM mode is one whose magnetic field lies perpendicular to the surface normal (z-axis). A TE mode is one whose electric field lies perpendicular to the surface normal (z-axis).

A given FSS has a periodicity that is defined by a unit cell of the structure. The smallest such unit cell is termed a primitive unit cell and is generally represented by a parallelogram. In QDAS this is specified by the base dimension d_x, the height d_y and the skew angle α as illustrated in figure 1-1. The unit cell is assumed to lie in a plane perpendicular to the z-axis, aligned with respect to the x and y axes as illustrated.

A plane wave is assumed to be incident on the structure with incidence angles θ_{in} and ϕ_{in} as illustrated in figure 1-2. The angle θ_{in} is the elevation angle from the surface normal while ϕ_{in} is the azimuth projection angle with respect to the x axis. In QDAS all angles, transmitted and reflected, will be defined in this coordinate system, where the z axis points in the direction of the incident wave. The incident wave will always be assumed to arrive from out of the *left hand* half plane. The polarisation of a wave will always refer to the direction of the electric field. If a plane wave has a direction specified by the angles θ and ϕ in the above coordinate system, then principal polarisations will be assumed to lie in the direction of increasing θ, referred to by the unit vector $\underline{\hat{\theta}}$, or in the direction of increasing ϕ,

[2] There have been acceleration schemes published which compute over an arbitrarily large number of modes sufficient to achieve convergence [12]. However, to the author's knowledge none have been demonstrated to be effective over arbitrary dielectric layered composites. The structure of the software has been designed to allow a ready implementation of an acceleration scheme should one become available.

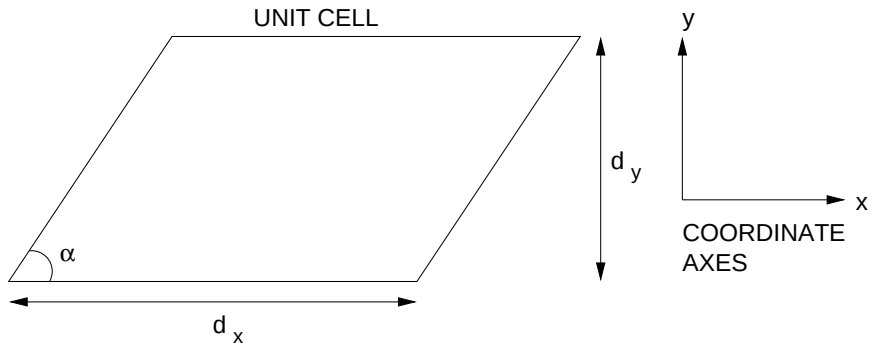

Figure 1-1: A unit cell of a single FSS

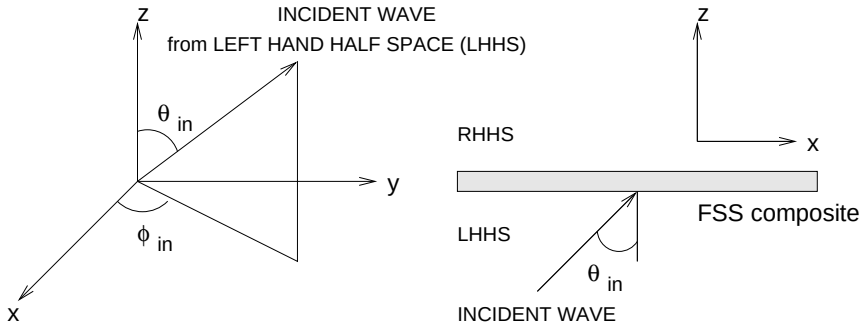

Figure 1-2: Wave angle definitions

referred to by the unit vector $\underline{\hat{\phi}}$. A $\underline{\hat{\theta}}$ directed wave is TM while a $\underline{\hat{\phi}}$ wave is TE. At normal incidence a wave is TEM (both TE and TM).

In QDAS an $e^{+j\omega t}$ harmonic time dependence is assumed for all electric, magnetic and linearly dependent fields, where ω is the angular frequency. The cyclic frequency $f = \omega/2\pi$. All materials will be assumed linear so that the harmonic form of Maxwell's equations are assumed to be valid. The free-space wave number $k_0 = 2\pi/\lambda_0 = \omega/C_0$ where λ_0 is the free space wavelength and C_0 is the speed of light in vacuum.

With the above definitions the wave number components in the x and y directions, associated with each Floquet mode, are respectively,

$$\begin{aligned} u_{pq} &= k_0 \sin\theta_{in} \cos\phi_{in} + \frac{2\pi p}{d_x} \\ v_{pq} &= k_0 \sin\theta_{in} \sin\phi_{in} + \frac{2\pi q}{d_y} - \frac{2\pi p \cot\alpha}{d_x} \end{aligned} \qquad \text{1-1}$$

while the Floquet modes themselves are defined by,

$$\underline{\phi}_{pqr}(\underline{x}) = \begin{cases} \dfrac{1}{\sqrt{d_x d_y}} \left(\dfrac{v_{pq}\underline{\hat{x}} - u_{pq}\underline{\hat{y}}}{t_{pq}} \right) \phi_{pq}(\underline{x}) & \text{for } r = 1 \text{ (TE)} \\ \dfrac{1}{\sqrt{d_x d_y}} \left(\dfrac{u_{pq}\underline{\hat{x}} + v_{pq}\underline{\hat{y}}}{t_{pq}} \right) \phi_{pq}(\underline{x}) & \text{for } r = 2 \text{ (TM)} \end{cases} \qquad \text{1-2}$$

where

$$t_{pq} = \sqrt{(u_{pq})^2 + (v_{pq})^2} \qquad 1\text{-}3$$

and

$$\phi_{pq}(\underline{x}) = e^{-j(u_{pq}x + v_{pq}y)} \qquad 1\text{-}4$$

The Floquet modes, as defined, are transverse fields which are mutually orthogonal over a unit cell. In other words,

$$\iint_{\mathcal{C}} \underline{\phi}_{pqr}(\underline{x}).\underline{\phi}^{\star}_{p'q'r'}(\underline{x})\, dxdy = \delta_{pp'}\delta_{qq'}\delta_{rr'} \qquad 1\text{-}5$$

for all integers p, q, p', q' and $r, r' = 1, 2$. The index $r = 1$ corresponds to a TE mode and $r = 2$ to a TM mode. The domain of integration $\mathcal{C}$ represents a unit cell; i.e. the integration is performed for all $x, y \in \mathcal{C}$. The term δ_{ij} is the Kroneka-delta symbol which is unity when $i = j$ and zero otherwise. Each Floquet mode may be regarded as the transverse component of a (generally evanescent) plane wave, $\underline{\Phi}_{pqr}(x, y, z)$, which satisfies the periodic boundary conditions of a given FSS. If an FSS is situated at $z = z_0$ then in general, $\underline{\Phi}_{pqr}(x, y, z)$ is given by

$$\underline{\Phi}_{pqr}(x, y, z) = \underline{\phi}_{pqr}(\underline{x}) \exp(-j\gamma_{pq}|z - z_0|) \qquad 1\text{-}6$$

where the *propagation factor* γ_{pq} is defined by,

$$\gamma_{pq} = \sqrt{\epsilon_r \mu_r (k_0)^2 - (u_{pq})^2 - (v_{pq})^2} \qquad 1\text{-}7$$

Since ϵ_r and μ_r are generally complex and u_{pq}, v_{pq} and $k_0 > 0$ are arbitrary real numbers, some care is required over which branch of the complex square root to use. This is a much more delicate issue than the literature would indicate. For the reasons outlined in the next section, we choose the branch cut to lie along the positive imaginary axis.

1.4 Material properties

Let $\epsilon_r \equiv \epsilon_1 + j\epsilon_2$ and $\mu_r \equiv \mu_1 + j\mu_2$ for real $\epsilon_1, \epsilon_2, \mu_1$ and μ_2. Similarly, let $\gamma_{pq} \equiv \gamma_1 + j\gamma_2$ for real γ_1 and γ_2. Four assumptions are commonly made in the macroscopic description of a dielectric (magnetic) material;

- #1. The material is linear and non-active. In this case, there is no growth in the amplitude of a wave with distance from the FSS and we require $\gamma_2 \leq 0$ for any p, q, r or value of θ_{in} or ϕ_{in}.
- #2. The real parts of the permittivity and permeability, ϵ_1 and μ_1, are positive (indeed usually ≥ 1).
- #3. A wave generated by a source on the FSS propagates away from the source, within the medium, so that $\gamma_1 > 0$.
- #4. The electric and magnetic parameters ϵ_r and μ_r are independent of each other.

Equating the imaginary parts of the square of both sides of (1-7) implies,

$$k_0^2(\epsilon_1\mu_2 + \mu_1\epsilon_2) = 2\gamma_1\gamma_2 \qquad 1\text{-}8$$

Taken with conditions #1 to #4 it is necessary that $\mu_2 \leq 0$ and $\epsilon_2 \leq 0$. However, assumption #1 is invalid for certain kinds of active media which feature distributed amplification mechanisms that permit the exponential growth of a wave over a finite distance. Examples include semiconductors and free electron plasmas for which there may be a modeling requirement.

Assumption #2 may also be invalid for certain dispersive materials. For example, ϵ_1 can be negative in plasmas at certain frequencies and, more recently, composite materials have been created by Pendry and others with negative μ_1 (see e.g. [7]). Assumption #3 may be invalid for materials where assumption #2 is invalid. This is consistent with causality in dispersive materials provided a phase reversal (a transition to $\gamma_1 < 0$) occurs only over certain restricted frequency intervals. Finally, assumption #4 has been questioned in Landau and Lifshitz [6, §79]. They show that there is no fundamental distinction to be made between the curl of the magnetic moment and the time rate of change of the electric polarisation. This means that there is a relationship between the frequency dependence of the permeability and permittivity in spatially and frequency dispersive media, especially relevant to artificial magneto-dielectric materials where the dimensions of the constituent particles are large (even if small compared to a wavelength). In addition it may also imply the realisation of materials which, at certain frequencies, have $\mu_2 > 0$ (with $\epsilon_2 < 0$) or $\epsilon_2 > 0$ (with $\mu_2 < 0$) while still obeying assumption #1.[3]

If none of the assumptions are valid, it is not possible to define a fixed branch cut for the evaluation of the square root in (1-7) which does not result in a discontinuity over some range of permitted parameters! We have, somewhat arbitrarily, chosen the branch cut to lie along the positive imaginary axis. This permits the breaking of assumptions #2, #3 and #4 and allows a certain range of parameters which violate #1. Furthermore, for more 'normal' materials it avoids the numerical problem associated with a branch cut on the negative or positive real axis. This can occur using materials where the numerical value of the product $\epsilon_r\mu_r$ lies close to (and numerically, possibly, to either side of) the real axis.

1.5 Multiple FSS and the global unit cell

In general, if a composite contains more than one unit cell then the FSSs may couple through interactions with many Floquet modes. If the FSSs share the *same* unit cell, then the FSSs interact through the same set of Floquet modes defined for any single FSS. The problem, while complex, is physically straightforward. However if each FSS has a *different* unit cell, such that primitive unit cells define FSSs with different periodicities, then FSSs do not share

[3] This observation is rather speculative. It is almost universally assumed, even in [6, e.g. §80], that there is no transfer between the macroscopic electric and magnetic energy density. However, there is no obvious requirement for such a constraint in a material which is non-linear on a microscopic scale.

a common mode set and the Floquet modes of one FSS are not necessarily those of another. In this case a strict periodic analysis is only possible if there exists a unit cell, termed the *global unit cell* (GUC) which is the lowest common multiple of all others. The GUC defines the true periodicity of the entire composite.

In any exact periodic analysis it is therefore necessary to define a global unit cell. However, in practice there are many situations where the distance between FSS is large enough and the frequency low enough, that almost all the coupling between FSS is due to the principal wave described by the Floquet modal indices $p = q = 0$ (for $r = 1, 2$). This is an important special case that deserves attention. The principal wave does *not*, by itself, carry information concerning the periodicity of the FSS; if two or more FSS interact only through principal waves the FSS can be described by arbitrary unit cells without the existence of a GUC and this is permitted in the formulation. Such FSS are said to be *local* and are specified only through a *local* unit cell. Any local FSS is coupled to FSS on the left or the right only through Floquet modes with $p = q = 0$.

FSS are termed *incommensurate* if there does not exist a finite GUC. Because the interaction of incommensurate FSS is poorly understood, it is left to the user to designate that a particular FSS is local.

1.6 Basis functions

In any boundary element method it is necessary to represent unknown fields in terms of a sum of basis functions with unknown coefficients. In our formulation we will assume the basis functions are those employed by Rao, Wilton and Glisson (RWG) in a classic paper [11], commonly employed for electromagnetic boundary element problems. They offer a good compromise between accuracy and ease of computation and allow the representation of surface currents, either electric or magnetic, which are piece-wise continuous in their principal components. Higher order elements are possible, but are rarely used in electromagnetic problems because of the nature of the Green's function singularity and the vector nature of the surface fields and boundary conditions. The RWG basis functions assume the (electric) currents are spread across triangle pairs sharing a common side. The currents are a maximum at the common edge and linearly taper to zero at the opposite vertices.

A given FSS is defined as either a 'slot' or an 'element' structure. A slot structure requires the gap in conductor to be represented by a set of electric field basis functions, whereas an element structure requires the conductor in empty space to be represented by a set of electric current basis functions. Rao, Wilton and Glisson described the use of their basis functions for electric currents, as applied to element structures. In this case the electric current component normal to a common triangle edge is approximately continuous. For slotted structures, the vector directions are rotated by 90 degrees and used to locally describe the tangential electric fields and the tangential component of the electric field *parallel* to a common triangle edge is approximately continuous.

If a triangle defines part of a slotted FSS a triangle is assigned a complex tensor conductivity $\underline{\underline{\sigma}}$, entered in Cartesian coordinates. The components are entered as $\Re\sigma_{xx}$, $\Im\sigma_{xx}$, $\Re\sigma_{xy}$, $\Im\sigma_{xy}$, $\Re\sigma_{yx}$, $\Im\sigma_{yx}$, $\Re\sigma_{yy}$, $\Im\sigma_{yy}$. (The notation $\Re Z$ means the 'real part of Z' and $\Im Z$ means the 'imaginary part of Z'.) All zero values imply the slot is empty in a perfect conductor. These are, respectively, the parameters #11 to #18 in the triangle parameter list.

If a triangle defines part of an element FSS a triangle is assigned a complex tensor resistivity $\underline{\underline{\Omega}}$, entered in Cartesian coordinates. The components are entered as $\Re\Omega_{xx}$, $\Im\Omega_{xx}$, $\Re\Omega_{xy}$, $\Im\Omega_{xy}$, $\Re\Omega_{yx}$, $\Im\Omega_{yx}$, $\Re\Omega_{yy}$, $\Im\Omega_{yy}$. All zero values imply the element is a perfect conductor in free space.

An isotropic material should have the xx and yy subscripted quantities equal, with the xy and yx subscripted quantities zero. The model assumes that the values of resistivity or conductivity are piece-wise constant over a given triangle. Whether this is a good model, especially for anisotropic materials, is not known. Anisotropy may not be well modeled when employed with RWG basis functions because discontinuities in the non-principal current flows (e.g. the current flow parallel to a common side of a triangle pair for the element formulation) may coincide with an important flow in an anisotropic material. The user is warned that a lot more work is required to quantify this behaviour. However, preliminary tests show good agreement in cross comparisons with isotropic materials.

1.7 Grating lobes

When the frequency becomes sufficiently large (more precisely, if the wavelength in the left or right half space becomes sufficiently small compared with the unit cell dimensions), grating lobes can be excited. These correspond to angles other than those of the principal wave at which energy can propagate into the left or right half space. The principal wave is always characterised by the Floquet indices $p = q = 0$. Grating lobes are uniquely characterised by other pairs of p and q, based on the global unit cell (GUC). In a composite containing dielectrics, internal grating lobes will usually appear first which long-range couple FSS through modes other than $p = q = 0$. Internal grating lobes will often introduce resonances into the reflection and transmission characteristics of the principal waves, but are not extracted as special outputs.

Grating lobes which appear in the left or right hand half space are referred to as *external grating lobes*. These are of direct importance in the design of the composite. The angles at which these occur and the powers associated with each (for both co-polar and cross-polar fields) are program outputs.

1.8 Reflection and transmission matrices

The composite analysis is based on the determination of matrix relationships between the tangential components of left and right propagating modal fields. After a suitable matrix concatenation it is possible to relate the incoming with the outgoing tangential fields at the

left and right-most surfaces of the composite by a modal scattering matrix. Determination of this matrix forms the heart of the problem. The next part of the problem is to determine the reflected and transmitted amplitudes and powers of the wave fields that give rise to the tangential components. These reflections and transmissions are characterised by a 2×2 reflection or transmission polarisation matrix associated with each pair of Floquet modal indices p and q.

It is necessary to define the reflection and transmission polarisation matrix only for principal and external grating waves. Modal values of p and q not associated with external grating waves are not associated with propagating plane waves. Referring to the coordinate system in figure 1-2, it is assumed that reflected and transmitted wave angles may be different to those of the incident wave. Firstly, the wave may be a grating wave and secondly, we assume the right hand half plane may be a loss-less dielectric medium with real ϵ_r and μ_r different from unity. The incident plane wave is specified by the incidence angles (θ_{in}, ϕ_{in}) in free space in the left hand half plane. The transmitted plane wave (or waves) are specified by the angles (θ_{tx}, ϕ_{tx}) in the right hand half plane. The reflected plane wave (or waves) are specified by the angles (θ_{rx}, ϕ_{rx}) in the left hand half plane.

The principal incident polarisation directions, $\underline{\hat{\theta}}_{in}$ and $\underline{\hat{\phi}}_{in}$, are defined in Cartesian coordinates by,

$$\begin{aligned} \underline{\hat{\theta}}_{in} &= \cos\phi_{in}\cos\theta_{in}\underline{\hat{x}} + \sin\phi_{in}\cos\theta_{in}\underline{\hat{y}} - \sin\theta_{in}\underline{\hat{z}} \\ \underline{\hat{\phi}}_{in} &= -\sin\phi_{in}\underline{\hat{x}} + \cos\phi_{in}\underline{\hat{y}} \end{aligned} \qquad \text{1-9}$$

The polarisation of a general unit magnitude incident wave may be described by the unit electric vector,

$$\underline{E}_0 = \alpha_{in}^{(\phi)}\underline{\hat{\phi}}_{in} + \alpha_{in}^{(\theta)}\underline{\hat{\theta}}_{in} \qquad \text{1-10}$$

for complex scalars $\alpha_{in}^{(\phi)}$ and $\alpha_{in}^{(\theta)}$ such that $\alpha_{in}^{(\phi)}(\alpha_{in}^{(\phi)})^\star + \alpha_{in}^{(\theta)}(\alpha_{in}^{(\theta)})^\star = 1$.

A wave is said to be scattered if it is either transmitted into the right hand half plane or reflected into the left hand half plane. The scattering angles θ and ϕ, referred to the same coordinate system, define the new directions $\underline{\hat{\theta}}$ and $\underline{\hat{\phi}}$,

$$\begin{aligned} \underline{\hat{\theta}} &= \cos\phi\cos\theta\underline{\hat{x}} + \sin\phi\cos\theta\underline{\hat{y}} - \sin\theta\underline{\hat{z}} \\ \underline{\hat{\phi}} &= -\sin\phi\underline{\hat{x}} + \cos\phi\underline{\hat{y}} \end{aligned} \qquad \text{1-11}$$

If there are no grating waves, there is only one pair of angles $(\theta, \phi) = (\theta_{tx}, \phi_{tx})$ for the transmitted and one pair $(\theta, \phi) = (\theta_{rx}, \phi_{rx})$ for the reflected waves. The scattered wave, associated with (θ, ϕ), may be defined by,

$$\underline{E}_{scat} = \alpha_s^{(\phi)}\underline{\hat{\phi}} + \alpha_s^{(\theta)}\underline{\hat{\theta}} \qquad \text{1-12}$$

The relation between $\underline{E}_0$ and $\underline{E}_{scat}$ may be defined by a polarisation matrix,

$$\begin{pmatrix} \alpha_s^{(\phi)} \\ \alpha_s^{(\theta)} \end{pmatrix} = \begin{pmatrix} S_{11} & S_{12} \\ S_{21} & S_{22} \end{pmatrix} \begin{pmatrix} \alpha_{in}^{(\phi)} \\ \alpha_{in}^{(\theta)} \end{pmatrix} \qquad \text{1-13}$$

For a reflected wave the coefficients S_{ij} refer to field reflection coefficients $\mathcal{R}_{ij}$ and for a transmitted wave to field transmission coefficients $\mathcal{T}_{ij}$. These coefficients may be converted into power coefficients and phases respectively,

$$\begin{aligned} P_{db}^{(ij)} &= 20\log_{10}(|S_{ij}|) \\ \Phi^{(ij)} &= \arg(S_{ij}) \end{aligned} \qquad \text{1-14}$$

The power coefficients are measured in dB and the phase is referenced with respect to the first (left-most) interface and output in degrees. The powers are those associated with a transverse plane wave propagating in the wave direction (θ, ϕ) assuming an incident wave with unit amplitude propagating in the direction (θ_{in}, ϕ_{in}). These are the quantities that are directly measured in a free space measurement bridge assuming a sufficiently large FSS with sufficiently large projected area in the scattered field direction and antennas with apertures large compared to a wavelength but small compared to the projected area of the FSS.

1.9 Power transmission and the grating angles

For a lossless FSS with no grating lobes in free space there are only two sets of scatter angles, $(\theta, \phi) = (\theta_{rx}, \phi_{rx})$ for the reflected wave for which $S_{ij} = \mathcal{R}_{ij}$ and $(\theta, \phi) = (\theta_{tx}, \phi_{tx})$ for the transmitted wave for which $S_{ij} = \mathcal{T}_{ij}$. In this special case, $(\theta_{rx}, \phi_{rx}) = (\pi - \theta_{in}, \phi_{in})$ and $(\theta_{tx}, \phi_{tx}) = (\theta_{in}, \phi_{in})$. Power conservation may be applied independently to the two incident polarisations and,

$$\begin{aligned} |\mathcal{R}_{11}|^2 + |\mathcal{R}_{12}|^2 + |\mathcal{T}_{11}|^2 + |\mathcal{T}_{12}|^2 &= 1 \\ |\mathcal{R}_{21}|^2 + |\mathcal{R}_{22}|^2 + |\mathcal{T}_{21}|^2 + |\mathcal{T}_{22}|^2 &= 1 \end{aligned} \qquad \text{1-15}$$

independent of the angles of incidence. *However*, it is *not* valid to sum power coefficients when there are grating lobes. The reason for this is that power conservation is appropriate to the input and output fluxes *normal* to the FSS and thus an incidence angle dependent projection factor must now be accounted for as given below.

In general, suppose that the right hand half space is a loss-less dielectric (magnetic) material with real permittivity and permeability $\epsilon_r > 0$ and $\mu_r > 0$. The left hand half space is assumed to be free space. Suppose there are grating reflection and transmission lobes with wave coefficients S_{ij} defined by $\mathcal{R}_{ij}^k$ and $\mathcal{T}_{ij}^k$. The superfix k denoting a unique grating angle, which includes the principal wave direction. The set of reflected waves is specified by the indices $k \in [1, K_R]$, with reflection angles $(\theta_{rx}^{(k)}, \phi_{rx}^{(k)})$. The set of transmitted waves is specified by the indices $k \in [1, K_T]$, with transmission angles $(\theta_{tx}^{(k)}, \phi_{tx}^{(k)})$.

For a plane wave propagating at an angle θ normal to the FSS, the power flow perpendicular to the FSS in the right hand half plane is $|\cos\theta| I\sqrt{\epsilon_r/\mu_r}$ where I is the intensity of the plane wave. Similarly in the left hand half plane, without the $\sqrt{\epsilon_r/\mu_r}$ factor. Therefore

conservation of power implies that,

$$Q_1 \equiv \frac{1}{|\cos\theta_{in}|}\left(\sum_{k=1}^{K_R}|\cos\theta_{rx}^{(k)}|(|\mathcal{R}_{11}^k|^2+|\mathcal{R}_{12}^k|^2)+\sqrt{\frac{\epsilon_r}{\mu_r}}\sum_{k=1}^{K_T}|\cos\theta_{tx}^{(k)}|(|\mathcal{T}_{11}^k|^2+|\mathcal{T}_{12}^k|^2)\right)\leq 1$$

$$Q_2 \equiv \frac{1}{|\cos\theta_{in}|}\left(\sum_{k=1}^{K_R}|\cos\theta_{rx}^{(k)}|(|\mathcal{R}_{21}^k|^2+|\mathcal{R}_{22}^k|^2)+\sqrt{\frac{\epsilon_r}{\mu_r}}\sum_{k=1}^{K_T}|\cos\theta_{tx}^{(k)}|(|\mathcal{T}_{21}^k|^2+|\mathcal{T}_{22}^k|^2)\right)\leq 1$$

1-16

with equality when the FSS composite is loss-less. The program outputs these "power conservation factors", Q_1 and Q_2 as diagnostics.

The grating angles $(\theta_{rx}^{(k)},\phi_{rx}^{(k)})$ and $(\theta_{tx}^{(k)},\phi_{tx}^{(k)})$ are functions of the frequency, angles of incidence and unit cell dimensions. Equating the x and y components of the wavenumber in the left hand half space we have,

$$\begin{aligned} k_0\sin\theta_{rx}^{(k)}\cos\phi_{rx}^{(k)} &= u_{pq} = k_0\sin\theta_{in}\cos\phi_{in}+\frac{2\pi p}{d_x} \\ k_0\sin\theta_{rx}^{(k)}\sin\phi_{rx}^{(k)} &= v_{pq} = k_0\sin\theta_{in}\sin\phi_{in}+\frac{2\pi q}{d_y}-\frac{2\pi p\cot\alpha}{d_x} \end{aligned} \qquad \text{1-17}$$

where k indexes all unique pairs of Floquet indices p and q such that $\theta_{rx}^{(k)}$ and $\phi_{rx}^{(k)}$ are real valued solutions. Let,

$$\begin{aligned} \hat{u}_{pq} &= \sin\theta_{in}\cos\phi_{in}+\frac{2\pi p}{k_0 d_x} \\ \hat{v}_{pq} &= \sin\theta_{in}\sin\phi_{in}+\frac{2\pi}{k_0}\left(\frac{q}{d_y}-\frac{p\cot\alpha}{d_x}\right) \end{aligned} \qquad \text{1-18}$$

then,

$$\theta_{rx}^{(k)} = \pi-\arcsin\sqrt{(\hat{v}_{pq})^2+(\hat{u}_{pq})^2} \qquad \text{1-19}$$

and

$$\phi_{rx}^{(k)} = \arctan_2(\hat{v}_{pq},\hat{u}_{pq}) \qquad \text{1-20}$$

where $\arctan_2(y,x)$ refers to the standard double argument inverse tangent function, $\arctan(y/x)$, which places the angle in the correct quadrant depending on whether x or y is less than or greater than zero.

Equating the x and y components of the wavenumber in the right hand half space,

$$\begin{aligned} k_0\sqrt{\epsilon_r\mu_r}\sin\theta_{tx}^{(k)}\cos\phi_{tx}^{(k)} &= u_{pq} \\ k_0\sqrt{\epsilon_r\mu_r}\sin\theta_{tx}^{(k)}\sin\phi_{tx}^{(k)} &= v_{pq} \end{aligned} \qquad \text{1-21}$$

giving the transmission angles as,

$$\theta_{tx}^{(k)} = \arcsin\left(\frac{\sqrt{(\hat{v}_{pq})^2 + (\hat{u}_{pq})^2}}{\epsilon_r \mu_r}\right) \qquad 1\text{-}22$$

and

$$\phi_{tx}^{(k)} = \arctan_2(\hat{v}_{pq}, \hat{u}_{pq}) \qquad 1\text{-}23$$

1.10 The tangential field coefficients

Central to the analysis is a representation of the tangential fields either side of an interface within the composite in terms of the vector Floquet modes $\underline{\phi}_{pqr}(\underline{x})$. Let the tangential component of the electric and magnetic fields just to the left of a given interface be $\underline{E}^{(t-)}$ and $\underline{H}^{(t-)}$, respectively. Similarly, let the tangential component of the electric and magnetic fields just to the right of the same interface be $\underline{E}^{(t+)}$ and $\underline{H}^{(t+)}$, respectively. We define the incident, reflected, transmitted and incoming *tangential electric field coefficients* by A_{pqr}, R_{pqr}, T_{pqr} and W_{pqr}, respectively. Any periodic incident field in the left hand half space has a tangential electric field represented by $\sum_{pqr} A_{pqr}\underline{\phi}_{pqr}(\underline{x})$. Similarly, the tangential reflected field in the left hand half space is represented by $\sum_{pqr} R_{pqr}\underline{\phi}_{pqr}(\underline{x})$. In the right hand half space, the transmitted and incoming fields are represented by similar sums over T_{pqr} and W_{pqr}.

Suppose, without loss of generality, we consider an interface at $z = 0$ with fields that are periodic with respect to a unit cell specified by d_x, d_y and α. Following Chen [4], $\underline{E}^{(t-)}$ and $\underline{E}^{(t+)}$ are given by,

$$\begin{aligned}\underline{E}^{(t-)}(x,y) &= \sum_{pqr} A_{pqr}\underline{\phi}_{pqr}(x,y) + \sum_{pqr} R_{pqr}\underline{\phi}_{pqr}(x,y) \\ \underline{E}^{(t+)}(x,y) &= \sum_{pqr} T_{pqr}\underline{\phi}_{pqr}(x,y) + \sum_{pqr} W_{pqr}\underline{\phi}_{pqr}(x,y)\end{aligned} \qquad 1\text{-}24$$

The sums are over all important Floquet modes, strictly $-\infty < p, q < \infty$, $r = 1, 2$. In practise, the sums are truncated and may be truncated to different numbers for each sum. This is discussed in more detail in later sections of this report. If the composite structure does not contain an FSS the sums only contain non-zero terms for $p = q = 0$ so we are at liberty to assume any values for d_x, d_y and α.

To represent the magnetic fields in terms of the tangential electric field coefficients, the modal admittances are required. Suppose the medium just to the left of the interface at $z = 0$ has relative permittivity and permeability $\epsilon_r^{(1)}$ and $\mu_r^{(1)}$. Similarly, let the medium just to the right of the interface have relative permittivity and permeability $\epsilon_r^{(2)}$ and $\mu_r^{(2)}$. The

modal admittances to the left and right of the interface, respectively $\xi^{(1)}_{pqr}$ and $\xi^{(2)}_{pqr}$, are given by

$$\xi^{(l)}_{pqr} = \begin{cases} \dfrac{\gamma^{(l)}_{pq}\xi_0}{\mu^{(l)}_r k_0} & \text{for } r = 1 \text{ (TE modes)} \\ \dfrac{\epsilon^{(l)}_r k_0 \xi_0}{\gamma^{(l)}_{pq}} & \text{for } r = 2 \text{ (TM modes)} \end{cases} \qquad \text{1-25}$$

for $l = 1, 2$, k_0 is the free space wave number, $\xi_0 = \sqrt{\epsilon_0/\mu_0} \approx 1/377$ is the admittance of free space and $\gamma^{(l)}_{pq}$ are the propagation factors (as in (1-7)) to either side of the interface,

$$\gamma^{(l)}_{pq} = \sqrt{\epsilon^{(l)}_r \mu^{(l)}_r (k_0)^2 - (u_{pq})^2 - (v_{pq})^2} \qquad \text{1-26}$$

with the branch cut defined as in (1-7).

The tangential magnetic fields may now be written ([4]) by,

$$\begin{aligned} -\underline{\hat{z}} \times \underline{H}^{(t-)}(x,y) &= \sum_{pqr} A_{pqr}\xi^{(1)}_{pqr}\underline{\phi}_{pqr}(x,y) - \sum_{pqr} R_{pqr}\xi^{(1)}_{pqr}\underline{\phi}_{pqr}(x,y) \\ -\underline{\hat{z}} \times \underline{H}^{(t+)}(x,y) &= \sum_{pqr} T_{pqr}\xi^{(2)}_{pqr}\underline{\phi}_{pqr}(x,y) - \sum_{pqr} W_{pqr}\xi^{(2)}_{pqr}\underline{\phi}_{pqr}(x,y) \end{aligned} \qquad \text{1-27}$$

The tangential wave coefficients are determined using boundary element methods, described later, with a different formulation for slotted and element structures.

1.11 Relation between tangential fields and polarisation matrix $\mathbf{S}_{ij}$

Once the tangential field coefficients have been calculated it is necessary to relate them to the wave reflection and transmission matrices defined by the polarisation matrix S_{ij}.

The incident field at each point on the interface, $\underline{E}_{in}(x,y)$, is taken to be of strength $\underline{E}_0$, i.e

$$\underline{E}_{in}(x,y) = \underline{E}_0\, \phi_{00}(\underline{x}) \qquad \text{1-28}$$

Let $\underline{E}^{(t)}_{in}(x,y)$ and $\underline{E}^{(t)}_0$ be the tangential components,

$$\begin{aligned} \underline{E}^{(t)}_{in}(x,y) &= \underline{E}_{in}(x,y) - (\underline{E}_{in}(x,y).\underline{\hat{z}})\underline{\hat{z}} \\ \underline{E}^{(t)}_0 &= \underline{E}_0 - (\underline{E}_0.\underline{\hat{z}})\underline{\hat{z}} \end{aligned} \qquad \text{1-29}$$

Suppose that $\underline{E}_{in}(x,y)$ is either a TE polarised wave ($r = 1$) or a TM polarised wave ($r = 2$). In this case (1-24) implies that,

$$\underline{E}^{(t)}_{in}(x,y) = \begin{cases} A_{001}\,\underline{\phi}_{001}(x,y) & \text{, for } r = 1 \\ A_{002}\,\underline{\phi}_{002}(x,y) & \text{, for } r = 2 \end{cases} \qquad \text{1-30}$$

and so,

$$\underline{E}_0^{(t)} = \frac{1}{\sqrt{d_x d_y}} \begin{cases} A_{001}(\sin\phi_{in}\underline{\hat{x}} - \cos\phi_{in}\underline{\hat{y}}) & \text{, for } r = 1 \\ A_{002}(\cos\phi_{in}\underline{\hat{x}} + \sin\phi_{in}\underline{\hat{y}}) & \text{, for } r = 2 \end{cases} \qquad \text{1-31}$$

However, in section 1.7, we described the incident fields in terms of the coefficients $\alpha_{in}^{(\phi)}$ and $\alpha_{in}^{(\theta)}$. For a TE incident field ($r = 1$) $\underline{E}_0 = \alpha_{in}^{(\phi)}\underline{\hat{\phi}}_{in}$ and for a TM incident field ($r = 2$) $\underline{E}_0 = \alpha_{in}^{(\theta)}\underline{\hat{\theta}}_{in}$. Thus,

$$\underline{E}_0^{(t)} = \begin{cases} \alpha_{in}^{(\phi)}(-\sin\phi_{in}\underline{\hat{x}} + \cos\phi_{in}\underline{\hat{y}}) & \text{, for } r = 1 \\ \alpha_{in}^{(\theta)}\cos\theta_{in}(\cos\phi_{in}\underline{\hat{x}} + \sin\phi_{in}\underline{\hat{y}}) & \text{, for } r = 2 \end{cases} \qquad \text{1-32}$$

Comparing (1-31) and (1-32) implies,

$$A_{00r} = \sqrt{d_x d_y} \begin{cases} -\alpha_{in}^{(\phi)} & \text{, for } r = 1 \\ \cos\theta_{in}\alpha_{in}^{(\theta)} & \text{, for } r = 2 \end{cases} \qquad \text{1-33}$$

where d_x and d_y refer to the unit cell dimensions of the first FSS in the composite. If the composite contains no FSS, d_x and d_y can be chosen arbitrarily since $A_{00s}\underline{\phi}_{00s}$ are independent of d_x and d_y. If the composite contains FSS but no global unit cell (GUC) exists then there is the possibility that d_x and d_y refer to a *local* FSS and not the global unit cell. However, QDAS makes the assumption that an FSS is either defined by a GUC or it is defined as *local* with couplings to the rest of the structure and the outside world only through the principal waves. In this case scatter angles are those of the principal waves which are independent of d_x and d_y.

A similar argument can be made for the reflection and transmission coefficients. Let $\alpha_{refl}^{(\phi)}$ and $\alpha_{refl}^{(\theta)}$ be the reflected scattered wave coefficients and $\alpha_{tran}^{(\phi)}$ and $\alpha_{tran}^{(\theta)}$ be the transmitted scattered wave coefficients (generically, $\alpha_s^{(\phi)}$ and $\alpha_s^{(\theta)}$ as defined in (1-12)). The tangential component of a reflected wave, at the grating angles (θ_{rx}, ϕ_{rx}) and modal indices (p, q), is given by

$$\underline{E}_{refl}^{(t)} = \frac{1}{\sqrt{d_x d_y}} \left(R_{pq1}(\sin\phi_{rx}\underline{\hat{x}} - \cos\phi_{rx}\underline{\hat{y}}) + R_{pq2}(\cos\phi_{rx}\underline{\hat{x}} + \sin\phi_{rx}\underline{\hat{y}}) \right) \qquad \text{1-34}$$

with different values of R_{pq1} and R_{pq2} for each r. The tangential component of a transmitted wave, at the grating angles (θ_{tx}, ϕ_{tx}) and modal indices (p, q), is given by

$$\underline{E}_{tran}^{(t)} = \frac{1}{\sqrt{d_x d_y}} \left(T'_{pq1}(\sin\phi_{tx}\underline{\hat{x}} - \cos\phi_{tx}\underline{\hat{y}}) + T'_{pq2}(\cos\phi_{tx}\underline{\hat{x}} + \sin\phi_{tx}\underline{\hat{y}}) \right) \qquad \text{1-35}$$

where the primes on T_{pqs} are used to indicate they belong to the last interface, which is generally not the first. Again there are different values of T'_{pq1} and T'_{pq2} for each r. Note that in the transmitted case, we still define d_x and d_y as the dimensions of the *first* FSS in the composite. This is because all angles and periodicities are referenced with respect to the

left hand half plane in (1-34) and (1-35) and the transmitted field is represented here by the Floquet modes of the first interface. If every FSS is defined by a GUC there is no issue. If the final FSS is defined as local then we assume $p = q = 0$ and there are no non-recognised angles.

Because R_{pq1}, R_{pq2}, T'_{pq1} and T'_{pq2} are generally dependent on r, we represent them by the coefficients $z_{rs}^{(R)}$ and $z_{rs}^{(T)}$, respectively, with implicit p, q dependence. Thus define,

$$\begin{array}{ll} z_{1s}^{(R)} = R_{pqs} & \text{for } r = 1 \\ z_{2s}^{(R)} = R_{pqs} & \text{for } r = 2 \\ z_{1s}^{(T)} = T'_{pqs} & \text{for } r = 1 \\ z_{2s}^{(T)} = T'_{pqs} & \text{for } r = 2 \end{array} \qquad \text{1-36}$$

Now suppose we assume that R_{pq1}, R_{pq2}, T'_{pq1} and T'_{pq2} are all calculated with either $A_{001} = 1$, $A_{002} = 0$ (TE case) or $A_{001} = 0$, $A_{002} = 1$ (TM case). In other words let,

$$\begin{array}{lll} A_{001} = 1 & A_{002} = 0 & \text{for } r = 1 \\ A_{001} = 0 & A_{002} = 1 & \text{for } r = 2 \end{array} \qquad \text{1-37}$$

This implies that the reflected and transmitted tangential fields, for $\alpha_{in}^{(\theta)} = 1$, $\alpha_{in}^{(\phi)} = 0$ or $\alpha_{in}^{(\theta)} = 0$, $\alpha_{in}^{(\phi)} = 1$ must be scaled according to (1-33). Once the tangential fields are determined, the coefficients $\alpha_s^{(\theta)}$ and $\alpha_s^{(\phi)}$ may be found by the inverse scaling with (1-33) for θ_{in} replaced by θ_{tx} for the transmitted waves and θ_{rx} for the reflected waves. This allows us to write the polarisation matrix, $S_{ij} = \mathcal{R}_{ij}$ for the reflected waves defined in (1-13) by,

$$\begin{pmatrix} \mathcal{R}_{11} & \mathcal{R}_{12} \\ \mathcal{R}_{21} & \mathcal{R}_{22} \end{pmatrix} = \begin{pmatrix} z_{11}^{(R)} & -z_{12}^{(R)} / \cos\theta_{rx} \\ -z_{21}^{(R)} \cos\theta_{in} & z_{22}^{(R)} \cos\theta_{in} / \cos\theta_{rx} \end{pmatrix} \qquad \text{1-38}$$

and $S_{ij} = \mathcal{T}_{ij}$ for the transmitted waves by,

$$\begin{pmatrix} \mathcal{T}_{11} & \mathcal{T}_{12} \\ \mathcal{T}_{21} & \mathcal{T}_{22} \end{pmatrix} = \begin{pmatrix} z_{11}^{(T)} & -z_{12}^{(T)} / \cos\theta_{tx} \\ -z_{21}^{(T)} \cos\theta_{in} & z_{22}^{(T)} \cos\theta_{in} / \cos\theta_{tx} \end{pmatrix} \qquad \text{1-39}$$

A note on angle convention

Using the angle convention described earlier, θ_{rx} and θ_{tx} follow the direction of the reflected (transmitted) waves and the polarisation matrices are defined *with the wave*. Suppose, for example, we were to consider a wave incident at normal incidence on to a dielectric or conducting slab. In this case $\theta_{in} = 0°$, $\theta_{tx} = 0°$ but $\theta_{rx} = 180°$. The reflection polarisation matrix for a perfect conductor thus takes the form, $\begin{pmatrix} 1 & 0 \\ 0 & -1 \end{pmatrix}$ rather than the identity matrix expected in the coordinate system of the source. Under our definition, a right circular polarised wave is correctly transformed into a left circular polarised wave. If we required $\theta_{rx} = \theta_{in}$ (in the coordinate system of the source) we must reverse the signs of $\mathcal{R}_{12}$ and $\mathcal{R}_{22}$.

2 Canonical structures and general coupling methods

2.1 Introduction

A general FSS composite is assumed to contain zero or more individual FSS surfaces separated by any number of arbitrarily thick layers of dielectric/magnetic material. Each interface, whether an FSS or not, will reflect and transmit wave components. We will employ Chu's tangential field description, described in section 1.9, at each interface. The central problem is then to calculate the tangential field coefficients, A_{pqr}, R_{pqr}, T_{pqr} and W_{pqr} at each interface. Once these are known at the front and back surface of the composite, the wave transmission and reflection matrices are readily found as described in section 1.10.

Consider a general composite, as illustrated in figure 2-1 below. In the figure, a dashed line represents an FSS whereas a straight line represents a non-FSS (dielectric) interface. We analyse the structure "left to right" with an incident wave from the left hand half plane and a transmitted wave into the right hand half plane.

In general, each interface of the composite is illuminated by two sets of incoming waves one from the left with coefficients A_{pqr} and one from the right with coefficients W_{pqr}. Each interface scatters a reflected wave set with coefficients R_{pqr} and a transmitted wave set T_{pqr}. We assume here that all Floquet indices (p, q, r) are referenced with respect to the global unit cell or else $p = q = 0$ (if the interface is a local FSS). These may be ascribed a superfix or a prime to differentiate between sets from different interfaces, where appropriate. This is illustrated in figure 2-2 below.

The coefficients associated with interface n are related to those of interface $n + 1$ by the propagation factor, $\gamma_{pq}^{(n)}$, defined as in (1-7) by,

$$\gamma_{pq}^{(n)} = \sqrt{\epsilon_n \mu_n (k_0)^2 - (u_{pq})^2 - (v_{pq})^2} \qquad 2\text{-}1$$

where ϵ_n and μ_n are the relative permittivity and permeability of the medium between interfaces n and $n + 1$. If d is the layer thickness between these interfaces,

$$\begin{aligned} A_{pqr}^{(n+1)} &= \exp(-j\gamma_{pq}^{(n)} d) T_{pqr}^{(n)} \\ W_{pqr}^{(n)} &= \exp(-j\gamma_{pq}^{(n)} d) R_{pqr}^{(n+1)} \end{aligned} \qquad 2\text{-}2$$

It is important to note the sign in the exponent. As defined, any passive material has the real part of the exponent as non positive. For large values of d or large Floquet mode indices (p or q) it is generally not possible to invert these expressions because the exponent may be very large and negative such that $A_{pqr}^{(n+1)} \to 0$ or $W_{pqr}^{(n)} \to 0$. This has important consequences on the stability of any numerical method. In particular, a concatenation scheme must be used which does not contain the inverse expressions.

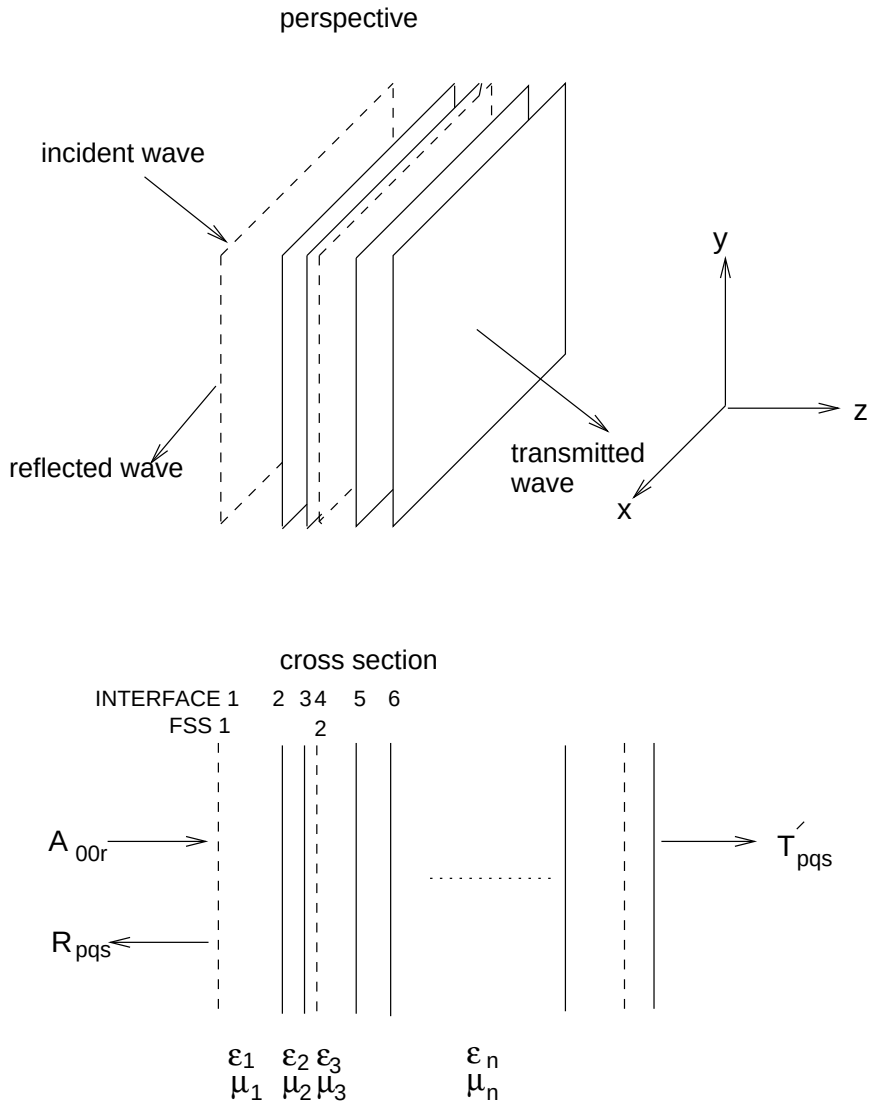

Figure 2-1: A general FSS composite

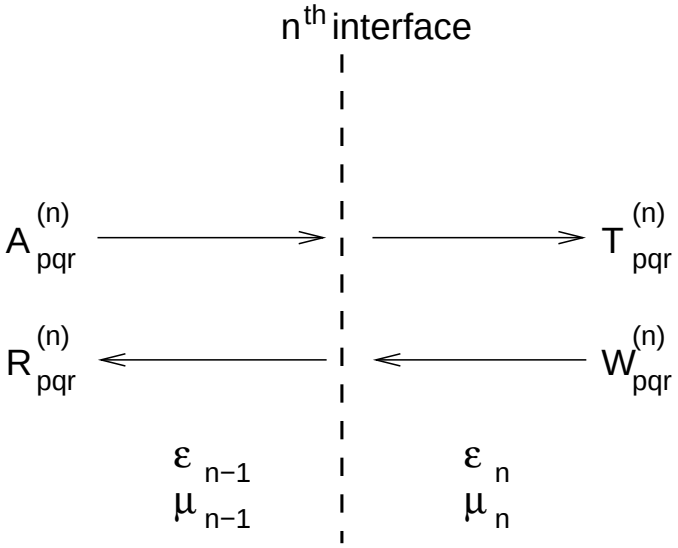

Figure 2-2: A single interface showing tangential wave coefficients

2.2 Matrix concatenation

A method, originally employed for FSS by Cwik and Mittra [5], can be constructed which does not involve the badly conditioned inverses described above and we have employed a similar method elsewhere [10]. The basic procedure involves successive contractions of the r^{th} and $(r+1)^{th}$ "canonical FSS structures". Each contraction generates a new structure of the same canonical form which, taken with the next part of the structure generates another one. The process continues until all the old sub-structures are amalgamated. To illustrate the process, we will employ the method described in [10] where a canonical structure corresponds to a single interface (FSS or non-FSS) together with the permittivity and permeability to left and right. This is not always efficient, as we describe in the next section, but is probably the simplest.

The concatenation is illustrated in figure 2-3 for a four interface structure. The coefficients A_{pqr}, R_{pqr}, T_{pqr} and W_{pqr} are grouped as the vectors $\underline{A}$, $\underline{R}$, $\underline{T}$ and $\underline{W}$, respectively, where the i_{th} vector element is associated with a unique tuple (p, q, r). The way in which the elements are ordered will be described later.

In general, there is a matrix relationship between coefficient vectors of a particular interface. Suppose we consider the first and second interface of an N-interface composite where $N \geq 2$. If $N = 1$ no concatenation is necessary. The matrix relations at the first and second interface may be written as,

$$\begin{pmatrix} \underline{T}_1 \\ \underline{R}_1 \end{pmatrix} = \begin{pmatrix} \mathbf{X}'_{11} & \mathbf{X}'_{12} \\ \mathbf{X}'_{21} & \mathbf{X}'_{22} \end{pmatrix} \begin{pmatrix} \underline{A}_1 \\ \underline{W}_1 \end{pmatrix} \qquad 2\text{-}3$$

and

$$\begin{pmatrix} \underline{T}_2 \\ \underline{R}_2 \end{pmatrix} = \begin{pmatrix} \mathbf{X}''_{11} & \mathbf{X}''_{12} \\ \mathbf{X}''_{21} & \mathbf{X}''_{22} \end{pmatrix} \begin{pmatrix} \underline{A}_2 \\ \underline{W}_2 \end{pmatrix} \qquad 2\text{-}4$$

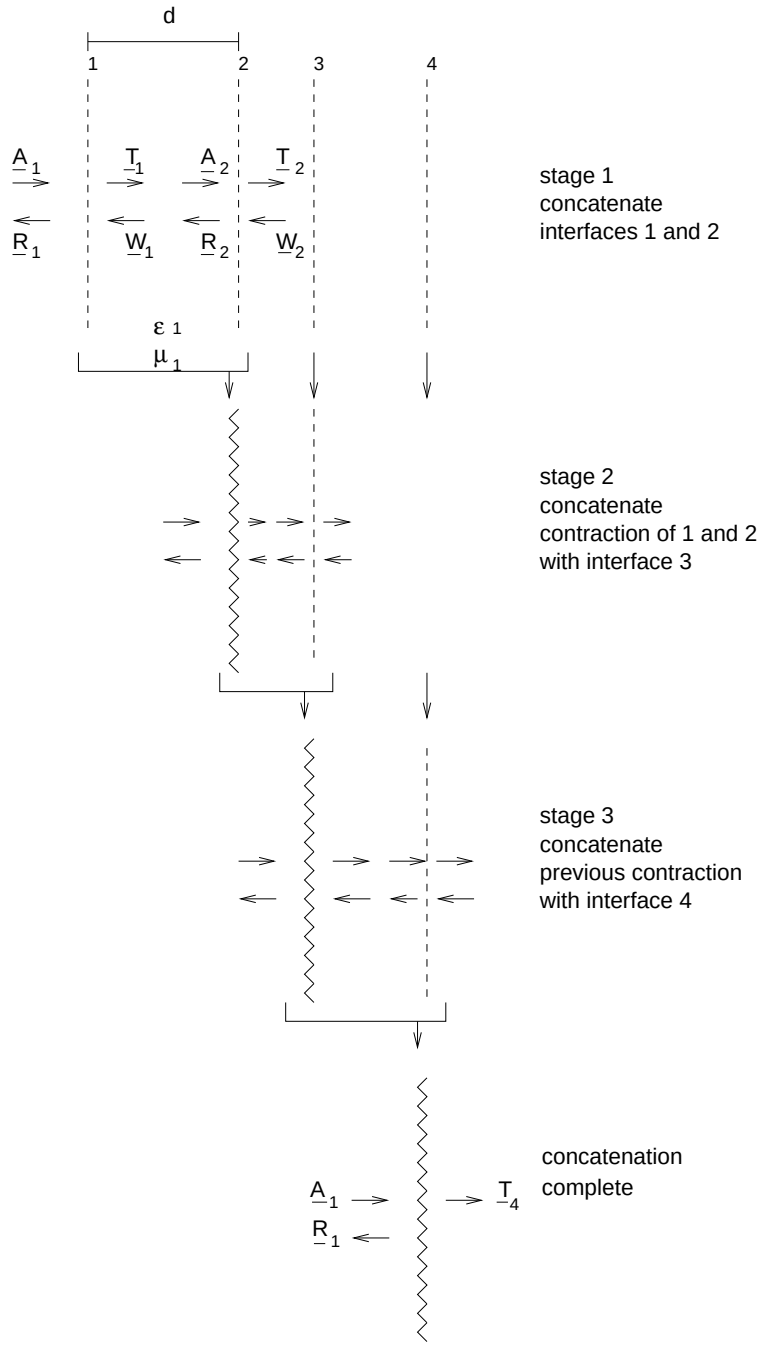

Figure 2-3: Interface concatenation in a multi-layer composite

In general, $\mathbf{X}'_{lm}$ and $\mathbf{X}''_{lm}$ $(l, m = 1, 2)$ are rectangular matrices, indexed by row and column numbers i and j. For an FSS, $\mathbf{X}'_{lm}$ and $\mathbf{X}''_{lm}$ are determined using the Floquet modal boundary element method described in section 3.3 and 3.4. For a non-FSS interface, they are zero except for the diagonal terms when the sets of indices $(p, q, r)_i = (p, q, r)_j$. These are described in section 2.5.

Note that even when $\mathbf{X}'_{lm}$ and $\mathbf{X}''_{lm}$ $(l, m = 1, 2)$ are square they do not generally possess an inverse. Equations (2-2) may be re-written in matrix form,

$$\begin{aligned} \underline{A}_2 &= \mathbf{H}\underline{T}_1 \\ \underline{W}_1 &= \mathbf{H}\underline{R}_2 \end{aligned} \qquad \text{2-5}$$

where $\mathbf{H}$ is the diagonal matrix whose i_{th} diagonal entry is determined by the indices $(p, q)_i$,

$$\mathbf{H} = diag_i \left(\exp(-j\{\gamma_{pq}\}_i^{(1)} d) \right) \qquad \text{2-6}$$

Remembering that the inverses to $\mathbf{H}$, $\mathbf{X}'_{lm}$ and $\mathbf{X}''_{lm}$ should not be evaluated (and may not exist), (2-6), (2-3) and (2-4) imply the contraction,

$$\begin{pmatrix} \underline{T}_2 \\ \underline{R}_1 \end{pmatrix} = \begin{pmatrix} \mathbf{Z}_{11} & \mathbf{Z}_{12} \\ \mathbf{Z}_{21} & \mathbf{Z}_{22} \end{pmatrix} \begin{pmatrix} \underline{A}_1 \\ \underline{W}_2 \end{pmatrix} \qquad \text{2-7}$$

where

$$\begin{aligned} \mathbf{Z}_{11} &= \mathbf{X}''_{11}\mathbf{H}(\mathbf{I}_p - \mathbf{L})^{-1}\mathbf{X}'_{11} && \text{2-8} \\ \mathbf{Z}_{12} &= \mathbf{X}''_{11}\mathbf{H}(\mathbf{I}_p - \mathbf{L})^{-1}\mathbf{X}'_{12}\mathbf{H}\mathbf{X}''_{22} + \mathbf{X}''_{12} && \text{2-9} \\ \mathbf{Z}_{21} &= \mathbf{X}'_{21} + \mathbf{X}'_{22}\mathbf{H}\mathbf{X}''_{21}\mathbf{H}(\mathbf{I}_p - \mathbf{L})^{-1}\mathbf{X}'_{11} && \text{2-10} \\ \mathbf{Z}_{22} &= \left[\mathbf{X}'_{22}\mathbf{H}\mathbf{X}''_{21}\mathbf{H}(\mathbf{I}_p - \mathbf{L})^{-1}\mathbf{X}'_{12} + \mathbf{X}'_{22}\right]\mathbf{H}\mathbf{X}''_{22} && \text{2-11} \end{aligned}$$

where $\mathbf{L}$ is the square, but not necessarily invertible matrix,

$$\mathbf{L} = \mathbf{X}'_{12}\mathbf{H}\mathbf{X}''_{21}\mathbf{H} \qquad \text{2-12}$$

and $\mathbf{I}_p$ is the *permutation* (permuted identity) matrix with unit entries only when $(p, q, r)_i = (p, q, r)_j$ on $\{\mathbf{L}\}_{ij}$, i.e. when the tuple $(p, q, r)_i$ on the i_{th} row of $\mathbf{X}'_{12}$ is the tuple $(p, q, r)_j$ on the j_{th} column of $\mathbf{X}''_{21}$.

$\mathbf{L}$ is square because, by construction, we assume the same Floquet modal index set for $\underline{T}_1$ and $\underline{A}_2$, even if some of the entries for $\underline{A}_2$ are zero.

Physically the contraction provides the outgoing wave sets from the substructure, formed from interfaces 1 and 2, given the incoming wave sets. The contraction process continues, bringing down the next interface to represent the terms $\mathbf{X}''_{lm}$ and,

$$\begin{aligned} \mathbf{X}'_{11} &\leftarrow \mathbf{Z}_{11} \\ \mathbf{X}'_{12} &\leftarrow \mathbf{Z}_{12} \\ \mathbf{X}'_{21} &\leftarrow \mathbf{Z}_{21} \\ \mathbf{X}'_{22} &\leftarrow \mathbf{Z}_{22} \end{aligned} \qquad \text{2-13}$$

until there are no interfaces remaining, whereupon the process terminates.

In the process described, the matrices $\mathbf{X}'_{lm}$ and $\mathbf{X}''_{lm}$ represent the relations between transmission and reflection to incident waves *for a single interface (FSS or non-FSS)*. As such, they are defined assuming a semi-infinite dielectric medium to left and right. Thus the n_{th} interface assumes a semi-infinite medium on its left defined by $\epsilon_{n-1}, \mu_{n-1}$ and a semi-infinite medium on its right defined by ϵ_n, μ_n. This is often not efficient, especially when there are several layers of dielectric between FSS.

2.3 Efficient canonical structures - a summary

The simplest canonical structure is the single interface, either an FSS or a non-FSS, together with the relative permittivity and permeability to left and right. By successively taking the r^{th} and the $(r+1)^{th}$ interface, as described above, the entire structure can be contracted one interface at a time. However, the process is inefficient if an interface is not an FSS. This is because if the distance between an FSS interface and a non-FSS interface is small a large number of (generally evanescent) coupling modes are required. This results in the construction and processing of very large matrices which is numerically intensive.

It is possible to assign an arbitrary number of non-FSS interfaces to a *single* FSS interface and determine the connection matrices $\mathbf{X}'_{lm}$ for the structure as a whole. In this case the canonical structure represents a single FSS together with an arbitrary number of non-FSS interfaces. However, the contraction process for such canonical structures is more complicated. Firstly, there is the manner in which two such structures should be attached and secondly there is the requirement to consider various special cases depending on whether the structure is first, last or in the middle of the composite. For example, on the first point, should we need a separating layer of dielectric between canonical groups? If we do, how do we decide how to choose this and what happens if such a layer is very thin (with the problems associated with the demonstration method above)? If we do not, then how do we decide on the number of coupling modes required?

In QDAS we will assume *two* possible formulations, which will be described as the *simple* and the *advanced* coupling scheme. The simple method is intended as a backup method if, for whatever reason, the advanced method should fail. Neither the simple nor the advanced method employs quite the formulation described earlier, though the simple method comes closest.

The *simple* coupling scheme employs a single FSS interface to construct the first $\mathbf{X}'_{lm}$ matrix and subsequent $\mathbf{X}''_{lm}$ matrices, as above. However, a non-FSS interface is not treated in the same manner except if it happens to be the first or last non-FSS which interfaces to the left-hand or right-hand half space. More generally, multiple layers of dielectric are separately joined to form a more general diagonal replacement for the diagonal matrix $\mathbf{H}$. However, the determination of coupling modes to left or right is still based on the thickness of the dielectric layers in immediate contact to the left or right. The coupling mode set between

the n_{th} and $(n+1)_{th}$ FSS is taken as the smallest superset of coupling modes just to the right of the n_{th} FSS (required to couple this interface to the next interface) and just to the left of the $(n+1)_{th}$ FSS (required to couple this interface to the previous interface). The method is described in full detail in section 2.5 and 2.6.

The *advanced* coupling scheme is rather different and more complex. This does away with the junction matrix $\mathbf{H}$ in the cascade process described above. Instead, the canonical structure is no longer an interface but an FSS contained within the region of multiple dielectric layers bounded (in general) between the previous FSS and the next FSS. The two exceptional cases are where the boundary interface is a non-FSS boundary to the left or right hand half spaces. This requires a special treatment of "closed" modes which are required at a given FSS but are not observed by the previous FSS on the left or the next FSS on the right. The method is described in section 2.7.

Before either method is described, it is necessary to determine a contraction for an arbitrary stack of non-FSS interfaces. The method is similar to that described in section 2, except that the matrices are diagonal and may be computed without the use of a finite element approximation. This is described below.

2.4 Non-FSS contraction

Suppose that within the composite there is contained a region of L contiguous non-FSS interfaces separated by uniform regions of dielectric or magnetic material. We will permit a non-FSS interface to contain a uniform thin resistive sheet. This may be anisotropic, but for our purposes we will assume isotropy such that the l_{th} interface is specified by the scalar conductivity parameter σ_l in mhos. The absence of a resistive card is equivalent to setting $\sigma_l = 0$. We will assume there are a total of L contiguous non-FSS interfaces such that $L > 1$.

Figure 2-4 illustrates such a region. Because there is no cross-coupling of modes between Floquet modes of different index, we will write the scalar A_l as the $\{p,q,r\}_{th}$ mode coefficient A_{pqr} associated with the l_{th} interface. Similarly for the mode coefficients R_l, T_l and W_l. Note that the dielectric interfaces are renumbered for this part of the analysis such that the first interface of the block is labeled by 1. Note also the index convention on the material properties as illustrated.

The electric current density $\underline{J}(\underline{x})$ on a conductive interface is related to the total tangential electric field $\underline{E}^{(t)}(\underline{x})$ by ohms law. On a non-FSS interface, the $\underline{x}$ dependence can be factored out since all tangential electric and magnetic fields and currents have a spatial dependence proportional to the scalar, $\phi_{pqr}(\underline{x})$. Let J_l be the scalar current coefficient associated with the $\{p,q,r\}_{th}$ mode at the l_{th} interface. Similarly, let E_l be the tangential electric field coefficient associated with the $\{p,q,r\}_{th}$ mode at the l_{th} interface.

Because the tangential electric field is continuous across any interface in the composite,

$$E_l = A_l + R_l = T_l + W_l \qquad 2\text{-}14$$

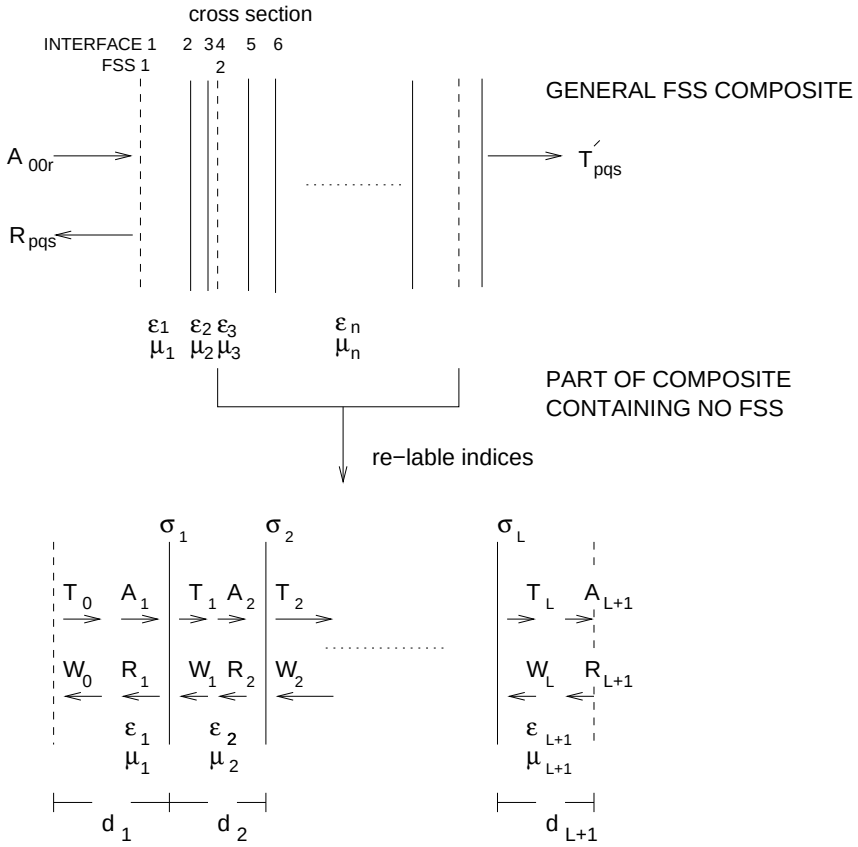

Figure 2-4: A part of the composite containing no FSS

and Ohm's law is represented as,

$$J_l = \sigma_l E_l \qquad 2\text{-}15$$

Let the characteristic admittance to the left of the l_{th} interface be designated by $\xi_l \equiv \xi_{pqr}^{(l)}$, as defined in (1-25). Similarly, let the modal admittance to the left of the l_{th} interface be designated by $\gamma_l \equiv \gamma_{pq}^{(l)}$ as defined in (1-26) with $\epsilon_l \equiv \epsilon_r^{(l)}$ and $\mu_l \equiv \mu_r^{(l)}$. The difference in tangential magnetic field is proportional to the electric current such that,

$$\xi_l(A_l - R_l) - \xi_{l+1}(T_l - W_l) = J_l \qquad 2\text{-}16$$

If d_{l+1} is the distance between the l_{th} and $(l+1)_{th}$ (for $1 \le l \le L$) interface then,

$$\begin{aligned} A_{l+1} &= \exp(-j\gamma_{l+1}d_{l+1})T_l \\ W_l &= \exp(-j\gamma_{l+1}d_{l+1})R_{l+1} \\ &\quad \text{for } 1 \le l \le L \end{aligned} \qquad 2\text{-}17$$

We may thus write,

$$\begin{pmatrix} A_{l+1} \\ R_l \end{pmatrix} = \mathcal{Z}_l^{(A)} \begin{pmatrix} A_l \\ R_{l+1} \end{pmatrix} \text{ for } 1 \le l \le L \qquad 2\text{-}18$$

where the matrix $\mathcal{Z}_l^{(A)}$,

$$\mathcal{Z}_l^{(A)} \equiv \begin{pmatrix} Z_{11}^{(Al)} & Z_{12}^{(Al)} \\ Z_{21}^{(Al)} & Z_{22}^{(Al)} \end{pmatrix} \qquad 2\text{-}19$$

is defined, using (2-14) to (2-17), by

$$\mathcal{Z}_l^{(A)} = \frac{1}{\xi_l + \xi_{l+1} + \sigma_l} \begin{pmatrix} 2\xi_l \exp(-j\gamma_{l+1}d_{l+1}) & -(\xi_l - \xi_{l+1} + \sigma_l)\exp(-2j\gamma_{l+1}d_{l+1}) \\ (\xi_l - \xi_{l+1} - \sigma_l) & 2\xi_{l+1}\exp(-j\gamma_{l+1}d_{l+1}) \end{pmatrix} \qquad 2\text{-}20$$

Note that $\mathcal{Z}_l^{(A)}$ relates outgoing to incoming fields just to the left of the $(l+1)_{th}$ interface and just to the left of the l_{th} interface. The superfix "(A)" is employed to show that this differs from the expression in (2-7).

The concatenation process begins by constructing $\mathcal{Z}_l^{(A)}$ for $l = 1$ and $l = 2$ with elements designated, respectively, by $Z_{ij}^{(A1)}$ $(i,j = 1,2)$ and $Z_{ij}^{(A2)}$ $(i,j = 1,2)$. We then determine $\mathcal{Z}_{1,2}^{(A)}$ with elements $Z_{ij}^{(A1,2)}$ defined by,

$$\begin{pmatrix} A_3 \\ R_1 \end{pmatrix} = \mathcal{Z}_{1,2}^{(A)} \begin{pmatrix} A_1 \\ R_3 \end{pmatrix} \qquad 2\text{-}21$$

such that,

$$\mathcal{Z}_{1,2}^{(A)} = \frac{1}{1 - Z_{12}^{(A1)}Z_{21}^{(A2)}} \begin{pmatrix} Z_{11}^{(A1)}Z_{11}^{(A2)} & Z_{12}^{(A2)} + Z_{12}^{(A1)}\det \mathcal{Z}_2^{(A)} \\ Z_{21}^{(A1)} + Z_{21}^{(A2)}\det \mathcal{Z}_1^{(A)} & Z_{22}^{(A1)}Z_{22}^{(A2)} \end{pmatrix} \qquad 2\text{-}22$$

The concatenation continues by making the substitution,

$$\begin{aligned} \mathcal{Z}_1^{(A)} &\leftarrow \mathcal{Z}_{1,2}^{(A)} \quad \text{with elements} \quad Z_{ij}^{(A1)} \leftarrow Z_{ij}^{(A1,2)} \\ \mathcal{Z}_2^{(A)} &\leftarrow \mathcal{Z}_3^{(A)} \quad \text{with elements} \quad Z_{ij}^{(A2)} \leftarrow Z_{ij}^{(A3)} \end{aligned} \tag{2-23}$$

in (2-22), for which $\mathcal{Z}_{1,2}^{(A)} \rightarrow \mathcal{Z}_{1,3}^{(A)}$. If $L > 3$ there are a further $L-3$ substitutions,

$$\begin{aligned} \mathcal{Z}_1^{(A)} &\leftarrow \mathcal{Z}_{1,l}^{(A)} \\ \mathcal{Z}_2^{(A)} &\leftarrow \mathcal{Z}_{l+1}^{(A)} \quad \text{for } l = 3, 4, ...L-1 \end{aligned} \tag{2-24}$$

until we are left with the expression for $\mathcal{Z}_{1,L}^{(A)}$ such that,

$$\begin{pmatrix} A_{L+1} \\ R_1 \end{pmatrix} = \mathcal{Z}_{1,L}^{(A)} \begin{pmatrix} A_1 \\ R_{L+1} \end{pmatrix} \tag{2-25}$$

We believe the concatenation is well conditioned provided the physics does not permit trapped waves. In a loss-less system, trapped waves can occur if more than one interface is perfectly conducting or a dielectric layer is impermeable (i.e. if $\epsilon_l \rightarrow \infty$ or $\mu_l \rightarrow \infty$). These are necessary but not sufficient conditions. For example, ill-conditioning is expected if interfaces 1 and 2 are almost perfectly conducting and if $d_1 = 0, \lambda/2, \lambda, ...$ where λ is the wavelength in the material defined by ϵ_2, μ_2.

Finally, we construct the matrix $\mathcal{Z}_{1,L}^{(B)}$ which relates the coefficients T_0, W_0, at a distance d_1 to the left of the first interface, to A_{L+1} and R_{L+1} such that,

$$\begin{pmatrix} A_{L+1} \\ W_0 \end{pmatrix} = \mathcal{Z}_{1,L}^{(B)} \begin{pmatrix} T_0 \\ R_{L+1} \end{pmatrix} \tag{2-26}$$

If the elements of $\mathcal{Z}_{1,L}^{(A)}$ are $Z_{ij}^{(A1,L)}$ for $i, j = 1, 2$, then

$$\mathcal{Z}_{1,L}^{(B)} \equiv \begin{pmatrix} Z_{11}^{(B1,L)} & Z_{12}^{(B1,L)} \\ Z_{21}^{(B1,L)} & Z_{22}^{(B1,L)} \end{pmatrix} = \begin{pmatrix} Z_{11}^{(A1,L)} \exp(-j\gamma_1 d_1) & Z_{12}^{(A1,L)} \\ Z_{21}^{(A1,L)} \exp(-2j\gamma_1 d_1) & Z_{22}^{(A1,L)} \exp(-j\gamma_1 d_1) \end{pmatrix} \tag{2-27}$$

2.5 The simple coupling scheme

In the QDAS *simple* coupling scheme, a non-FSS contraction is employed as above whenever possible. This leads to a requirement to consider two special and one generic coupling between FSS within a general composite. The generic case is the coupling between two successive FSS, as illustrated in figure 2-5. Special cases need to be considered if the first or last interface (the bounding surfaces of the composite) are not FSS. One case is the coupling between the first (non-FSS) dielectric interface and the first FSS. The second case is the coupling between the last (non-FSS) dielectric interface and the last FSS. A degenerate case occurs when both special cases apply to the same FSS, i.e. if there is one and only one FSS bounded on both sides by at least one layer of dielectric. These cases are illustrated in figure 2-6.

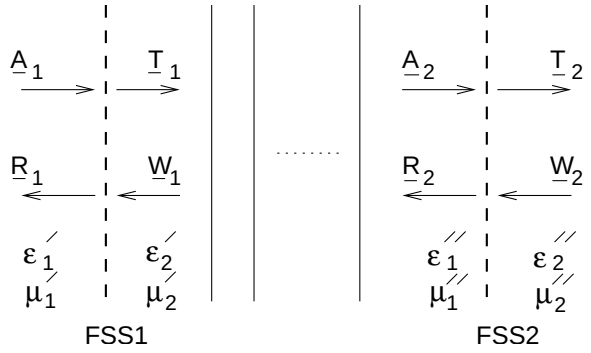

Figure 2-5: Generic coupling between two FSS in the simple coupling scheme

Let us consider the generic case first, with any two contiguous FSS labeled in figure 2-5 by "FSS1" and "FSS2". To avoid unnecessary notational complexity, we will suffix the field coefficients by the integers 1 and 2. The permittivity and permeability immediately to the left and right of FSS1 are designated by ϵ'_1, μ'_1 and ϵ'_2, μ'_2 respectively. To the left and right of FSS2 they are designated by ϵ''_1, μ''_1 respectively.

As in (2-3) and (2-4), we assume a known matrix form relating $\underline{T}_1$ and $\underline{R}_1$ to $\underline{A}_1$ and $\underline{W}_1$ and relating $\underline{T}_2$ and $\underline{R}_2$ to $\underline{A}_2$ and $\underline{W}_2$,

$$\begin{pmatrix} \underline{T}_1 \\ \underline{R}_1 \end{pmatrix} = \begin{pmatrix} \mathbf{X}'_{11} & \mathbf{X}'_{12} \\ \mathbf{X}'_{21} & \mathbf{X}'_{22} \end{pmatrix} \begin{pmatrix} \underline{A}_1 \\ \underline{W}_1 \end{pmatrix} \qquad 2\text{-}28$$

and

$$\begin{pmatrix} \underline{T}_2 \\ \underline{R}_2 \end{pmatrix} = \begin{pmatrix} \mathbf{X}''_{11} & \mathbf{X}''_{12} \\ \mathbf{X}''_{21} & \mathbf{X}''_{22} \end{pmatrix} \begin{pmatrix} \underline{A}_2 \\ \underline{W}_2 \end{pmatrix} \qquad 2\text{-}29$$

where $\mathbf{X}'_{lm}$ and $\mathbf{X}''_{lm}$ $(l, m = 1, 2)$ are rectangular matrices, indexed by row and column numbers i and j. The finite element calculation of these matrices is described later in section 3.

Suppose that the dielectric structure between FSS1 and FSS2 is represented by the connection matrix $\mathcal{Z}_{1,L}^{(B)}$, defined by (2-27). This is a 2×2 matrix for each mode $\{p, q, r\}$. The vectors $\underline{A}_2$, $\underline{W}_1$, $\underline{T}_1$ and $\underline{R}_2$ are each indexed by a unique mode number $\{p, q, r\}$. In our simple coupling scheme we will assume *either* that FSS1 and FSS2 are referenced with respect to the same global unit cell, *or* that the only permitted coupling modes are given by $p = q = 0$.[4] The mode set $\{p, q, r\}$ is therefore common to all four vectors.

The coupling of $\underline{A}_2$ to $\underline{T}_1$, $\underline{A}_2$ to $\underline{R}_2$, $\underline{W}_1$ to $\underline{T}_1$ and $\underline{W}_1$ to $\underline{R}_2$ may thus be represented by a rectangular or square matrix, with at most one non-zero entry in each row or column corresponding to the entry where both vectors share the same value of $\{p, q, r\}$. This is a *permuted diagonal* matrix which, if rectangular, includes rows or columns of zeros. Formally, let δ_{ij} be the Kronecka-delta symbol, defined as 1 if $i = j$ and 0 otherwise. Let the vectors $\underline{V}_1$ and $\underline{V}_2$ have entries $\{V_1\}_{p_1 q_1 r_1}$ and $\{V_2\}_{p_2 q_2 r_2}$. If they couple as above then,

$$\{V_1\}_{p_1 q_1 r_1} = Z_{p_2 q_2 r_2} \{V_2\}_{p_2 q_2 r_2} \delta_{p_1 p_2} \delta_{q_1 q_2} \delta_{r_1 r_2} \qquad 2\text{-}30$$

and the associated (generally rectangular) permuted diagonal matrix $pdiag(Z)$ may be written as,

$$\underline{V}_1 = pdiag(Z) \underline{V}_2 \qquad 2\text{-}31$$

in vector/matrix notation.

We may then write,

$$\begin{aligned} \mathbf{Z}_{11}^{(B)} &= pdiag(Z_{11}^{(B1,L)}) \\ \mathbf{Z}_{12}^{(B)} &= pdiag(Z_{12}^{(B1,L)}) \\ \mathbf{Z}_{21}^{(B)} &= pdiag(Z_{21}^{(B1,L)}) \\ \mathbf{Z}_{22}^{(B)} &= pdiag(Z_{22}^{(B1,L)}) \end{aligned} \qquad 2\text{-}32$$

so that,

$$\begin{pmatrix} \underline{A}_2 \\ \underline{W}_1 \end{pmatrix} = \begin{pmatrix} \mathbf{Z}_{11}^{(B)} & \mathbf{Z}_{12}^{(B)} \\ \mathbf{Z}_{21}^{(B)} & \mathbf{Z}_{22}^{(B)} \end{pmatrix} \begin{pmatrix} \underline{T}_1 \\ \underline{R}_2 \end{pmatrix} \qquad 2\text{-}33$$

Just as in section 2.2, it is important to note that even when the matrices $\mathbf{X}'_{ij}$, $\mathbf{X}''_{ij}$ and $\mathbf{Z}_{ij}^{(B)}$ are square, they may be badly conditioned and their inverses may not exist. This fact drives the formulation adopted below.

First, we will define the square *permutation* matrix $\mathbf{I}_p$ as in section 2.2, but applied in a slightly more general context. This matrix has one and only one non-zero element in each row and column, with value unity. If the row number is indexed by the Floquet modal indices $\{p_1 q_1 r_1\}$ and the column number by the indices $\{p_2 q_2 r_2\}$ then the entry to $\mathbf{I}_p$ is unity if and only if $p_1 = p_2$, $q_1 = q_2$ and $r_1 = r_2$. Thus, depending on context, $\mathbf{I}_p$ may be of arbitrary

[4] In the *advanced* coupling scheme, described in section 2.7, this is generalised slightly in that $(\underline{T}_1, \underline{W}_1)$ is permitted a different mode set to $(\underline{A}_2, \underline{R}_2)$ provided coupling from $\underline{T}_1$ to $\underline{A}_2$ and $\underline{W}_1$ to $\underline{R}_2$ is only through the $p = q = 0$ mode.

rank and permuted arbitrarily. However, context guarantees uniqueness. For example, if the square matrix $\mathbf{M}$ relates the vectors $\underline{A}_1$ and $\underline{W}_1$ by,

$$\underline{A}_1 = \mathbf{M}\underline{W}_1 \tag{2-34}$$

then the operation $\mathbf{I}_p + \mathbf{M}$ is defined by,

$$\underline{A}_1 = (\mathbf{I}_p + \mathbf{M})\underline{W}_1 \tag{2-35}$$

i.e. the rows of $\mathbf{I}_p$ are indexed as $\underline{W}_1$ and the columns as $\underline{A}_1$.

With these definitions, it is possible to re-arrange (2-28), (2-29) and (2-33) as follows. Let,

$$\mathbf{L}_1 = \mathbf{Z}_{11}^{(B)}\mathbf{X}'_{12}(\mathbf{I}_p - \mathbf{Z}_{21}^{(B)}\mathbf{X}'_{12})^{-1} \tag{2-36}$$

and

$$\mathbf{L}_2 = \mathbf{Z}_{22}^{(B)}\mathbf{X}''_{21}(\mathbf{I}_p - \mathbf{Z}_{12}^{(B)}\mathbf{X}''_{21})^{-1} \tag{2-37}$$

where $(\mathbf{M})^{-1}$ refers to the inverse of an arbitrary well conditioned square matrix $\mathbf{M}$. Also let,

$$\mathbf{M}_1 = \mathbf{X}''_{11}(\mathbf{I}_p - [\mathbf{L}_1\mathbf{Z}_{22}^{(B)} + \mathbf{Z}_{12}^{(B)}]\mathbf{X}''_{21})^{-1} \tag{2-38}$$

and

$$\mathbf{M}_2 = \mathbf{X}'_{22}(\mathbf{I}_p - [\mathbf{L}_2\mathbf{Z}_{11}^{(B)} + \mathbf{Z}_{21}^{(B)}]\mathbf{X}'_{12})^{-1} \tag{2-39}$$

Let us now define the matrices $\mathbf{W}_{ij}$ by,

$$\begin{pmatrix} \underline{T}_2 \\ \underline{R}_1 \end{pmatrix} = \begin{pmatrix} \mathbf{W}_{11} & \mathbf{W}_{12} \\ \mathbf{W}_{21} & \mathbf{W}_{22} \end{pmatrix} \begin{pmatrix} \underline{A}_1 \\ \underline{W}_2 \end{pmatrix} \tag{2-40}$$

It may then be shown that,

$$\begin{aligned} \mathbf{W}_{11} &= \mathbf{M}_1(\mathbf{Z}_{11}^{(B)} + \mathbf{L}_1\mathbf{Z}_{21}^{(B)})\mathbf{X}'_{11} \\ \mathbf{W}_{12} &= \mathbf{X}''_{12} + \mathbf{M}_1(\mathbf{Z}_{12}^{(B)} + \mathbf{L}_1\mathbf{Z}_{22}^{(B)})\mathbf{X}''_{22} \\ \mathbf{W}_{21} &= \mathbf{X}'_{21} + \mathbf{M}_2(\mathbf{Z}_{21}^{(B)} + \mathbf{L}_2\mathbf{Z}_{11}^{(B)})\mathbf{X}'_{11} \\ \mathbf{W}_{22} &= \mathbf{M}_2(\mathbf{Z}_{22}^{(B)} + \mathbf{L}_2\mathbf{Z}_{12}^{(B)})\mathbf{X}''_{22} \end{aligned} \tag{2-41}$$

Concatenation of successive FSS proceeds, as demonstrated in section 2.2, by using the same formulae with the substitutions in (2-36) to (2-40),

$$\begin{aligned} \mathbf{X}'_{11} &\leftarrow \mathbf{W}_{11} \\ \mathbf{X}'_{12} &\leftarrow \mathbf{W}_{12} \\ \mathbf{X}'_{21} &\leftarrow \mathbf{W}_{21} \\ \mathbf{X}'_{22} &\leftarrow \mathbf{W}_{22} \end{aligned} \tag{2-42}$$

and

$$\begin{aligned} \mathbf{X}''_{11} &\leftarrow \mathbf{X}'''_{11} \\ \mathbf{X}''_{12} &\leftarrow \mathbf{X}'''_{12} \\ \mathbf{X}''_{21} &\leftarrow \mathbf{X}'''_{21} \\ \mathbf{X}''_{22} &\leftarrow \mathbf{X}'''_{22} \end{aligned} \qquad 2\text{-}43$$

where the triple-primed quantities relate field coefficients on the next FSS, e.g. on the third FSS,

$$\begin{pmatrix} \underline{T}_3 \\ \underline{R}_3 \end{pmatrix} = \begin{pmatrix} \mathbf{X}'''_{11} & \mathbf{X}'''_{12} \\ \mathbf{X}'''_{21} & \mathbf{X}'''_{22} \end{pmatrix} \begin{pmatrix} \underline{A}_3 \\ \underline{W}_3 \end{pmatrix} \qquad 2\text{-}44$$

The process continues until the N^{th} FSS is concatenated under the substitution

$$\begin{aligned} \mathbf{X}''_{11} &\leftarrow \mathbf{X}_{11}^{(N)\prime} \\ \mathbf{X}''_{12} &\leftarrow \mathbf{X}_{12}^{(N)\prime} \\ \mathbf{X}''_{21} &\leftarrow \mathbf{X}_{21}^{(N)\prime} \\ \mathbf{X}''_{22} &\leftarrow \mathbf{X}_{22}^{(N)\prime} \end{aligned} \qquad 2\text{-}45$$

where,

$$\begin{pmatrix} \underline{T}_N \\ \underline{R}_N \end{pmatrix} = \begin{pmatrix} \mathbf{X}_{11}^{(N)\prime} & \mathbf{X}_{12}^{(N)\prime} \\ \mathbf{X}_{21}^{(N)\prime} & \mathbf{X}_{22}^{(N)\prime} \end{pmatrix} \begin{pmatrix} \underline{A}_N \\ \underline{W}_N \end{pmatrix} \qquad 2\text{-}46$$

This will coincide with a full concatenation of all interfaces in the composite only if the last interface in the composite is an FSS and the first interface of the composite is an FSS. To analyse a general composite we need to account for the special (but important) cases where the first or last interface in the composite is not an FSS. These cases are illustrated in figure 2-6.

The simplest method to analyse these special cases, appropriate in our simple coupling scheme, is to consider the first or last non-FSS interface as a special FSS. Thus, if the first interface is not an FSS, we consider this as FSS1 with the matrices $\mathbf{X}'_{11}$, $\mathbf{X}'_{12}$, $\mathbf{X}'_{21}$ and $\mathbf{X}'_{22}$ taking special forms. Similarly for the last FSS, where $\mathbf{X}_{11}^{(N)\prime}$, $\mathbf{X}_{12}^{(N)\prime}$, $\mathbf{X}_{21}^{(N)\prime}$ and $\mathbf{X}_{22}^{(N)\prime}$ take special forms. In both cases, suppose that the permittivity and permeability to left and right of the "special FSS" are μ_1, ϵ_1 and μ_2, ϵ_2, respectively. We will drop the prime superfix notation, since the same result will apply to both first or last FSS. To each mode $\{p, q, r\}$ defined on the global unit cell, or $p = q = 0$ if the first true FSS is defined as "local", it is straight forward to show that,

$$\mathbf{X}_{11} = pdiag\left(\frac{2\xi_{pqr}^{(1)}}{\xi_{pqr}^{(1)} + \xi_{pqr}^{(2)} + \sigma_s}\right) \qquad 2\text{-}47$$

$$\mathbf{X}_{12} = pdiag\left(\frac{\xi_{pqr}^{(2)} - \xi_{pqr}^{(1)} - \sigma_s}{\xi_{pqr}^{(1)} + \xi_{pqr}^{(2)} + \sigma_s}\right) \qquad 2\text{-}48$$

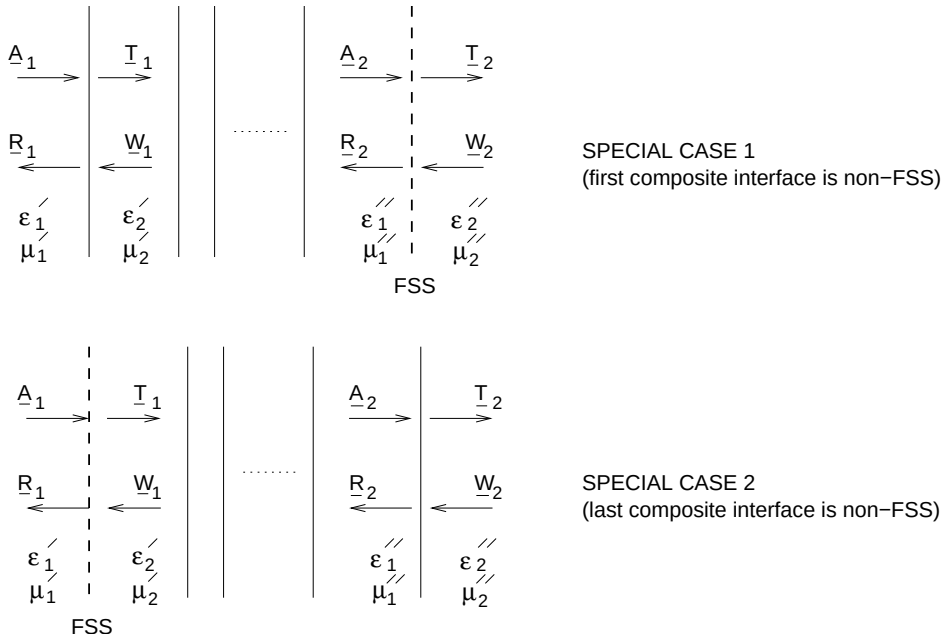

Figure 2-6: Coupling between an FSS and the first or last non-FSS interface in the composite

$$\mathbf{X}_{21} = pdiag\left(\frac{\xi_{pqr}^{(1)} - \xi_{pqr}^{(2)} - \sigma_s}{\xi_{pqr}^{(1)} + \xi_{pqr}^{(2)} + \sigma_s}\right) \qquad 2\text{-}49$$

$$\mathbf{X}_{22} = pdiag\left(\frac{2\xi_{pqr}^{(2)}}{\xi_{pqr}^{(1)} + \xi_{pqr}^{(2)} + \sigma_s}\right) \qquad 2\text{-}50$$

where σ_s is the surface conductivity at the interface and $\xi_{pqr}^{(1)}$ and $\xi_{pqr}^{(2)}$ refer to the modal admittances to the left and right of the interface, respectively, as defined in (1-25).

Note that, unlike the *advanced* coupling scheme described in section 2.7, if the first (or last) FSS is defined as "local" (i.e. the FSS is not considered to share the global unit cell of the composite) it is assumed that coupling to the first (or last) non-FSS interface is only through the principal $p = q = 0$ mode. This constraint is necessary in the above scheme since if the first or last composite interface is not an FSS it is still treated as an FSS within the mechanics of the algorithm. As discussed in section 1.4, non-principal couplings are not permitted between two FSS which do not share a common global unit cell.

2.6 Determination of coupling modes in the simple coupling scheme

The coupling scheme described above does not specify which $\{p, q, r\}$ elements are required in the definition of the field coefficient vectors $\underline{A}$, $\underline{R}$, $\underline{T}$ and $\underline{W}$. There is no single optimal method known to perform this task. The issue is one of compromising between algorithm complexity, computational resources and predictive accuracy. Ideally, a complete mode set

using the same mode set applied in the finite element analysis, defined by the modal limits P and Q could be used. However, the number of such coupling modes would require the computation and manipulation of very large matrices which would be impractical on existing computers. This number should be significantly reduced.

In the limit where two FSS are separated by a large distance, the only significant coupling modes are the principal ($p = q = 0$) modes and any grating modes which may exist. All other modes decay exponentially with distance from the two FSS, and can be ignored. In the limit where two FSS are almost co-located, all modes must *a-priori* be assumed to couple and the full set defined by P and Q should be used, consistent with the approximations made for each FSS individually. In practise, most applications require FSS separated by distances between these two limits.

We adopt the use of a decay factor s_n, set by the user prior to analysis for the n_{th} FSS, defined such that $0 < s_n < 1$. Let $\gamma_{pq}^{(n-1)}$ be the admittance to the left of the FSS and $\gamma_{pq}^{(n)}$ be the admittance to the right. Let d_{n-1} be the distance to the next interface (FSS or non-FSS) on the left and d_n be the distance to the next interface (FSS or non-FSS) on the right. In the simple coupling scheme, we assume that each FSS has a *left mode set* and a *right mode set* of accounted modes. These are the modes to left or right which are not assumed negligible. The coupling mode set between the n_{th} and $(n+1)_{th}$ FSS is generally taken to be the superset of the right mode set of the n_{th} FSS and the left mode set of the $(n+1)_{th}$ FSS. The exception is where an FSS is defined as "local" in which case the coupling mode set between the n_{th} and $(n+1)_{th}$ FSS and between the n_{th} and $(n-1)_{th}$ FSS are assumed to contain only the modes $(p = q = 0, r = 1)$ and $(p = q = 0, r = 2)$.

A mode in the left mode set is assumed present only if,

$$|\exp(-j\gamma_{pq}^{(n-1)} d_{n-1})| > s_n \qquad 2\text{-}51$$

Similarly, a mode in the right mode set is assumed present only if,

$$|\exp(-j\gamma_{pq}^{(n)} d_n)| > s_n \qquad 2\text{-}52$$

This assumes required couplings are based on the distance to the nearest interface, *whether this is an FSS or not*, and is a principal source of inefficiency in the simple scheme. However, this is unavoidable using the analysis described in the previous section because the coefficients $A_{pqr}^{(n)}$ and $R_{pqr}^{(n)}$, associated with the n_{th} FSS, will generally couple through a reflection at the previous interface even if this interface is not an FSS. The same is true of the coefficients $T_{pqr}^{(n)}$ and $W_{pqr}^{(n)}$ through a reflection at the next interface.

Some experimentation of s_n is generally necessary to check for convergence, but typically we have found a value $s_n \approx 0.1$ is good. If s_n is made too small, a large number of coupling modes are calculated involving significant increase in computation time with an insignificant improvement in accuracy. If s_n is too large, computer time can be significantly reduced but accuracy may suffer. We should emphasize that the pruning criterion is neither unique nor maximally efficient, though it has been found to work quite effectively in practice.

2.7 The advanced coupling scheme

In the simple coupling scheme of the previous sections, the basic canonical structure is an FSS interface together with a definition of the material just to its left and right. Concatenation takes place between these canonical structures and only the definition of the connection matrices $\mathbf{X}_{ij}^{(n)\prime}$ changes depending on the type of FSS. As mentioned above, an important source of inefficiency in the simple coupling scheme is the requirement to base the number of required Floquet coupling modes on the distance between an FSS and the nearest interface, even if this interface is a non FSS. This is because of the modal reflection that occurs at such an interface, even if such a mode does not propagate to the next FSS. In practice this means that if there is a thin layer of dielectric to one side of an FSS, significant coupling is required to take into account the mutual interactions, even if the nearest neighbour FSS is far off as illustrated in figure 2-7. This can result in considerable computation time and memory requirement, due solely to the choice of the basic canonical structure.

A more general canonical structure may be generated which associates an arbitrary number of dielectric layers to the left and right of a given FSS, together with a definition of the material properties to the left of the left-most dielectric interface and to the right of the right-most interface, as illustrated in figure 2-8. This is sometimes referred to as a "sandwich" structure and has been adopted elsewhere; a restricted version, consisting of a single interface to left and right, has been employed by the author in MANEAC (Multiple Array Numerical Electromagnetic Analysis Code; a rather outdated UK classified FSS analysis program). The problem is that such canonical structures must still be separated by a dielectric gap in order for concatenation to proceed along the previous lines. This requires a propagation threshold to be set on the separation layer and this can still result in inefficiency. For example, if a large number of very thin dielectric layers separate one FSS from another it would not be possible to choose the separation layer to be large enough to apply sufficient pruning to the coupling modes. Furthermore, such an approach makes a logical distinction between the separation layer and the layers of the "sandwich" which is not physical. Either the user must signify the distinction, or a level of pre-processing is required to choose the optimal separation layer.

Although the sandwich structure is an improvement on the single FSS interface, we decided to consider a formulation which was numerically efficient with any possible dielectric layering. The important point is to recognise that wave components reflected back from an FSS to itself by multiple layers of dielectric should be treated in a different manner to those which reach the next FSS. These two classes of modes will be referred to as *closed* and *open*. Both closed and open modes can be evanescent. Any given mode must be in either one or the other class or not present at all; i.e. it is not possible for a coupling mode to be both closed and open. In this approach, we may do away with the concept of a separation layer. The concept is illustrated in figure 2-9, where a "black box" terminates the closed modes. The "black box" is represented by interactions within the canonical structure that are not observed outside it; closed modes do not escape or interact outside of the structure. Interestingly, as

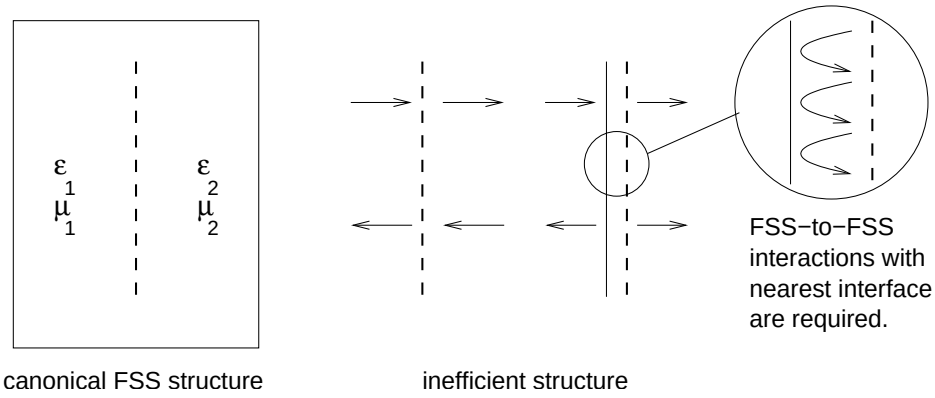

Figure 2-7: Inefficiencies in the simple FSS canonical structure

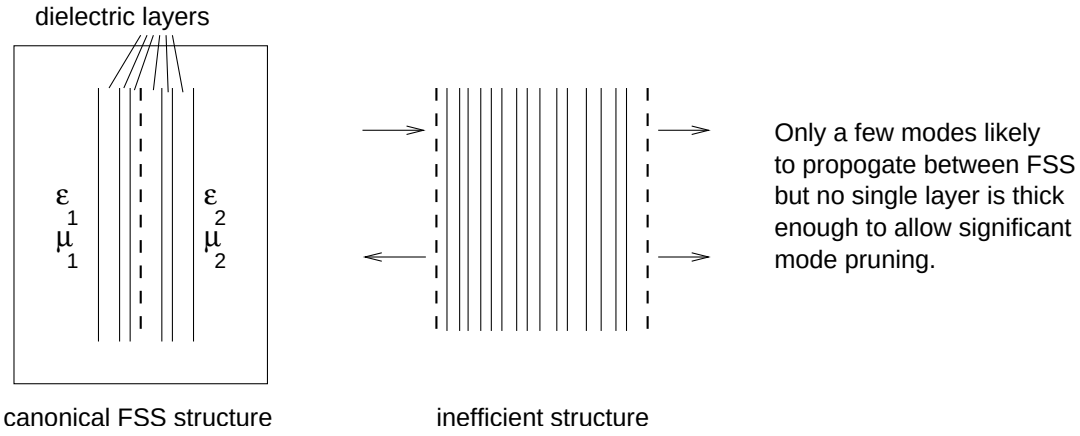

Figure 2-8: Inefficiencies in a “sandwich” canonical structure

we will show in sections 3.3 and 3.4, the formulation of an FSS as a slotted or an element structure requires a different accounting of the closed modes.

Just as for the simple coupling scheme, we need to consider four cases in order to allow analysis of a general structure by concatenation. Case 1 is where a given FSS is not bounded on either side by another FSS. Case 2 is where a given FSS has no FSS to its right. Case 3 is where a given FSS has no FSS to its left. Case 4 is where the given FSS has an FSS to both its left and its right.

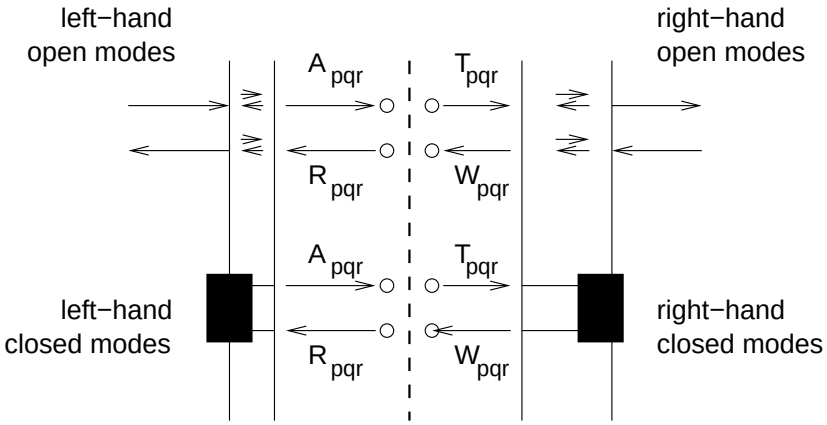

Figure 2-9: The advanced coupling scheme

The concatenation of such canonical structures follows that of the simple scheme with just one difference; only the open modes are propagated using the matrix $\mathbf{Z}_{ij}^{(B)}$. The closed modes are accounted for within the matrices $\mathbf{X}_{ij}^{(n)\prime}$. As in the simple coupling scheme, the special cases 1,2 and 3 are considered with $\mathbf{X}_{ij}^{(n)\prime}$ taking the special forms appropriate to a terminating dielectric interface, equations (2-47) to (2-50).

Referring to figure 2-5, suppose that FSS1 and FSS2 are both considered under the advanced coupling scheme. The subset of open modes for $\underline{T}_1$ are defined as those modes for which $\underline{A}_2$ are significant, with associated reflected open modes in $\underline{W}_1$. Similarly, the subset of open modes for $\underline{R}_2$ are those modes for which $\underline{W}_1$ are significant with associated reflected open modes in $\underline{A}_2$. If the same criterion for significance is applied to both open mode sets, reciprocity[5] implies that the open modes of $\underline{T}_1$ and $\underline{R}_2$ are the same. Thus $\mathbf{Z}_{ij}^{(B)}$ are permuted diagonal matrices referring to the open mode set and the previous definition remains valid under this set.

The matrix $\mathbf{Z}_{11}^{(B)}$ or $\mathbf{Z}_{22}^{(B)}$ is used to determine the significance criterion for coupling between FSS sharing a global unit cell. Either may be used since reciprocity implies that $|\mathbf{Z}_{11}^{(B)}| =$

[5]We assume reciprocal materials in QDAS, such that admittances are independent of whether waves are traveling left to right, or right to left.

$|\mathbf{Z}_{22}^{(B)}|$. Thus, for a given $\{p, q, r\}$, a mode is considered open between FSS1 and FSS2 if,

$$|Z_{11}^{(B1,L)}(p, q, r)| > s_n \qquad \text{2-53}$$

where, as for the simple coupling scheme, the threshold parameter $0 < s_n < 1$ is set by the user for a given FSS. Unlike the simple coupling scheme, if $\mathbf{Z}_{ij}^{(B)}$ refers to a multi-layer structure, it is possible that resonant conditions may be developed such that an open mode set, chosen using (2-53), is strongly dependent on frequency. In QDAS, under both simple and advanced coupling methods, the coupling sets are assumed to be *independent of frequency* (or angle of incidence) with the mode set calculated at a given frequency (and angle of incidence). As a general rule, it is advisable to set the marker frequency at which this is calculated to be the highest frequency in the run, since this takes best account of the generation of internal grating lobes for which $|Z_{11}^{(B1,L)}(p, q, r)|$ or $|\exp(-j\gamma_{pq}^{(n-1)}d_{n-1})|$ can equal unity. In the advanced coupling scheme, the possibility of an insufficiently large coupling set of open modes is greater than for the simple scheme so it may be advisable to perform simulations at different marker frequencies for complex multi-layer structures.

If FSS1 or FSS2 is defined as "local", i.e. not sharing a global unit cell, then only the principal $p = q = 0$ mode are assumed to propagate. A warning will be issued if this is inconsistent with the the above criterion set on the global unit cell, but calculations may be meaningful and accurate in some circumstances and computation is permitted.

Unlike for the simple coupling scheme, if the first (last) interface is not an FSS, open coupling modes are taken to be those modes which propagate into the left hand (right hand) half space. This is maximally efficient and deals effectively with grating modes. Those modes which are not grating or principal modes do not couple into the left hand (right hand) half space and may be considered closed modes.

3 Finite element analysis and the coupling schemes

3.1 Introduction

In this section we will describe the representation of an FSS in terms either of slots or of elements and the triangular basis functions employed. Together with a Floquet modal analysis, the FSS interaction matrices, $\mathbf{X}_{ij}^{(l)\prime}$, are determined for application under both the advanced and the simple coupling scheme. Those for the simple coupling scheme are given as a special case of the advanced method. A significant element in the formulation is the mode separation between open and closed modes.

Special features include the representation of each element of a slot or element by a thin anisotropic conductive/resistive material. Thus slots can be filled with a thin material of non-zero conductivity and elements can be composed of a thin material with non-zero resistivity. Each element of the structure can be assigned a different material value. However, we should point out that strongly anisotropic materials may not be well approximated by the piecewise-constant impedance approximation using RWG basis functions for the currents/fields and such materials should be analysed with care. Further analysis and experimental validation is required for such materials. The use of impedance elements permits the analysis of active FSS or FSS containing lumped impedances such as varicap or PIN diodes.

The triangular mesh representation of a unit cell can be completely arbitrary for maximum generality. However, a method is employed to detect the use of multiple triangles of the same size and shape. Under a Floquet modal analysis, such translational invariance can significantly reduce analysis time and permits a compromise between complete generality and the efficient (but less general) Fast Fourier Analysis of structures on a uniformly meshed grid.

We also implement a method which allows the continuous flow of currents across a unit cell boundary. The finite element input is described by the user in terms of nodes (by nodal coordinates) and triangles (by nodes). The node references defining the triangles include integers to indicate which unit cell they refer to. This provides a relatively simple and quite general way for the program to identify current flows across cell boundaries. Any structures containing lines (e.g. meander lines) require this description.

3.2 Mode separation

Each FSS, in both simple and advanced coupling schemes, has sets of left modes (associated with the field coefficients A_{pqr} and R_{pqr}) and right modes (associated with the field coefficients T_{pqr} and W_{pqr}. Both left and right modes are further split as open and closed modes in the advanced coupling scheme (as illustrated in figure 2-9). Let us define the set $\mathcal{L}_o$ as the set of left open modes, the set $\mathcal{L}_c$ as the set of left closed modes, the set $\mathcal{R}_o$ as the set of right open modes and the set $\mathcal{R}_c$ as the set of right closed modes. Members of these sets are represented by a triple mode index $\{p, q, r\}$.

The set $\mathcal{L}_o$ represents those modes, deemed to be significant, which reach the next FSS on the left of the given FSS or, if there is not one, those which propagate into the left hand half space as grating (or principal) modes. The set $\mathcal{R}_o$ represents those modes, deemed to be significant, which reach the next FSS on the right of the given FSS or, if there is not one, those which propagate into the right hand half space as grating (or principal) modes. The set $\mathcal{L}_c$ represents those remaining left modes which do not reach the next FSS on the left, if there is one. If there is no left FSS then it represents those modes which do not penetrate into the left hand half space. The set $\mathcal{R}_c$ represents those remaining right modes which do not reach the next FSS on the right, if there is one. If there is no right FSS then it represents those modes which do not penetrate into the right hand half space.

In determining mutual interactions, a given FSS is represented by a total number of modes specified by $-P \leq p \leq P$, $-Q \leq q \leq Q$ and $r = 1, 2$ where P and Q are large positive integers. If an FSS is characterised by a global unit cell, P and Q are common to every FSS. If an FSS is defined as "local", P and Q are defined specific to the given FSS. In the absence of effective acceleration schemes (see section 4.6), the total mode set so defined is used to approximate the sum-to-infinity in the Floquet modal analysis. Let the total number of such modes be the set $\mathcal{T}$.

We will assume,

$$\begin{aligned} \mathcal{R}_o \cap \mathcal{R}_c &= 0 \\ \mathcal{R}_o \cup \mathcal{R}_c &= \mathcal{T} \\ \mathcal{L}_o \cap \mathcal{L}_c &= 0 \\ \mathcal{L}_o \cup \mathcal{L}_c &= \mathcal{T} \end{aligned} \qquad \text{3-1}$$

It would be possible to use a subset smaller than $\mathcal{T}$ in the expressions for the unions in (3-1), to provide a small increase in computation speed[6]. Such a set could be chosen on a criterion similar to condition (2-53) but based on the magnitudes of $Z_{12}^{(B1,L)}(p,q,r)$ and $Z_{21}^{(B1,L)}(p,q,r)$. However, this is an issue we have not explored. Special cases include $\mathcal{R}_o = 0$ and $\mathcal{L}_o = 0$ when there exists a right or left perfectly conducting termination within the structure, if there are layers of dielectric material sufficiently thick or lossy to absorb all propagating waves, or under special resonant conditions. Such resonant conditions can occur when multiple layers of dielectric interact so as to forbid transmission at certain frequencies.

In general, between two FSS (case 4 of section 2.7) the sets $\mathcal{R}_o$, $\mathcal{R}_c$, $\mathcal{L}_o$ and $\mathcal{L}_c$ are non-empty. If the first interface of the composite coincides with the first FSS (special case of case 3 of section 2.7) then $\mathcal{L}_c = 0$. Similarly if the last interface of the composite coincides with the last FSS (special case of case 2 of section 2.7) then $\mathcal{R}_c = 0$. Only if an FSS is isolated in free space (special case of case 1 of section 2.7) do we generally expect both $\mathcal{R}_c = 0$ and $\mathcal{L}_c = 0$.

[6] Most computational saving occurs as a result of reduction in the size of the open mode sets, due to the matrix operations required in computing the $\mathbf{W}_{ij}$ matrices (2-40). Reduction in the size of the closed mode sets results in far smaller savings, since this only allows the neglecting of certain terms in the construction of the χ_{pqr} admittances for slots (3-25), or $\overline{\chi}_{pqr}$ for elements (3-86).

Between two FSS, a mode set is assumed open if condition (2-53) holds and the associated closed mode set is implied by (3-1).

3.3 The formulation for slotted FSS

Adopting the notation in section 1.9, and following Chen's principles [4], the tangential electric field across an FSS interface of zero thickness, $\underline{E}_t(x,y)$, is continuous since there are no true magnetic currents. Thus,

$$\underline{E}_t(x,y) = \underline{E}^{(t-)}(x,y) = \underline{E}^{(t+)}(x,y) \qquad 3\text{-}2$$

and

$$\sum_{pqr}^{\infty} A_{pqr}\underline{\phi}_{pqr}(x,y) + \sum_{pqr}^{\infty} R_{pqr}\underline{\phi}_{pqr}(x,y) = \sum_{pqr}^{\infty} T_{pqr}\underline{\phi}_{pqr}(x,y) + \sum_{pqr}^{\infty} W_{pqr}\underline{\phi}_{pqr}(x,y) \qquad 3\text{-}3$$

with the sum superfix, ∞, indicating a summation over all modes; $-\infty < p,q < +\infty$, $r = 1,2$. Because these expressions are valid for all x,y on a unit cell (on regions of perfect conductor $\underline{E}^{(t-)}(x,y) = \underline{E}^{(t+)}(x,y) = 0$), inner products of Floquet modes taken with respect to the local unit cell imply that,

$$A_{pqr} + R_{pqr} = T_{pqr} + W_{pqr} \text{ for all modes } p,q,r. \qquad 3\text{-}4$$

Expression (3-4) is valid for any single FSS interface, whether represented by slots or elements.

We may define the unit cell as consisting of perfect conductor except for an aperture region which may contain a thin resistive material. Using (1-24), the expression (3-2) may thus be written as,

$$\underline{E}^{(t-)}(x,y) = \begin{cases} \sum_{pqr}^{\infty}(A_{pqr} + R_{pqr})\underline{\phi}_{pqr}(x,y) & \text{for } x,y \in \text{FSS aperture.} \\ 0 & \text{otherwise.} \end{cases} \qquad 3\text{-}5$$

and

$$\underline{E}^{(t+)}(x,y) = \begin{cases} \sum_{pqr}^{\infty}(T_{pqr} + W_{pqr})\underline{\phi}_{pqr}(x,y) & \text{for } x,y \in \text{FSS aperture.} \\ 0 & \text{otherwise.} \end{cases} \qquad 3\text{-}6$$

The difference in the tangential magnetic field across an FSS differs by the induced electric current, $\underline{J}(x,y)$. For regions of empty aperture containing no conductive material the tangential magnetic field is continuous across the aperture. Thus,

$$2\sum_{pqr}^{\infty} A_{pqr}\xi^{(1)}_{pqr}\underline{\phi}_{pqr}(x,y) - \sum_{pqr}^{\infty} T_{pqr}(\xi^{(1)}_{pqr} + \xi^{(2)}_{pqr})\underline{\phi}_{pqr}(x,y) - \sum_{pqr}^{\infty} W_{pqr}(\xi^{(1)}_{pqr} - \xi^{(2)}_{pqr})\underline{\phi}_{pqr}(x,y) \qquad 3\text{-}7$$

$$= \begin{cases} \underline{J}(x,y) & \text{for } x,y \in \text{perfect conductor or non-empty parts of aperture.} \\ 0 & \text{for } x,y \in \text{empty aperture.} \end{cases}$$

where $\xi^{(1)}_{pqr}$ is the modal admittance of the material to the left of the FSS and $\xi^{(2)}_{pqr}$ is the modal admittance of the material to the right of the FSS. This expression is valid for slotted or element structures.

Provided the conductivity is not infinite, i.e. over the aperture region, the electric current is related to the tangential electric field by,

$$\underline{J}(x,y) = \underline{\underline{\sigma}}_s(x,y)\underline{E}^{(t-)}(x,y) = \underline{\underline{\sigma}}_s(x,y)\underline{E}^{(t+)}(x,y) \qquad \text{for } x,y \in \text{aperture.} \tag{3-8}$$

where $\underline{\underline{\sigma}}_s(x,y)$ is the second order conductivity tensor, represented by a 2×2 matrix in a Cartesian (x,y) coordinate system. The expression is invalid over the perfect conducting non-aperture regions of the unit cell, since $\underline{\underline{\sigma}}_s(x,y) \to \infty$ and $\underline{E}^{(t)}(x,y) \to 0$. It remains valid, such that $\underline{\underline{\sigma}}_s(x,y) = \mathbf{0}$, in regions of empty aperture which do not contain a resistive material. The expression is employed only in the slot formulation, where the aperture is meshed by finite elements. Consequently,

$$\begin{aligned} 2\sum_{pqr}^{\infty} A_{pqr}\xi^{(1)}_{pqr}\underline{\phi}_{pqr}(x,y) - \sum_{pqr}^{\infty} T_{pqr}(\xi^{(1)}_{pqr} + \xi^{(2)}_{pqr})\underline{\phi}_{pqr}(x,y) - \sum_{pqr}^{\infty} W_{pqr}(\xi^{(1)}_{pqr} - \xi^{(2)}_{pqr})\underline{\phi}_{pqr}(x,y) \\ = \underline{\underline{\sigma}}_s(x,y)\sum_{pqr}^{\infty}(T_{pqr} + W_{pqr})\underline{\phi}_{pqr}(x,y) \qquad \text{for } x,y \in \text{aperture.} \end{aligned} \tag{3-9}$$

There are two finite element representations that we shall use. The first representation is of the conductivity. Generally, let us model $\underline{\underline{\sigma}}_s(x,y)$ as,

$$\underline{\underline{\sigma}}_s(x,y) = \sum_{k=1}^{K} \underline{\underline{\sigma}}_k p_k(x,y) \tag{3-10}$$

where the K tensor coefficients $\underline{\underline{\sigma}}_k$ are defined by the user and $p_k(x,y)$ are a set of piece-wise constant scalar shape functions. The second representation is of the tangential electric field in the aperture,

$$\underline{E}_t(x,y) = \sum_{pqr}^{\infty}(T_{pqr} + W_{pqr})\underline{\phi}_{pqr}(x,y) = \sum_{l=1}^{M} F_l\underline{\Psi}_l(x,y) \tag{3-11}$$

where $\underline{\Psi}_l(x,y)$ are a set of M complex vector-valued basis functions, assumed given and defined as zero for x,y not in the aperture. In our formulation we will assume RWG basis functions [11], comprising adjoining triangle pairs. The coefficients F_l are *a-priori* unknown.

Taking inner products with respect to the local unit cell, i.e. multiplying left and right hand sides of (3-11) as a dot product with $\underline{\phi}^{\star}_{pqr}(x,y)$ and integrating over the domain of the local unit cell, we may use the orthogonality relation (1-5). This, together with the fact that $\underline{E}_t(x,y) = 0$ for x,y not in the aperture implies,

$$A_{pqr} + R_{pqr} = T_{pqr} + W_{pqr} = \iint_{Ap} \underline{E}_t(x',y').\underline{\phi}^{\star}_{pqr}(x',y')dx'dy' \qquad \text{for all } p,q,r \tag{3-12}$$

where the integration is over the domain of the aperture, Ap.

We may now substitute (3-12) in to (3-9) to relate the unknown fields on the aperture in terms of the incident field coefficients A_{pqr} and W_{pqr},

$$\begin{aligned} &2\sum_{pqr}^{\infty} A_{pqr}\xi^{(1)}_{pqr}\underline{\phi}_{pqr}(x,y) + 2\sum_{pqr}^{\infty} W_{pqr}\xi^{(2)}_{pqr}\underline{\phi}_{pqr}(x,y) \\ &-\sum_{pqr}^{\infty}(\xi^{(1)}_{pqr}+\xi^{(2)}_{pqr})\underline{\phi}_{pqr}(x,y)\iint_{Ap}\underline{E}_t(x',y').\underline{\phi}^{\star}_{pqr}(x',y')dx'dy' \\ =\sum_{k=1}^{K}\sum_{pqr}^{\infty}&\left(\iint_{Ap}\underline{E}_t(x',y').\underline{\phi}^{\star}_{pqr}(x',y')dx'dy'\right)\underline{\underline{\sigma}}_k.\underline{\phi}_{pqr}(x,y)p_k(x,y) \qquad \text{for } x,y \in \text{aperture.} \end{aligned}$$

3-13

Suppose an FSS is embedded in multiple layers of dielectric as illustrated in figure 3-1. We

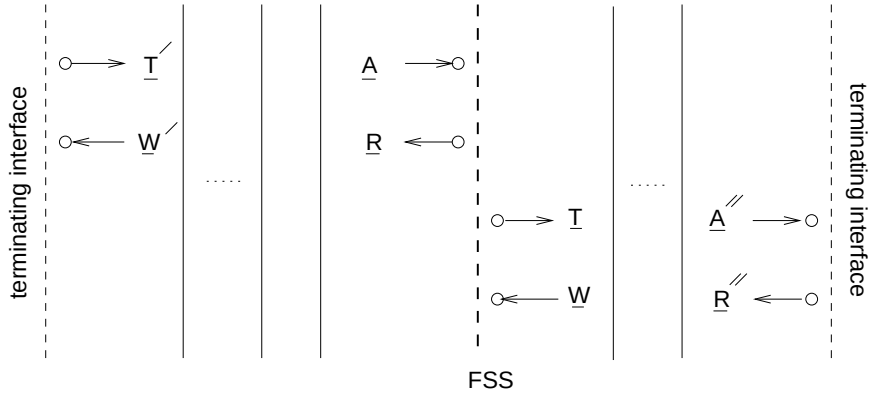

Figure 3-1: Wave coefficients to either side of an FSS embedded in layers of dielectric.

designate the matrices $\mathbf{Z}^{(B)}_{ij}$ and wave coefficients on the left and right using primed and double-primed suffices. Thus,

$$\begin{pmatrix} \underline{A} \\ \underline{W}' \end{pmatrix} = \begin{pmatrix} \mathbf{Z}^{(B)\prime}_{11} & \mathbf{Z}^{(B)\prime}_{12} \\ \mathbf{Z}^{(B)\prime}_{21} & \mathbf{Z}^{(B)\prime}_{22} \end{pmatrix} \begin{pmatrix} \underline{T}' \\ \underline{R} \end{pmatrix} \qquad 3\text{-}14$$

and

$$\begin{pmatrix} \underline{A}'' \\ \underline{W} \end{pmatrix} = \begin{pmatrix} \mathbf{Z}^{(B)\prime\prime}_{11} & \mathbf{Z}^{(B)\prime\prime}_{12} \\ \mathbf{Z}^{(B)\prime\prime}_{21} & \mathbf{Z}^{(B)\prime\prime}_{22} \end{pmatrix} \begin{pmatrix} \underline{T} \\ \underline{R}'' \end{pmatrix} \qquad 3\text{-}15$$

Under our definition, $\mathbf{Z}^{(B)\prime}_{ij}$ and $\mathbf{Z}^{(B)\prime\prime}_{ij}$ are (generally rectangular) permuted diagonal matrices. In terms of their non-zero elements, we designate the $\{p,q,r\}$ term of $\mathbf{Z}^{(B)\prime}_{ij}$ by $Z^{(B)\prime}_{ij,pqr}$ and the $\{p,q,r\}$ term of $\mathbf{Z}^{(B)\prime\prime}_{ij}$ by $Z^{(B)\prime\prime}_{ij,pqr}$. Both (3-14) and (3-15) are valid for any p,q,r belonging to open and closed mode sets, but note that an open mode in the left (primed) set may be a closed mode in the right (double primed) set. The latter effects are, as we shall show, important in an element formulation (section 3.4).

Next we split the sums of the coefficients A_{pqr} and W_{pqr} over open and closed mode sets. Because, by definition, closed modes do not propagate through to the terminating interfaces, (3-14) implies,

$$A_{pqr} = Z^{(B)\prime}_{12,pqr} R_{pqr} \qquad \text{for } (p,q,r) \in \mathcal{L}_c \tag{3-16}$$

Similarly, (3-15) implies,

$$W_{pqr} = Z^{(B)\prime\prime}_{21,pqr} T_{pqr} \qquad \text{for } (p,q,r) \in \mathcal{R}_c \tag{3-17}$$

In addition (3-12) implies,

$$T_{pqr} + W_{pqr} = \iint_{Ap} \underline{E}_t(x',y').\underline{\phi}^{\star}_{pqr}(x',y')dx'dy' \qquad \text{for } (p,q,r) \in \mathcal{R}_c \text{ or } \mathcal{R}_o \tag{3-18}$$

and

$$A_{pqr} + R_{pqr} = \iint_{Ap} \underline{E}_t(x',y').\underline{\phi}^{\star}_{pqr}(x',y')dx'dy' \qquad \text{for } (p,q,r) \in \mathcal{L}_c \text{ or } \mathcal{L}_o \tag{3-19}$$

Equations (3-18) and (3-19) are made distinct because it need not be the case that $\mathcal{R}_c = \mathcal{L}_c$.

Equations (3-16) and (3-19) imply,

$$A_{pqr} = \frac{Z^{(B)\prime}_{12,pqr}}{1 + Z^{(B)\prime}_{12,pqr}} \iint_{Ap} \underline{E}_t(x',y').\underline{\phi}^{\star}_{pqr}(x',y')dx'dy' \qquad \text{for } (p,q,r) \in \mathcal{L}_c \tag{3-20}$$

and (3-17) and (3-18) imply,

$$W_{pqr} = \frac{Z^{(B)\prime\prime}_{21,pqr}}{1 + Z^{(B)\prime\prime}_{21,pqr}} \iint_{Ap} \underline{E}_t(x',y').\underline{\phi}^{\star}_{pqr}(x',y')dx'dy' \qquad \text{for } (p,q,r) \in \mathcal{R}_c \tag{3-21}$$

We now split the sums over A_{pqr} and W_{pqr} in (3-13) over open and closed modes and substitute (3-11) and the expressions (3-20) and (3-21) over the closed modes to obtain,

$$\begin{aligned}
&2\sum_{pqr\in\mathcal{L}_o} A_{pqr}\xi^{(1)}_{pqr}\underline{\phi}_{pqr}(x,y) + 2\sum_{pqr\in\mathcal{L}_c} \frac{\xi^{(1)}_{pqr} Z^{(B)\prime}_{12,pqr}}{1 + Z^{(B)\prime}_{12,pqr}} \underline{\phi}_{pqr}(x,y) \iint_{Ap} \underline{E}_t(x',y').\underline{\phi}^{\star}_{pqr}(x',y')dx'dy' \\
&+2\sum_{pqr\in\mathcal{R}_o} W_{pqr}\xi^{(2)}_{pqr}\underline{\phi}_{pqr}(x,y) + 2\sum_{pqr\in\mathcal{R}_c} \frac{\xi^{(2)}_{pqr} Z^{(B)\prime\prime}_{21,pqr}}{1 + Z^{(B)\prime\prime}_{21,pqr}} \underline{\phi}_{pqr}(x,y) \iint_{Ap} \underline{E}_t(x',y').\underline{\phi}^{\star}_{pqr}(x',y')dx'dy' \\
&-\sum_{pqr}^{\infty} (\xi^{(1)}_{pqr} + \xi^{(2)}_{pqr}) \underline{\phi}_{pqr}(x,y) \iint_{Ap} \underline{E}_t(x',y').\underline{\phi}^{\star}_{pqr}(x',y')dx'dy' \\
&= \sum_{k=1}^{K}\sum_{l=1}^{M} F_l \underline{\sigma}_k.\underline{\Psi}_l(x,y)p_k(x,y) \qquad \text{for } x,y \in \text{aperture.}
\end{aligned} \tag{3-22}$$

We may group all the terms involving integrals together by introducing some symbols. Let us define,

$$U_{pqr}(\mathcal{L}_c) = \begin{cases} 1 & \text{for } (p,q,r) \in \mathcal{L}_c \\ 0 & \text{otherwise} \end{cases} \quad 3\text{-}23$$

and

$$U_{pqr}(\mathcal{R}_c) = \begin{cases} 1 & \text{for } (p,q,r) \in \mathcal{R}_c \\ 0 & \text{otherwise} \end{cases} \quad 3\text{-}24$$

Then define the admittance coefficients,

$$\chi_{pqr} = -2U_{pqr}(\mathcal{L}_c)\frac{\xi^{(1)}_{pqr} Z^{(B)\prime}_{12,pqr}}{1 + Z^{(B)\prime}_{12,pqr}} - 2U_{pqr}(\mathcal{R}_c)\frac{\xi^{(2)}_{pqr} Z^{(B)\prime\prime}_{21,pqr}}{1 + Z^{(B)\prime\prime}_{21,pqr}} + \xi^{(1)}_{pqr} + \xi^{(2)}_{pqr} \quad \text{for all } p,q,r \quad 3\text{-}25$$

Equation (3-22) may then be re-written as,

$$\begin{aligned} &2\sum_{pqr\in\mathcal{L}_o} A_{pqr}\xi^{(1)}_{pqr}\underline{\phi}_{pqr}(x,y) + 2\sum_{pqr\in\mathcal{R}_o} W_{pqr}\xi^{(2)}_{pqr}\underline{\phi}_{pqr}(x,y) \\ &= \sum_{pqr}^{\infty} \chi_{pqr}\underline{\phi}_{pqr}(x,y)\iint_{Ap} \underline{E}_t(x',y').\underline{\phi}^{\star}_{pqr}(x',y')dx'dy' + \sum_{k=1}^{K}\sum_{l=1}^{M} F_l\underline{\underline{\sigma}}_k.\underline{\Psi}_l(x,y)p_k(x,y) \end{aligned} \quad 3\text{-}26$$

$$\text{for } x,y \in \text{aperture.}$$

Using (3-11) in the remaining integral, we may then take the dot product of (3-26) with the complex conjugate of the basis function, $\underline{\Psi}^{\star}_m(x,y)$. Integrating the expression over (x,y) in the domain of the aperture then yields the M equations $(1 \le m \le M)$,

$$2\sum_{pqr\in\mathcal{L}_o} A_{pqr}\xi^{(1)}_{pqr}C^{\star}_{pqr,m} + 2\sum_{pqr\in\mathcal{R}_o} W_{pqr}\xi^{(2)}_{pqr}C^{\star}_{pqr,m} = \sum_{pqr}^{\infty}\chi_{pqr}C^{\star}_{pqr,m}\sum_{l=1}^{M} F_l C_{pqr,l} + \sum_{l=1}^{M} R_{ml}F_l \quad 3\text{-}27$$

where the (generally complex) scalar coefficients $C_{pqr,l}$ and R_{ml} are defined by,

$$C_{pqr,l} = \iint_{Ap} \underline{\Psi}_l(x',y').\underline{\phi}^{\star}_{pqr}(x',y')dx'dy' \quad 3\text{-}28$$

and

$$R_{ml} = \sum_{k=1}^{K}\iint_{Ap} [\underline{\underline{\sigma}}_k.\underline{\Psi}_l(x',y')].\underline{\Psi}^{\star}_m(x',y')p_k(x',y')dx'dy' \quad 3\text{-}29$$

The finite Floquet mode approximation is then applied to replace the sum to infinity in (3-27) by the set $\mathcal{T} : (-P \le p \le P), (-Q \le q \le Q), (r = 1,2)$. Evaluation of $C_{pqr,l}$ and R_{ml} depends on the choice of basis functions $\Psi_m(x,y)$ and (piece-wise constant) impedance shape functions $p_k(x,y)$. This is described in section 4.

We will now adopt matrix notation with an ordering convention. Let $\mathbf{M}$ be a matrix with elements M_{ij}, let $\mathbf{V}$ be a matrix with elements V_{ij} and let $(MV)_{ij}$ be the elements of the

matrix **MV**. We assume that the ordering of the $(p,q,r)_{th}$ row or column is arbitrary, but that any matrix-matrix or vector-matrix operation of the form **MV** has elements defined by,

$$(MV)_{ij} = \sum_{pqr \in \mathcal{S}} M_{i,k(pqr)} V_{k(pqr),j} \qquad 3\text{-}30$$

where k is the ordering of the $(p,q,r)_{th}$ row or column and $\mathcal{S}$ is any set of $\{p,q,r\}$. In other words, matrix multiplications always assume an ordering which is the same in the column number of the first matrix as the row number of the second. Similarly, any sum of matrices or vectors assumes the same ordering $k(pqr)$ of terms.

Let $\boldsymbol{C}_{Lo}$ be the rectangular matrix, comprising terms $C_{pqr,l}$ for $(p,q,r) \in \mathcal{L}_o$, with M columns and L_o rows, where L_o is the number of entries in the set $\mathcal{L}_o$.

Let $\boldsymbol{C}_{Ro}$ be the rectangular matrix, comprising terms $C_{pqr,l}$ for $(p,q,r) \in \mathcal{R}_o$, with M columns and R_o rows, where R_o is the number of entries in the set $\mathcal{R}_o$.

Let $\boldsymbol{C}$ be the rectangular matrix, comprising terms $C_{pqr,l}$ for $(p,q,r) \in \mathcal{T}$, with M columns and $T = 2(2P+1)(2Q+1)$ rows, where T is the number of entries in the set $\mathcal{T}$.[7]

Let $\underline{F}$ be the vector of elements F_l of dimension M.

Let the superfix † associated with a matrix represent its complex conjugate transpose.

Let $\boldsymbol{\chi}$ be the permuted diagonal matrix defined by $\boldsymbol{\chi} = pdiag(\chi_{pqr})$ (where *pdiag* is defined in section 2.5), under the additional restriction that $\boldsymbol{\chi}$ is assumed square. This assumes $(p,q,r) \in \mathcal{T}$ with $\boldsymbol{\chi}$ of dimension $T \times T$, where $T = 2(2P+1)(2Q+1)$ is the size of $\mathcal{T}$.

Let $\boldsymbol{\xi}^{(1)}_{Lo}$ be the permuted diagonal matrix, $bdiag(\xi^{(1)}_{pqr})$, for $(p,q,r) \in \mathcal{L}_o$, under the additional restriction that $\boldsymbol{\xi}^{(1)}_{Lo}$ is assumed square of size $L_o \times L_o$.

Let $\boldsymbol{\xi}^{(2)}_{Ro}$ be the permuted diagonal matrix, $bdiag(\xi^{(2)}_{pqr})$, for $(p,q,r) \in \mathcal{R}_o$, under the additional restriction that $\boldsymbol{\xi}^{(2)}_{Ro}$ is assumed square of size $R_o \times R_o$.

Any suffix Ro, Rc, Lo, Lc applied to a vector indicates that the members of the vector are indexed by the mode (p,q,r) for $(p,q,r) \in \mathcal{R}_o$, $\mathcal{R}_c$, $\mathcal{L}_o$ or $\mathcal{L}_c$, respectively. The associated vector will be of size Ro, Rc, Lo or Lc, respectively.

[7] Clearly, $\boldsymbol{C}_{Ro}$ and $\boldsymbol{C}_{Lo}$ are submatrices of $\boldsymbol{C}$. Usually, $\boldsymbol{C}$ is very much larger than either $\boldsymbol{C}_{Ro}$ or $\boldsymbol{C}_{Lo}$. Within the QDAS software it was decided not to store all elements of $\boldsymbol{C}$ since this requires either significant memory resources or rapid IO to hard disk. Furthermore, it also makes it hard to investigate convergence schemes where the effective size of T may need to be much larger than usually employed. However, the elements of $\boldsymbol{C}_{Ro}$ and $\boldsymbol{C}_{Lo}$ are stored. The efficiency of this approach depends on the computation time in the construction of $\boldsymbol{C}$, its relation to other computation times, and the number of times $\boldsymbol{C}$ is used. In fact, $\boldsymbol{C}$ is used only twice, for the calculation of the $\mathbf{Y}$ matrix defined below, so even if calculation of the elements of $\boldsymbol{C}$ dominates QDAS (which it does only sometimes) there is at most a factor of 2 that can be gained by efficient memory storage and data transfer to and from hard disk.

We define the $\mathbf{Y}$ matrix, of size $M \times M$, by,

$$\boldsymbol{Y} = \boldsymbol{C}^{\dagger}\boldsymbol{\chi}\boldsymbol{C} + \boldsymbol{R} \qquad 3\text{-}31$$

This matrix is assumed invertible using M linearly independent basis functions. With the above definitions (3-27) may be rewritten as,

$$2\boldsymbol{C}^{\dagger}_{Lo}\boldsymbol{\xi}^{(1)}_{Lo}\underline{A}_{Lo} + 2\boldsymbol{C}^{\dagger}_{Ro}\boldsymbol{\xi}^{(2)}_{Ro}\underline{W}_{Ro} = \boldsymbol{Y}\underline{F} \qquad 3\text{-}32$$

giving the expression for the unknown coefficients of $\underline{F}$ in terms of the incoming wave coefficients,

$$\underline{F} = 2\boldsymbol{Y}^{-1}(\boldsymbol{C}^{\dagger}_{Lo}\boldsymbol{\xi}^{(1)}_{Lo}\underline{A}_{Lo} + \boldsymbol{C}^{\dagger}_{Ro}\boldsymbol{\xi}^{(2)}_{Ro}\underline{W}_{Ro}) \qquad 3\text{-}33$$

In fact, while $\underline{F}$ is necessary to determine the electric fields over the aperture, its explicit calculation is not necessary to compute the transmission and reflection coefficients of the aggregate composite. Currently, QDAS does not determine $\underline{F}$ explicitly.

Equation (3-18) may also be cast in matrix form as,

$$\underline{T}_{Ro} + \underline{W}_{Ro} = \boldsymbol{C}_{Ro}\underline{F} \qquad 3\text{-}34$$

Substituting (3-33) in (3-34) and re-arranging the expression gives,

$$\underline{T}_{Ro} = 2\boldsymbol{C}_{Ro}\boldsymbol{Y}^{-1}\boldsymbol{C}^{\dagger}_{Lo}\boldsymbol{\xi}^{(1)}_{Lo}\underline{A}_{Lo} + (2\boldsymbol{C}_{Ro}\boldsymbol{Y}^{-1}\boldsymbol{C}^{\dagger}_{Ro}\boldsymbol{\xi}^{(2)}_{Ro} - \boldsymbol{I})\underline{W}_{Ro} \qquad 3\text{-}35$$

Equation (3-19) may similarly be case in matrix form as,

$$\underline{A}_{Lo} + \underline{R}_{Lo} = \boldsymbol{C}_{Lo}\underline{F} \qquad 3\text{-}36$$

Substituting (3-33) in (3-36) and re-arranging the expression gives,

$$\underline{R}_{Lo} = (2\boldsymbol{C}_{Lo}\boldsymbol{Y}^{-1}\boldsymbol{C}^{\dagger}_{Lo}\boldsymbol{\xi}^{(1)}_{Lo} - \boldsymbol{I})\underline{A}_{Lo} + 2\boldsymbol{C}_{Lo}\boldsymbol{Y}^{-1}\boldsymbol{C}^{\dagger}_{Ro}\boldsymbol{\xi}^{(2)}_{Ro}\underline{W}_{Ro} \qquad 3\text{-}37$$

We determine the combined set of modes, $\mathcal{S}_o = \mathcal{L}_o \cup \mathcal{R}_o$. We may then define $\mathbf{C}_{So}$ as the rectangular matrix, comprising terms $C_{pqr,l}$ for $(p,q,r) \in \mathcal{S}_o$, with M columns and S_o rows, where S_o is the number of entries in the set $\mathcal{S}_o$ ($max(R_o, L_o) \leq S_o \leq R_o + L_o$). We then define the matrix,

$$\boldsymbol{Q}_{SoSo} = \boldsymbol{C}_{So}\boldsymbol{Y}^{-1}\boldsymbol{C}^{\dagger}_{So} \qquad 3\text{-}38$$

All elements of the matrix $\boldsymbol{Q}_{SoSo}$ are held resident in memory while computation of interaction matrices, $\boldsymbol{X}^{(n)\prime}_{ij}$, is underway for the given FSS. The elements of $\boldsymbol{Q}_{SoSo}$ are used to construct the submatrices (by appropriate choice of row and column number),

$$\begin{aligned}
\boldsymbol{Q}_{LoLo} &= \boldsymbol{C}_{Lo}\boldsymbol{Y}^{-1}\boldsymbol{C}^{\dagger}_{Lo} \\
\boldsymbol{Q}_{LoRo} &= \boldsymbol{C}_{Lo}\boldsymbol{Y}^{-1}\boldsymbol{C}^{\dagger}_{Ro} \\
\boldsymbol{Q}_{RoLo} &= \boldsymbol{C}_{Ro}\boldsymbol{Y}^{-1}\boldsymbol{C}^{\dagger}_{Lo} \\
\boldsymbol{Q}_{RoRo} &= \boldsymbol{C}_{Ro}\boldsymbol{Y}^{-1}\boldsymbol{C}^{\dagger}_{Ro}
\end{aligned} \qquad 3\text{-}39$$

Using this representation, we achieve the final result. If the $\boldsymbol{X}_{ij}^{(n)\prime}$ matrices, associated with the n^{th} slot FSS in the advanced coupling scheme, connect open modes via the definition,

$$\begin{pmatrix} \underline{T}_{Ro} \\ \underline{R}_{Lo} \end{pmatrix} = \begin{pmatrix} \boldsymbol{X}_{11}^{(n)\prime} & \boldsymbol{X}_{12}^{(n)\prime} \\ \boldsymbol{X}_{21}^{(n)\prime} & \boldsymbol{X}_{22}^{(n)\prime} \end{pmatrix} \begin{pmatrix} \underline{A}_{Lo} \\ \underline{W}_{Ro} \end{pmatrix} \qquad 3\text{-}40$$

then,

$$\begin{pmatrix} \boldsymbol{X}_{11}^{(n)\prime} & \boldsymbol{X}_{12}^{(n)\prime} \\ \boldsymbol{X}_{21}^{(n)\prime} & \boldsymbol{X}_{22}^{(n)\prime} \end{pmatrix} = \begin{pmatrix} 2\boldsymbol{Q}_{RoLo}\boldsymbol{\xi}_{Lo}^{(1)} & 2\boldsymbol{Q}_{RoRo}\boldsymbol{\xi}_{Ro}^{(2)} - \boldsymbol{I} \\ 2\boldsymbol{Q}_{LoLo}\boldsymbol{\xi}_{Lo}^{(1)} - \boldsymbol{I} & 2\boldsymbol{Q}_{LoRo}\boldsymbol{\xi}_{Ro}^{(2)} \end{pmatrix} \qquad 3\text{-}41$$

In the simple coupling scheme, we may simply redefine all modes as open modes and ignore any such modes which fall below the threshold defined in section 2.6. We may thus use the above expression with $\mathcal{L}_c = \mathcal{R}_c = 0$ and $\mathcal{L}_o$ and $\mathcal{R}_o$ chosen as subsets of $\mathcal{T}$ according to the threshold criterion. Here, (3-25) simplifies to,

$$\chi_{pqr} = \xi_{pqr}^{(1)} + \xi_{pqr}^{(2)} \qquad 3\text{-}42$$

In general, we would still expect $\mathcal{R}_o \neq \mathcal{L}_o$, so little further simplification is possible.

3.4 The formulation for element FSS

An FSS defined as consisting of elements assumes a finite element representation of the electric current on the conductor and is efficient when the fraction of conductor on a unit cell is significantly less than 50%. This contrasts with the previous aperture formulation which assumes a finite element representation of the electric field on the aperture, efficient when the fraction of aperture on a unit cell is significantly less than 50%. For complex shapes where the percentage of perfect conductor is similar to the percentage of empty slot, either formulation can be used with similar efficiency.

Equations (3-2) to (3-7) remain valid for the element formulation. However, equation (4) is no longer useful since we need a representation for the electric current valid for regions of perfect conductor. In its place, we must use the inverse expression as the constitutive relation,

$$\underline{E}_t(x,y) = \underline{\underline{\Omega}}_s(x,y)\underline{J}(x,y) \qquad 3\text{-}43$$

where $\underline{\underline{\Omega}}_s(x,y)$ is the matrix representation of the resistivity tensor,

$$\underline{\underline{\Omega}}_s(x,y) = [\underline{\underline{\sigma}}_s(x,y)]^{-1} \qquad 3\text{-}44$$

$\underline{E}_t(x,y)$ is defined in (3-43) provided x, y are not in empty aperture. Using the expression (1-24) for $\underline{E}_t(x,y)$, (3-43) becomes,

$$\sum_{pqr}^{\infty}(T_{pqr} + W_{pqr})\underline{\phi}_{pqr}(x,y) = \underline{\underline{\Omega}}_s(x,y)\underline{J}(x,y) \qquad \text{for } x,y \in \text{FSS element} \qquad 3\text{-}45$$

Note that it is no longer possible to use the expression for $\underline{J}(x,y)$ in (3-43) for substitution in (3-7).

We now employ M basis functions, $\underline{\jmath}_l(x,y)$ (for $1 \leq l \leq M$) to model the current flow over non empty regions of the unit cell. Any linearly independent set of functions, which locally and approximately satisfy Maxwell's equations, are acceptable. We will use ones which complement the slot field functions, defined by

$$\underline{\jmath}_l(x,y) = \hat{\underline{n}} \times \underline{\Psi}_l(x,y) \tag{3-46}$$

where $\hat{\underline{n}}$ is the surface normal to an FSS and $\underline{\Psi}_l$ are the basis functions used to represent the electric field over slots. These are described in section 4. The electric current on any non-empty point on the unit cell may thus be represented by,

$$\underline{J}(x,y) = \begin{cases} \sum_{l=1}^{M} F_l \underline{\jmath}_l(x,y) & \text{for } x,y \in \text{element} \\ 0 & \text{otherwise} \end{cases} \tag{3-47}$$

Substituting (3-47) in to (3-7), we may then form the dot product of (3-7) with $\underline{\phi}^{\star}_{pqr}$ and integrate over the whole unit cell. Using the orthogonality of Floquet modes (indexed by $\{p,q,r\}$ over the local unit cell), (3-7) becomes,

$$2A_{pqr}\xi^{(1)}_{pqr} - T_{pqr}(\xi^{(1)}_{pqr} + \xi^{(2)}_{pqr}) - W_{pqr}(\xi^{(1)}_{pqr} - \xi^{(2)}_{pqr}) = \sum_{l=1}^{M} F_l \iint_{El} \underline{\jmath}_l(x',y').\underline{\phi}^{\star}_{pqr}(x',y')dx'dy' \quad \text{for all p,q,r} \tag{3-48}$$

where the domain of integration, El, represents the "element"; i.e. the non-empty region of the unit cell made from perfectly or partially conducting thin material.

We assume a mode separation into sets $\mathcal{L}_o$, $\mathcal{L}_c$, $\mathcal{R}_o$ and $\mathcal{R}_c$ as defined in the aperture formulation. We will also assume a structure and notation set out in figure 3-1 and equations (3-14), (3-15), (3-16) and (3-17).

Equations (3-16) and (3-4) imply,

$$A_{pqr}(1 + Z^{(B)\prime}_{12,pqr}) = Z^{(B)\prime}_{12,pqr}(T_{pqr} + W_{pqr}) \qquad \text{for } (p,q,r) \in \mathcal{L}_c \tag{3-49}$$

Also, (3-17) and (3-48) imply,

$$2A_{pqr}\xi^{(1)}_{pqr} - T_{pqr}(\xi^{(1)}_{pqr} + \xi^{(2)}_{pqr}) - Z^{(B)\prime\prime}_{21,pqr}T_{pqr}(\xi^{(1)}_{pqr} - \xi^{(2)}_{pqr}) = \sum_{l=1}^{M} F_l \iint_{El} \underline{\jmath}_l(x',y').\underline{\phi}^{\star}_{pqr}(x',y')dx'dy' \quad \text{for } (p,q,r) \in \mathcal{R}_c \tag{3-50}$$

The problem is that in general $\mathcal{R}_c \neq \mathcal{L}_c$ and so we can not simply substitute the expression for A_{pqr} in (3-49) in to (3-50)! What is the solution?

We could attempt to construct equations which are valid for $(p,q,r) \in \mathcal{L}_c \cup \mathcal{R}_c$. The problem is that a member of such a set may coincide with an open mode in $\mathcal{L}_o$ or $\mathcal{R}_o$ and thus

invalidate the requirement of impedance information local to the FSS. We could attempt to restrict $\mathcal{L}_c = \mathcal{R}_c$. However, this is not compatible with our advanced concatenation method and would result in significant program complexity and possible serious inefficiency for certain layer arrangements. These difficulties do not arise with the aperture formulation because there, the sets $\mathcal{L}_c$ and $\mathcal{L}_o$ are only ever associated with the coefficients A_{pqr} and R_{pqr} and the sets $\mathcal{R}_c$ and $\mathcal{R}_o$ with T_{pqr} and W_{pqr}. Because equation (3-50) takes coefficients from both sides of the interface it is not possible to solve directly for A_{pqr} for $(p,q,r) \in \mathcal{R}_\Delta$, where $\mathcal{R}_\Delta = \mathcal{R}_c \cup \mathcal{L}_o$.

To find a solution, it is convenient to separate modes into further subsets. Define,

$$\begin{array}{lll} \mathcal{LR}_o = \mathcal{L}_o \cap \mathcal{R}_o & & \text{modes common to left and right open sets} \\ \mathcal{LR}_c = \mathcal{L}_c \cap \mathcal{R}_c & & \text{modes common to left and right closed sets} \\ \mathcal{L}_{\Delta o} = \mathcal{L}_o - \mathcal{LR}_o & = \mathcal{L}_o \cup \mathcal{R}_o - \mathcal{R}_o & \text{modes in } \mathcal{L}_o \text{ which do not occur in } \mathcal{R}_o \\ \mathcal{R}_{\Delta o} = \mathcal{R}_o - \mathcal{LR}_o & = \mathcal{L}_o \cup \mathcal{R}_o - \mathcal{L}_o & \text{modes in } \mathcal{R}_o \text{ which do not occur in } \mathcal{L}_o \\ \mathcal{L}_{\Delta c} = \mathcal{L}_c - \mathcal{LR}_c & = \mathcal{L}_c \cup \mathcal{R}_c - \mathcal{R}_c & \text{modes in } \mathcal{L}_c \text{ which do not occur in } \mathcal{R}_c \\ \mathcal{R}_{\Delta c} = \mathcal{R}_c - \mathcal{LR}_c & = \mathcal{L}_c \cup \mathcal{R}_c - \mathcal{L}_c & \text{modes in } \mathcal{R}_c \text{ which do not occur in } \mathcal{L}_c \end{array} \qquad 3\text{-}51$$

We assume, as before, that $\mathcal{L}_o \cup \mathcal{L}_c = \mathcal{R}_o \cup \mathcal{R}_c = \mathcal{T}$ and $\mathcal{L}_o \cap \mathcal{L}_c = \mathcal{R}_o \cap \mathcal{R}_c = 0$. This implies,

$$\mathcal{L}_{\Delta c} \subseteq \mathcal{R}_{\Delta o} \qquad 3\text{-}52$$

$$\mathcal{R}_{\Delta c} \subseteq \mathcal{L}_{\Delta o} \qquad 3\text{-}53$$

$$\mathcal{R}_{\Delta o} \subseteq \mathcal{L}_{\Delta c} \qquad 3\text{-}54$$

$$\mathcal{L}_{\Delta o} \subseteq \mathcal{R}_{\Delta c} \qquad 3\text{-}55$$

But pairs (3-52), (3-54) and (3-53), (3-55) can both be true only with equality, that is,

$$\begin{array}{lll} \mathcal{L}_{\Delta c} = \mathcal{R}_{\Delta o} & & \\ \mathcal{R}_{\Delta c} = \mathcal{L}_{\Delta o} & & 3\text{-}56 \\ & & 3\text{-}57 \end{array}$$

Now we return to (3-48), re-arrange to obtain the expression for T_{pqr} valid for all (p,q,r), and substitute this in to (3-45) so that,

$$\sum_{pqr}^{\infty} \frac{\underline{\phi}_{pqr}(x,y)}{\xi^{(1)}_{pqr} + \xi^{(2)}_{pqr}} \left(2A_{pqr}\xi^{(1)}_{pqr} + 2W_{pqr}\xi^{(2)}_{pqr} - \sum_{l=1}^{M} F_l \iint_{El} \underline{J}_l(x',y').\underline{\phi}^{\star}_{pqr}(x',y')dx'dy' \right) \qquad 3\text{-}58$$

$$= \underline{\underline{\Omega}}_s(x,y) \sum_{l=1}^{M} F_l \underline{J}_l(x,y) \qquad \text{for } x,y \in \text{FSS element.}$$

As in the piece-wise constant model of conductance, we will assume a piece-wise constant model of the resistance and expand,

$$\underline{\underline{\Omega}}_s(x,y) = \sum_{k=1}^{K} \underline{\underline{\Omega}}_k p_k(x,y) \qquad 3\text{-}59$$

where $p_k(x,y)$ are a set of K piece-wise constant scalar shape functions.

We now apply the above defined mode groupings to the sums over A_{pqr} and W_{pqr} in (3-58), assuming that the sums to infinity are approximated by the sums over $\mathcal{T}$. The sum over A_{pqr} can be represented in terms only of left modes,

$$\sum_{pqr}^{\infty}...A_{pqr} \approx \sum_{pqr\in\mathcal{T}}...A_{pqr} = \sum_{pqr\in\mathcal{LR}_o}...A_{pqr} + \sum_{pqr\in\mathcal{L}_{\Delta o}}...A_{pqr} + \sum_{pqr\in\mathcal{LR}_c}...A_{pqr} + \sum_{pqr\in\mathcal{L}_{\Delta c}}...A_{pqr} \qquad 3\text{-}60$$

Similarly, the sum over W_{pqr} can be represented in terms only of right modes,

$$\sum_{pqr}^{\infty}...W_{pqr} \approx \sum_{pqr\in\mathcal{T}}...W_{pqr} = \sum_{pqr\in\mathcal{LR}_o}...W_{pqr} + \sum_{pqr\in\mathcal{R}_{\Delta o}}...W_{pqr} + \sum_{pqr\in\mathcal{LR}_c}...W_{pqr} + \sum_{pqr\in\mathcal{R}_{\Delta c}}...W_{pqr} \qquad 3\text{-}61$$

Using (3-57) to replace the sums over $\mathcal{L}_{\Delta c}$ and $\mathcal{R}_{\Delta c}$ by $\mathcal{R}_{\Delta o}$ and $\mathcal{L}_{\Delta o}$ and substituting (3-59) in (3-58), equation (3-58) becomes,

$$2\sum_{pqr\in\mathcal{L}_{\Delta o}} \frac{\underline{\phi}_{pqr}(x,y)}{\xi^{(1)}_{pqr}+\xi^{(2)}_{pqr}}(A_{pqr}\xi^{(1)}_{pqr}+W_{pqr}\xi^{(2)}_{pqr}) + 2\sum_{pqr\in\mathcal{R}_{\Delta o}} \frac{\underline{\phi}_{pqr}(x,y)}{\xi^{(1)}_{pqr}+\xi^{(2)}_{pqr}}(A_{pqr}\xi^{(1)}_{pqr}+W_{pqr}\xi^{(2)}_{pqr})$$

$$+2\sum_{pqr\in\mathcal{LR}_o} \frac{\underline{\phi}_{pqr}(x,y)}{\xi^{(1)}_{pqr}+\xi^{(2)}_{pqr}}(A_{pqr}\xi^{(1)}_{pqr}+W_{pqr}\xi^{(2)}_{pqr}) + 2\sum_{pqr\in\mathcal{LR}_c} \frac{\underline{\phi}_{pqr}(x,y)}{\xi^{(1)}_{pqr}+\xi^{(2)}_{pqr}}(A_{pqr}\xi^{(1)}_{pqr}+W_{pqr}\xi^{(2)}_{pqr})$$

$$-\sum_{pqr\in\mathcal{T}} \frac{\underline{\phi}_{pqr}(x,y)}{\xi^{(1)}_{pqr}+\xi^{(2)}_{pqr}} \iint_{El} \sum_{l=1}^{M} F_l \underline{\jmath}_l(x',y').\underline{\phi}^{\star}_{pqr}(x',y')dx'dy' = \sum_{k=1}^{K} \underline{\underline{\Omega}}_k.\left(p_k(x,y)\sum_{l=1}^{M} F_l \underline{\jmath}_l(x,y)\right) \qquad 3\text{-}62$$

We may now employ,

$$\begin{array}{rcl} A_{pqr} & = & Z^{(B)\prime}_{12,pqr}R_{pqr} \quad \text{for } (p,q,r)\in\mathcal{LR}_c \\ W_{pqr} & = & Z^{(B)\prime\prime}_{21,pqr}T_{pqr} \quad \text{for } (p,q,r)\in\mathcal{LR}_c \end{array} \qquad 3\text{-}63$$

and

$$\begin{array}{rcl} A_{pqr} & = & Z^{(B)\prime}_{12,pqr}R_{pqr} \quad \text{for } (p,q,r)\in\mathcal{L}_{\Delta c} \quad \text{i.e. } (p,q,r)\in\mathcal{R}_{\Delta o} \\ W_{pqr} & = & Z^{(B)\prime\prime}_{21,pqr}T_{pqr} \quad \text{for } (p,q,r)\in\mathcal{R}_{\Delta c} \quad \text{i.e. } (p,q,r)\in\mathcal{L}_{\Delta o} \end{array} \qquad 3\text{-}64$$

Substituting (3-48) in to the second line of (3-64) implies,

$$2A_{pqr}\xi^{(1)}_{pqr} - W_{pqr}\left(\frac{\xi^{(1)}_{pqr}+\xi^{(2)}_{pqr}}{Z^{(B)\prime\prime}_{21,pqr}} + \xi^{(1)}_{pqr} - \xi^{(2)}_{pqr}\right) = \sum F_l \iint_{El} \underline{\jmath}_l(x',y').\underline{\phi}^{\star}_{pqr}(x',y')dx'dy' \qquad 3\text{-}65$$
$$\text{for } (p,q,r)\in\mathcal{L}_{\Delta o}$$

Using,

$$A_{pqr} + R_{pqr} = T_{pqr} + W_{pqr} \qquad \text{for all p,q,r} \qquad 3\text{-}66$$

an alternative form for (3-48) is,

$$2W_{pqr}\xi^{(2)}_{pqr} - R_{pqr}(\xi^{(1)}_{pqr} + \xi^{(2)}_{pqr}) + A_{pqr}(\xi^{(1)}_{pqr} - \xi^{(2)}_{pqr}) = \sum_{l=1}^{M} F_l \iint_{El} \underline{\jmath}_l(x', y').\underline{\phi}^{\star}_{pqr}(x', y')dx'dy'$$
$$\text{for all p,q,r} \tag{3-67}$$

Substituting (3-67) in to the first line of (3-64) implies,

$$2W_{pqr}\xi^{(2)}_{pqr} - A_{pqr}\left(\frac{\xi^{(1)}_{pqr} + \xi^{(2)}_{pqr}}{Z^{(B)\prime}_{12,pqr}} - \xi^{(1)}_{pqr} + \xi^{(2)}_{pqr}\right) = \sum F_l \iint_{El} \underline{\jmath}_l(x', y').\underline{\phi}^{\star}_{pqr}(x', y')dx'dy' \tag{3-68}$$
$$\text{for } (p, q, r) \in \mathcal{R}_{\Delta o}$$

For convenience, let us define,

$$\delta'_{pqr} = \frac{Z^{(B)\prime}_{12,pqr}}{(1 - Z^{(B)\prime}_{12,pqr})\xi^{(1)}_{pqr} + (1 + Z^{(B)\prime}_{12,pqr})\xi^{(2)}_{pqr}} \tag{3-69}$$

and

$$\delta''_{pqr} = \frac{Z^{(B)\prime\prime}_{21,pqr}}{(1 + Z^{(B)\prime\prime}_{21,pqr})\xi^{(1)}_{pqr} + (1 - Z^{(B)\prime\prime}_{21,pqr})\xi^{(2)}_{pqr}} \tag{3-70}$$

Equations (3-68) and (3-65) may then be represented respectively as,

$$A_{pqr} = 2W_{pqr}\xi^{(2)}_{pqr}\delta'_{pqr} - \delta'_{pqr}\sum_{l=1}^{M} F_l \iint_{El} \underline{\jmath}_l(x', y').\underline{\phi}^{\star}_{pqr}(x', y')dx'dy' \quad \text{for } (p, q, r) \in \mathcal{R}_{\Delta o} \tag{3-71}$$

and

$$W_{pqr} = 2A_{pqr}\xi^{(1)}_{pqr}\delta''_{pqr} - \delta''_{pqr}\sum_{l=1}^{M} F_l \iint_{El} \underline{\jmath}_l(x', y').\underline{\phi}^{\star}_{pqr}(x', y')dx'dy' \quad \text{for } (p, q, r) \in \mathcal{L}_{\Delta o} \tag{3-72}$$

In addition, we require expressions for A_{pqr} and W_{pqr} for the common closed modes, $(p, q, r) \in \mathcal{LR}_c$. These may be obtained from (3-50) since $\mathcal{LR}_c \subseteq \mathcal{R}_c$. Substituting (3-63) in to (3-50), we observe that (3-65) is valid here too,

$$2A_{pqr}\xi^{(1)}_{pqr} - W_{pqr}\left(\frac{\xi^{(1)}_{pqr} + \xi^{(2)}_{pqr}}{Z^{(B)\prime\prime}_{21,pqr}} + \xi^{(1)}_{pqr} - \xi^{(2)}_{pqr}\right) = \sum_{l=1}^{M} F_l \iint_{El} \underline{\jmath}_l(x', y').\underline{\phi}^{\star}_{pqr}(x', y')dx'dy' \tag{3-73}$$
$$\text{for } (p, q, r) \in \mathcal{LR}_c$$

Equations (3-66) and (3-63) imply,

$$W_{pqr} = \left(\frac{Z^{(B)\prime\prime}_{21,pqr}(Z^{(B)\prime}_{12,pqr} + 1)}{Z^{(B)\prime}_{12,pqr}(Z^{(B)\prime\prime}_{21,pqr} + 1)}\right) A_{pqr} \quad \text{for } (p, q, r) \in \mathcal{LR}_c \tag{3-74}$$

Substituting (3-74) in (3-73) we obtain an expression for A_{pqr} for the common closed modes,

$$A_{pqr} = S^{(A)}_{pqr} \sum_{l=1}^{M} F_l \iint_{El} \underline{\jmath}_l(x', y').\underline{\phi}^{\star}_{pqr}(x', y')dx'dy' \qquad \text{for } (p, q, r) \in \mathcal{LR}_c \tag{3-75}$$

where $S^{(A)}_{pqr}$ are defined by,

$$S^{(A)}_{pqr} = \frac{Z^{(B)\prime}_{12,pqr}(Z^{(B)\prime\prime}_{21,pqr} + 1)}{\xi^{(1)}_{pqr}(Z^{(B)\prime\prime}_{21,pqr} + 1)(Z^{(B)\prime}_{12,pqr} - 1) + \xi^{(2)}_{pqr}(Z^{(B)\prime\prime}_{21,pqr} - 1)(Z^{(B)\prime}_{12,pqr} + 1)} \tag{3-76}$$

Similarly, using (3-74), we may obtain an expression for W_{pqr} for the common closed modes,

$$W_{pqr} = S^{(W)}_{pqr} \sum_{l=1}^{M} F_l \iint_{El} \underline{\jmath}_l(x', y').\underline{\phi}^{\star}_{pqr}(x', y')dx'dy' \qquad \text{for } (p, q, r) \in \mathcal{LR}_c \tag{3-77}$$

where $S^{(W)}_{pqr}$ are defined by,

$$S^{(W)}_{pqr} = \frac{Z^{(B)\prime\prime}_{21,pqr}(Z^{(B)\prime}_{12,pqr} + 1)}{\xi^{(1)}_{pqr}(Z^{(B)\prime\prime}_{21,pqr} + 1)(Z^{(B)\prime}_{12,pqr} - 1) + \xi^{(2)}_{pqr}(Z^{(B)\prime\prime}_{21,pqr} - 1)(Z^{(B)\prime}_{12,pqr} + 1)} \tag{3-78}$$

Analogous to the slot formulation, we will introduce the following symbol definitions,

$$U_{pqr}(\mathcal{L}_{\Delta o}) = \begin{cases} 1 & \text{for } (p, q, r) \in \mathcal{L}_{\Delta o} = \mathcal{R}_{\Delta c} \\ 0 & \text{otherwise} \end{cases} \tag{3-79}$$

$$U_{pqr}(\mathcal{R}_{\Delta o}) = \begin{cases} 1 & \text{for } (p, q, r) \in \mathcal{R}_{\Delta o} = \mathcal{L}_{\Delta c} \\ 0 & \text{otherwise} \end{cases} \tag{3-80}$$

$$U_{pqr}(\mathcal{LR}_o) = \begin{cases} 1 & \text{for } (p, q, r) \in \mathcal{LR}_o \\ 0 & \text{otherwise} \end{cases} \tag{3-81}$$

$$U_{pqr}(\mathcal{LR}_c) = \begin{cases} 1 & \text{for } (p, q, r) \in \mathcal{LR}_c \\ 0 & \text{otherwise} \end{cases} \tag{3-82}$$

We may now substitute (3-75), (3-77), (3-71) and (3-72) over valid domains in to (3-62). Since $\mathcal{LR}_o \subseteq \mathcal{L}_o$, $\mathcal{L}_{\Delta o} \subseteq \mathcal{L}_o$ and also $\mathcal{LR}_o \subseteq \mathcal{R}_o$, $\mathcal{R}_{\Delta o} \subseteq \mathcal{R}_o$, we may group sums over $\mathcal{L}_o$ and $\mathcal{R}_o$. Thus (3-62) becomes,

$$
\begin{aligned}
&2\sum_{(p,q,r)\in\mathcal{L}_o}\frac{A_{pqr}\left[U_{pqr}(\mathcal{LR}_o)\xi^{(1)}_{pqr}+U_{pqr}(\mathcal{L}_{\Delta o})\left\{\xi^{(1)}_{pqr}+2\xi^{(1)}_{pqr}\xi^{(2)}_{pqr}\delta''_{pqr}\right\}\right]\underline{\phi}_{pqr}(x,y)}{\xi^{(1)}_{pqr}+\xi^{(2)}_{pqr}}\\
&+2\sum_{(p,q,r)\in\mathcal{R}_o}\frac{W_{pqr}\left[U_{pqr}(\mathcal{LR}_o)\xi^{(2)}_{pqr}+U_{pqr}(\mathcal{R}_{\Delta o})\left\{\xi^{(2)}_{pqr}+2\xi^{(1)}_{pqr}\xi^{(2)}_{pqr}\delta'_{pqr}\right\}\right]\underline{\phi}_{pqr}(x,y)}{\xi^{(1)}_{pqr}+\xi^{(2)}_{pqr}}\\
&-\sum_{(p,q,r)\in\mathcal{T}}\left(\frac{1+2U_{pqr}(\mathcal{L}_{\Delta o})\xi^{(2)}_{pqr}\delta''_{pqr}+2U_{pqr}(\mathcal{R}_{\Delta o})\xi^{(1)}_{pqr}\delta'_{pqr}-2U_{pqr}(\mathcal{LR}_c)\left\{\xi^{(1)}_{pqr}S^{(A)}_{pqr}+\xi^{(2)}_{pqr}S^{(B)}_{pqr}\right\}}{\xi^{(1)}_{pqr}+\xi^{(2)}_{pqr}}\right)\times\\
&\times\sum_{l=1}^{M}F_l\underline{\phi}_{pqr}(x,y)\iint_{El}\underline{\jmath}_l(x',y').\underline{\phi}^{\star}_{pqr}(x',y')dx'dy'\\
&=\sum_{k=1}^{K}\underline{\underline{\Omega}}_k.\left(p_k(x,y)\sum_{l=1}^{M}F_l\underline{\jmath}_l(x,y)\right)\qquad\text{for } x,y \text{ in FSS element.}
\end{aligned}
\tag{3-83}
$$

For convenience let us define,

$$
\begin{aligned}
\eta^{(1)}_{pqr} &= \frac{\xi^{(1)}_{pqr}}{\xi^{(1)}_{pqr}+\xi^{(2)}_{pqr}}\\
\eta^{(2)}_{pqr} &= \frac{\xi^{(2)}_{pqr}}{\xi^{(1)}_{pqr}+\xi^{(2)}_{pqr}}
\end{aligned}
\tag{3-84}
$$

$$
\begin{aligned}
\overline{\eta}^{(1)}_{pqr} &= \eta^{(1)}_{pqr}\left[U_{pqr}(\mathcal{LR}_o)+U_{pqr}(\mathcal{L}_{\Delta o})\left\{1+2\xi^{(2)}_{pqr}\delta''_{pqr}\right\}\right]\\
\overline{\eta}^{(2)}_{pqr} &= \eta^{(2)}_{pqr}\left[U_{pqr}(\mathcal{LR}_o)+U_{pqr}(\mathcal{R}_{\Delta o})\left\{1+2\xi^{(1)}_{pqr}\delta'_{pqr}\right\}\right]
\end{aligned}
\tag{3-85}
$$

and

$$
\overline{\chi}_{pqr}=\frac{1+2U_{pqr}(\mathcal{L}_{\Delta o})\xi^{(2)}_{pqr}\delta''_{pqr}+2U_{pqr}(\mathcal{R}_{\Delta o})\xi^{(1)}_{pqr}\delta'_{pqr}-2U_{pqr}(\mathcal{LR}_c)\left\{\xi^{(1)}_{pqr}S^{(A)}_{pqr}+\xi^{(2)}_{pqr}S^{(B)}_{pqr}\right\}}{\xi^{(1)}_{pqr}+\xi^{(2)}_{pqr}}
\tag{3-86}
$$

Forming the dot product of $\underline{\jmath}^{\star}_m(x,y)$ with (3-83) and integrating over the unit cell conducting elements, we then obtain the expression,

$$
2\sum_{(p,q,r)\in\mathcal{L}_o}A_{pqr}\overline{\eta}^{(1)}_{pqr}\overline{C}^{\star}_{pqr,m}+2\sum_{(p,q,r)\in\mathcal{R}_o}W_{pqr}\overline{\eta}^{(2)}_{pqr}\overline{C}^{\star}_{pqr,m}=\sum_{(p,q,r)\in\mathcal{T}}\overline{\chi}_{pqr}\overline{C}^{\star}_{pqr,m}\sum_{l=1}^{M}F_l\overline{C}_{pqr,l}+\sum_{l=1}^{M}\overline{R}_{ml}F_l
\tag{3-87}
$$

where for elements,

$$
\overline{C}_{pqr,l}=\iint_{El}\underline{\jmath}_l(x',y').\underline{\phi}^{\star}_{pqr}(x',y')dx'dy'
\tag{3-88}
$$

and

$$
\overline{R}_{ml}=\sum_{k=1}^{K}\iint_{El}[\underline{\underline{\Omega}}_k.\underline{\jmath}_l(x',y')].\underline{\jmath}^{\star}_m(x',y')p_k(x',y')dx'dy'
\tag{3-89}
$$

Using the matrix notation defined for the slot formulation, modified by the overline symbol to designate overline coefficients,

$$2\overline{\boldsymbol{C}}_{Lo}^{\dagger}\overline{\boldsymbol{\eta}}_{Lo}^{(1)}\underline{A}_{Lo} + 2\overline{\boldsymbol{C}}_{Ro}^{\dagger}\overline{\boldsymbol{\eta}}_{Ro}^{(2)}\underline{W}_{Ro} = \overline{\boldsymbol{Y}}\,\underline{F} \tag{3-90}$$

where $\overline{\boldsymbol{Y}}$ is now defined by,

$$\overline{\boldsymbol{Y}} = \overline{\boldsymbol{C}}^{\dagger}\overline{\boldsymbol{\chi}}\overline{\boldsymbol{C}} + \overline{\boldsymbol{R}} \tag{3-91}$$

giving the expression for the unknown coefficients of $\underline{F}$ in terms of the incoming wave coefficients,

$$\underline{F} = 2\overline{\boldsymbol{Y}}^{-1}(\boldsymbol{C}_{Lo}^{\dagger}\overline{\boldsymbol{\eta}}_{Lo}^{(1)}\underline{A}_{Lo} + \boldsymbol{C}_{Ro}^{\dagger}\overline{\boldsymbol{\eta}}_{Ro}^{(2)}\underline{W}_{Ro}) \tag{3-92}$$

which are the analogues of (3-31) and (3-33). Here, as there, it is not necessary to explicitly determine $\underline{F}$ unless the electric currents are required.

Next we need to determine the coefficients T_{pqr} for $(p,q,r) \in \mathcal{R}_o$ and R_{pqr} for $(p,q,r) \in \mathcal{L}_o$, given $\underline{A}_{Lo}$ and $\underline{W}_{Ro}$. The procedure is more complex than for the slotted case. First we will obtain T_{pqr} for $(p,q,r) \in \mathcal{R}_{\Delta o}$. Substituting A_{pqr} from (3-48) in to (3-71) we obtain,

$$T_{pqr} = \alpha_{pqr}^{(R\Delta o)}W_{pqr} + \beta_{pqr}^{(R\Delta o)}\sum_{l=1}^{M} F_l\underline{\phi}_{pqr}(x,y)\iint_{El}\underline{\jmath}_l(x',y').\underline{\phi}_{pqr}^{\star}(x',y')dx'dy' \quad \text{for } (p,q,r) \in \mathcal{R}_{\Delta o} \tag{3-93}$$

where

$$\alpha_{pqr}^{(R\Delta o)} = \frac{\xi_{pqr}^{(2)}(Z_{12,pqr}^{(B)\prime}+1) + \xi_{pqr}^{(1)}(Z_{12,pqr}^{(B)\prime}-1)}{\xi_{pqr}^{(2)}(Z_{12,pqr}^{(B)\prime}+1) - \xi_{pqr}^{(1)}(Z_{12,pqr}^{(B)\prime}-1)} \tag{3-94}$$

and

$$\beta_{pqr}^{(R\Delta o)} = \frac{-(1+Z_{12,pqr}^{(B)\prime})}{\xi_{pqr}^{(1)}(1-Z_{12,pqr}^{(B)\prime}) + \xi_{pqr}^{(2)}(1+Z_{12,pqr}^{(B)\prime})} \tag{3-95}$$

Let us designate this set of T_{pqr} by $T_{pqr}^{(\Delta o)}$.

Next we will obtain T_{pqr} for $(p,q,r) \in \mathcal{LR}_o$. This time we require A_{pqr} for $(p,q,r) \in \mathcal{LR}_o$ since these propagating terms contribute to the fields and currents on the FSS. Equation (3-48) remains valid so that, under a re-arrangement of terms,

$$T_{pqr} = 2\eta_{pqr}^{(1)}A_{pqr} + \alpha_{pqr}^{(LR_o)}W_{pqr} + \beta_{pqr}^{(LR_o)}\sum_{l=1}^{M} F_l\underline{\phi}_{pqr}(x,y)\iint_{El}\underline{\jmath}_l(x',y').\underline{\phi}_{pqr}^{\star}(x',y')dx'dy' \quad \text{for } (p,q,r) \in \mathcal{LR}_o \tag{3-96}$$

where

$$\alpha_{pqr}^{(LR_o)} = \frac{\xi_{pqr}^{(2)} - \xi_{pqr}^{(1)}}{\xi_{pqr}^{(2)} + \xi_{pqr}^{(1)}} \tag{3-97}$$

and

$$\beta_{pqr}^{(LR_o)} = -\frac{1}{\xi_{pqr}^{(2)} + \xi_{pqr}^{(1)}} \tag{3-98}$$

Let us designate this set of T_{pqr} by $T_{pqr}^{(LR_o)}$.

Since $\mathcal{LR}_o \cap \mathcal{R}_{\Delta o} = 0$, the expressions (3-93) and (3-96) for T_{pqr} may be formally combined as,

$$T_{pqr} = U_{pqr}(\mathcal{R}_{\Delta o})T_{pqr}^{(\Delta o)} + U_{pqr}(\mathcal{LR}_o)T_{pqr}^{(LR_o)} \qquad \text{for all } (p,q,r) \in \mathcal{L}_o \tag{3-99}$$

which allows us a simple vector/matrix notation with $\underline{T}_{Ro}$ being the vector with elements T_{pqr} for $(p,q,r) \in \mathcal{L}_o$, ordered as in the slot formulation convention.

We define the permuted diagonal matrix $\boldsymbol{\alpha}_{Ro} = pdiag(\alpha_{pqr}^{(Ro)})$, where

$$\alpha_{pqr}^{(Ro)} = \begin{cases} \alpha_{pqr}^{(R\Delta o)} & \text{for } (p,q,r) \in \mathcal{R}_{\Delta o} \\ \alpha_{pqr}^{(LR_o)} & \text{for } (p,q,r) \in \mathcal{LR}_o \end{cases} \tag{3-100}$$

Similarly, we define the permuted diagonal matrix $\boldsymbol{\beta}_{Ro} = pdiag(\beta_{pqr}^{(Ro)})$, where

$$\beta_{pqr}^{(Ro)} = \begin{cases} \beta_{pqr}^{(R\Delta o)} & \text{for } (p,q,r) \in \mathcal{R}_{\Delta o} \\ \beta_{pqr}^{(LR_o)} & \text{for } (p,q,r) \in \mathcal{LR}_o \end{cases} \tag{3-101}$$

We also define the permuted diagonal matrices $\boldsymbol{\eta}_{RL}^{(1)} = pdiag(\eta_{pqr}^{(1,RL)})$, where

$$\eta_{pqr}^{(1,RL)} = \begin{cases} \eta_{pqr}^{(1)} & \text{for } (p,q,r) \in \mathcal{LR}_o \\ 0 & \text{otherwise} \end{cases} \tag{3-102}$$

and $\boldsymbol{\eta}_{RL}^{(2)} = pdiag(\eta_{pqr}^{(2,RL)})$, where

$$\eta_{pqr}^{(2,RL)} = \begin{cases} \eta_{pqr}^{(2)} & \text{for } (p,q,r) \in \mathcal{LR}_o \\ 0 & \text{otherwise} \end{cases} \tag{3-103}$$

Also, $\overline{\boldsymbol{\eta}}_{Lo}^{(1)} = pdiag(\overline{\eta}_{pqr}^{(1)})$ (with valid entries for $(p,q,r) \in \mathcal{L}_o$) and $\overline{\boldsymbol{\eta}}_{Ro}^{(2)} = pdiag(\overline{\eta}_{pqr}^{(2)})$ (with valid entries for $(p,q,r) \in \mathcal{R}_o$).

Using this notation and using (3-92) we obtain,

$$\underline{T}_{Ro} = 2(\boldsymbol{\eta}_{RL}^{(1)} + \boldsymbol{\beta}_{Ro}\boldsymbol{Q}_{RoLo}\overline{\boldsymbol{\eta}}_{Lo}^{(1)})\underline{A}_{Lo} + (\boldsymbol{\alpha}_{Ro} + 2\boldsymbol{\beta}_{Ro}\boldsymbol{Q}_{RoRo}\overline{\boldsymbol{\eta}}_{Ro}^{(2)})\underline{W}_{Ro} \tag{3-104}$$

where

$$\begin{aligned} \boldsymbol{Q}_{RoLo} &= \overline{\boldsymbol{C}}_{Ro}\overline{\boldsymbol{Y}}^{-1}\overline{\boldsymbol{C}}_{Lo}^{\dagger} \\ \boldsymbol{Q}_{RoRo} &= \overline{\boldsymbol{C}}_{Ro}\overline{\boldsymbol{Y}}^{-1}\overline{\boldsymbol{C}}_{Ro}^{\dagger} \end{aligned} \tag{3-105}$$

The same methods for the construction and storage of elements of the $\boldsymbol{Q}$ matrices are employed as described in the aperture formulation.

The next step is to determine the reflection coefficients R_{pqr} following the earlier method (equation (3-93) on). R_{pqr} are required for $(p,q,r) \in \mathcal{L}_o$, first for $(p,q,r) \in \mathcal{L}_{\Delta o}$ and then for $(p,q,r) \in \mathcal{LR}_o$.

Using the second equation of (3-64) and (3-66), we have

$$A_{pqr} + R_{pqr} = W_{pqr}\left(1 + \frac{1}{Z^{(B)\prime\prime}_{21,pqr}}\right) \qquad \text{for } (p,q,r) \in \mathcal{L}_{\Delta o} \tag{3-106}$$

Substituting this in (3-72) implies,

$$R_{pqr} = \alpha^{(L\Delta o)}_{pqr} A_{pqr} + \beta^{(L\Delta o)}_{pqr} \sum_{l=1}^{M} F_l \iint_{El} \underline{\jmath}_l(x',y').\underline{\phi}^{\star}_{pqr}(x',y')dx'dy' \qquad \text{for } (p,q,r) \in \mathcal{L}_{\Delta o} \tag{3-107}$$

where

$$\alpha^{(L\Delta o)}_{pqr} = \frac{\xi^{(1)}_{pqr}(Z^{(B)\prime\prime}_{21,pqr}+1) + \xi^{(2)}_{pqr}(Z^{(B)\prime\prime}_{21,pqr}-1)}{\xi^{(1)}_{pqr}(Z^{(B)\prime\prime}_{21,pqr}+1) - \xi^{(2)}_{pqr}(Z^{(B)\prime\prime}_{21,pqr}-1)} \tag{3-108}$$

and

$$\beta^{(L\Delta o)}_{pqr} = \frac{-(1+Z^{(B)\prime\prime}_{21,pqr})}{\xi^{(1)}_{pqr}(1+Z^{(B)\prime\prime}_{21,pqr}) + \xi^{(2)}_{pqr}(1-Z^{(B)\prime\prime}_{21,pqr})} \tag{3-109}$$

Using, for example, (3-96) and (3-66) we also have,

$$R_{pqr} = 2\eta^{(2)}_{pqr} W_{pqr} - \alpha^{(LR_o)}_{pqr} A_{pqr} + \beta^{(LR_o)}_{pqr} \sum_{l=1}^{M} F_l \underline{\phi}_{pqr}(x,y) \iint_{El} \underline{\jmath}_l(x',y').\underline{\phi}^{\star}_{pqr}(x',y')dx'dy' \qquad \text{for } (p,q,r) \in \mathcal{LR}_o \tag{3-110}$$

Equations (3-107) and (3-110) may be cast in vector/matrix notation as before. Let the permuted diagonal matrix $\boldsymbol{\alpha}_{Lo} = pdiag(\alpha^{(Lo)}_{pqr})$, where

$$\alpha^{(Lo)}_{pqr} = \begin{cases} \alpha^{(L\Delta o)}_{pqr} & \text{for } (p,q,r) \in \mathcal{L}_{\Delta o} \\ -\alpha^{(LR_o)}_{pqr} & \text{for } (p,q,r) \in \mathcal{LR}_o \end{cases} \tag{3-111}$$

Similarly, we define the permuted diagonal matrix $\boldsymbol{\beta}_{Lo} = pdiag(\beta^{(Lo)}_{pqr})$, where

$$\beta^{(Lo)}_{pqr} = \begin{cases} \beta^{(L\Delta o)}_{pqr} & \text{for } (p,q,r) \in \mathcal{L}_{\Delta o} \\ \beta^{(LR_o)}_{pqr} & \text{for } (p,q,r) \in \mathcal{LR}_o \end{cases} \tag{3-112}$$

Also define,

$$\begin{aligned} \boldsymbol{Q}_{LoRo} &= \overline{\boldsymbol{C}}_{Lo}\overline{\boldsymbol{Y}}^{-1}\overline{\boldsymbol{C}}^{\dagger}_{Ro} \\ \boldsymbol{Q}_{LoLo} &= \overline{\boldsymbol{C}}_{Lo}\overline{\boldsymbol{Y}}^{-1}\overline{\boldsymbol{C}}^{\dagger}_{Lo} \end{aligned} \tag{3-113}$$

We then obtain the vector/matrix form,

$$\underline{R}_{Lo} = 2(\boldsymbol{\eta}^{(2)}_{RL} + \boldsymbol{\beta}_{Lo}\boldsymbol{Q}_{LoRo}\overline{\boldsymbol{\eta}}^{(2)}_{Ro})\underline{W}_{Ro} + (\boldsymbol{\alpha}_{Lo} + 2\boldsymbol{\beta}_{Lo}\boldsymbol{Q}_{LoLo}\overline{\boldsymbol{\eta}}^{(1)}_{Lo})\underline{A}_{Lo} \tag{3-114}$$

Equations (3-104) and (3-114) define the $\boldsymbol{X}_{ij}^{(n)\prime}$ coupling matrices between open modes for the element formulation. Using the previous notation if,

$$\begin{pmatrix} \underline{T}_{Ro} \\ \underline{R}_{Lo} \end{pmatrix} = \begin{pmatrix} \boldsymbol{X}_{11}^{(n)\prime} & \boldsymbol{X}_{12}^{(n)\prime} \\ \boldsymbol{X}_{21}^{(n)\prime} & \boldsymbol{X}_{22}^{(n)\prime} \end{pmatrix} \begin{pmatrix} \underline{A}_{Lo} \\ \underline{W}_{Ro} \end{pmatrix} \qquad 3\text{-}115$$

then for elements,

$$\begin{pmatrix} \boldsymbol{X}_{11}^{(n)\prime} & \boldsymbol{X}_{12}^{(n)\prime} \\ \boldsymbol{X}_{21}^{(n)\prime} & \boldsymbol{X}_{22}^{(n)\prime} \end{pmatrix} = \begin{pmatrix} 2(\boldsymbol{\eta}_{RL}^{(1)} + \boldsymbol{\beta}_{Ro}\boldsymbol{Q}_{RoLo}\overline{\boldsymbol{\eta}}_{Lo}^{(1)}) & \boldsymbol{\alpha}_{Ro} + 2\boldsymbol{\beta}_{Ro}\boldsymbol{Q}_{RoRo}\overline{\boldsymbol{\eta}}_{Ro}^{(2)} \\ \boldsymbol{\alpha}_{Lo} + 2\boldsymbol{\beta}_{Lo}\boldsymbol{Q}_{LoLo}\overline{\boldsymbol{\eta}}_{Lo}^{(1)} & 2(\boldsymbol{\eta}_{RL}^{(2)} + \boldsymbol{\beta}_{Lo}\boldsymbol{Q}_{LoRo}\overline{\boldsymbol{\eta}}_{Ro}^{(2)}) \end{pmatrix} \qquad 3\text{-}116$$

This completes the advanced coupling element formulation. In the simple coupling scheme we perform the same simplification as in the slotted case. In particular, we redefine all modes as open modes and ignore any such modes which fall below the threshold defined in section 2.6. We may thus use the above expression with $\mathcal{L}_c = \mathcal{R}_c = 0$ and $\mathcal{L}_o$ and $\mathcal{R}_o$ chosen as subsets of $\mathcal{T}$ according to the threshold criterion. In fact, this disguises a subtlety since it is possible that the coupling modes to left and right of the FSS may not necessarily match even in the simple coupling scheme. Thus it is not necessarily true that $U_{pqr}(\mathcal{L}\mathcal{R}_o) = 1$ for all accounted modes (p, q, r). Similarly, it is not necessarily true that $U_{pqr}(\mathcal{L}_{\Delta o})$ or $U_{pqr}(\mathcal{R}_{\Delta o}) = 0$ for all accounted modes. However, this would require elements of the advanced formulation which we do not want for the simple scheme. Accordingly, we will *assume* left and right thresholds chosen sufficiently small that $U_{pqr}(\mathcal{L}\mathcal{R}_o) \approx 1$ and $U_{pqr}(\mathcal{L}_{\Delta o}) \approx U_{pqr}(\mathcal{R}_{\Delta o}) \approx 0$ in the simple coupling scheme.

This approximation allows us to ignore terms involving $Z_{12}^{(B)\prime}$ and $Z_{21}^{(B)\prime\prime}$ and we have,

$$\left.\begin{array}{c} \overline{\eta}_{pqr}^{(1)} = \eta_{pqr}^{(1)} \\ \overline{\eta}_{pqr}^{(2)} = \eta_{pqr}^{(2)} \\ \alpha_{pqr}^{(Ro)} = \alpha_{pqr}^{(LR_o)} \\ \alpha_{pqr}^{(Lo)} = -\alpha_{pqr}^{(LR_o)} \\ \beta_{pqr}^{(Ro)} = \beta_{pqr}^{(Lo)} = \beta_{pqr}^{(LR_o)} \\ \overline{\chi}_{pqr} = -\beta_{pqr}^{(LR_o)} \end{array}\right\} \quad \text{for all accounted } (p, q, r) \qquad 3\text{-}117$$

completing the element formulation under the simple coupling scheme.

3.5 The equivalent impedance and admittance of an FSS

It is possible to regard any FSS in an arbitrary composite as electrically equivalent to a uniform thin impedance layer at the same position in the composite. This is a useful design aid in the design of composites in terms of impedance layers, e.g. for Jaumann absorbers and Salisbury screens. In many applications, where differences in evanescent couplings to an FSS are not critically dependent on the rest of the composite, the equivalent impedance may be approximately independent of the layer thicknesses. Formally, the equivalent impedance of an FSS will be independent of the composite dimensions if coupling is primarily through the zero-order Floquet modes.

The equivalent impedance or admittance of a general FSS within a general composite will be a tensor quantity, represented by a 2×2 complex valued matrix. We would usually expect the Eigenvectors of the matrix to be orthogonal, in which case the matrix is diagonalised by a real valued rotation matrix, characterised by a rotation angle α. However, further study is required on this topic and no such constraint is made here.

As illustrated in the previous sections, the vectors of incoming and outgoing transmission and reflection coefficients at any interface in the composite take the form,

$$\begin{pmatrix} \underline{T} \\ \underline{R} \end{pmatrix} = \begin{pmatrix} \boldsymbol{X}_{11} & \boldsymbol{X}_{12} \\ \boldsymbol{X}_{21} & \boldsymbol{X}_{22} \end{pmatrix} \begin{pmatrix} \underline{A} \\ \underline{W} \end{pmatrix} \qquad \text{3-118}$$

From this matrix, we may consider the sub-set of zero-order Floquet mode coefficients, designated by a subscript 0 for the vectors and a superscript (0) for the matrix coupling terms. The subscripted 2-term vectors represent the $p = q = 0$ coefficients for the different polarisation states designated by $r = 1$ and $r = 2$,

$$\begin{pmatrix} \underline{T}_0 \\ \underline{R}_0 \end{pmatrix} = \begin{pmatrix} \boldsymbol{X}_{11}^{(0)} & \boldsymbol{X}_{12}^{(0)} \\ \boldsymbol{X}_{21}^{(0)} & \boldsymbol{X}_{22}^{(0)} \end{pmatrix} \begin{pmatrix} \underline{A}_0 \\ \underline{W}_0 \end{pmatrix} \qquad \text{3-119}$$

We say that the equivalent admittance (impedance) of an FSS (or any other thin) interface is defined as the admittance (impedance) of a uniform thin material which, replacing the FSS, has the same $\boldsymbol{X}_{ij}^{(0)}$ coupling matrices in (3-119). The equivalent admittance matrix, $\boldsymbol{\sigma}$, is defined by,

$$\underline{J} = \boldsymbol{\sigma} \underline{E}_{tan} \qquad \text{3-120}$$

and the equivalent impedance matrix, $\boldsymbol{\Omega}$, is defined by,

$$\underline{E}_{tan} = \boldsymbol{\Omega} \underline{J} \qquad \text{3-121}$$

It is possible for either of these 2×2 matrices to be singular in which case the other matrix is not properly defined. The total equivalent mean tangential electric field $\underline{E}_{tan}$ is defined by,

$$\underline{E}_{tan} = \underline{A}_0 + \underline{R}_0 = \underline{T}_0 + \underline{W}_0 \qquad \text{3-122}$$

The equivalent current $\underline{J}$ is defined by,

$$\underline{J} = \boldsymbol{\xi}_1(\underline{A}_0 - \underline{R}_0) - \boldsymbol{\xi}_2(\underline{T}_0 - \underline{W}_0) \qquad 3\text{-}123$$

where $\boldsymbol{\xi}_{1,2}$ are diagonal admittance matrices with elements,

$$\boldsymbol{\xi}_1 = \begin{pmatrix} \xi^{(1)}_{001} & 0 \\ 0 & \xi^{(1)}_{002} \end{pmatrix} \qquad 3\text{-}124$$

and

$$\boldsymbol{\xi}_2 = \begin{pmatrix} \xi^{(2)}_{001} & 0 \\ 0 & \xi^{(2)}_{002} \end{pmatrix} \qquad 3\text{-}125$$

The modal admittances $\xi^{(1)}_{00r}$ and $\xi^{(2)}_{00r}$ refer to the $p = q = 0$ admittances of the material just to the left and right of the interface, respectively, as defined earlier.

Substituting these expressions into (3-119) yields the following expressions,

$$\begin{aligned}
\boldsymbol{X}^{(0)}_{11} &= 2[\boldsymbol{\sigma} + \boldsymbol{\xi}_1 + \boldsymbol{\xi}_2]^{-1}\boldsymbol{\xi}_1 && 3\text{-}126\\
\boldsymbol{X}^{(0)}_{12} &= [\boldsymbol{\sigma} + \boldsymbol{\xi}_1 + \boldsymbol{\xi}_2]^{-1}[-\boldsymbol{\sigma} + \boldsymbol{\xi}_2 - \boldsymbol{\xi}_1] && 3\text{-}127\\
\boldsymbol{X}^{(0)}_{21} &= [\boldsymbol{\sigma} + \boldsymbol{\xi}_1 + \boldsymbol{\xi}_2]^{-1}[-\boldsymbol{\sigma} + \boldsymbol{\xi}_1 - \boldsymbol{\xi}_2] && 3\text{-}128\\
\boldsymbol{X}^{(0)}_{22} &= 2[\boldsymbol{\sigma} + \boldsymbol{\xi}_1 + \boldsymbol{\xi}_2]^{-1}\boldsymbol{\xi}_2 && 3\text{-}129
\end{aligned}$$

assuming the matrix inverses exist. Each of (3-126), (3-127), (3-128) or (3-129) provides an independent means to determine $\boldsymbol{\sigma}$ or $\boldsymbol{\Omega}$. The QDAS software allows $\boldsymbol{\sigma}$ and $\boldsymbol{\Omega}$ to be determined in any way. The corresponding definitions for $\boldsymbol{\sigma}$ and $\boldsymbol{\Omega}$ are given by,

$$\begin{aligned}
\boldsymbol{\sigma} &= 2\boldsymbol{\xi}_1[\boldsymbol{X}^{(0)}_{11}]^{-1} - (\boldsymbol{\xi}_1 + \boldsymbol{\xi}_2) && 3\text{-}130\\
\boldsymbol{\sigma} &= [\boldsymbol{\xi}_2 - \boldsymbol{\xi}_1 - (\boldsymbol{\xi}_1 + \boldsymbol{\xi}_2)\boldsymbol{X}^{(0)}_{12}][\boldsymbol{X}^{(0)}_{12} + \boldsymbol{I}]^{-1} && 3\text{-}131\\
\boldsymbol{\sigma} &= [\boldsymbol{\xi}_1 - \boldsymbol{\xi}_2 - (\boldsymbol{\xi}_1 + \boldsymbol{\xi}_2)\boldsymbol{X}^{(0)}_{21}][\boldsymbol{X}^{(0)}_{21} + \boldsymbol{I}]^{-1} && 3\text{-}132\\
\boldsymbol{\sigma} &= 2\boldsymbol{\xi}_2[\boldsymbol{X}^{(0)}_{22}]^{-1} - (\boldsymbol{\xi}_1 + \boldsymbol{\xi}_2) && 3\text{-}133
\end{aligned}$$

and

$$\begin{aligned}
\boldsymbol{\Omega} &= \boldsymbol{X}^{(0)}_{11}[2\boldsymbol{\xi}_1 - (\boldsymbol{\xi}_1 + \boldsymbol{\xi}_2)\boldsymbol{X}^{(0)}_{11}]^{-1} && 3\text{-}134\\
\boldsymbol{\Omega} &= [\boldsymbol{X}^{(0)}_{12} + \boldsymbol{I}][\boldsymbol{\xi}_2 - \boldsymbol{\xi}_1 - (\boldsymbol{\xi}_1 + \boldsymbol{\xi}_2)\boldsymbol{X}^{(0)}_{12}]^{-1} && 3\text{-}135\\
\boldsymbol{\Omega} &= [\boldsymbol{X}^{(0)}_{21} + \boldsymbol{I}][\boldsymbol{\xi}_1 - \boldsymbol{\xi}_2 - (\boldsymbol{\xi}_1 + \boldsymbol{\xi}_2)\boldsymbol{X}^{(0)}_{21}]^{-1} && 3\text{-}136\\
\boldsymbol{\Omega} &= \boldsymbol{X}^{(0)}_{22}[2\boldsymbol{\xi}_2 - (\boldsymbol{\xi}_1 + \boldsymbol{\xi}_2)\boldsymbol{X}^{(0)}_{22}]^{-1} && 3\text{-}137
\end{aligned}$$

where $\boldsymbol{I}$ is the 2×2 identity matrix and it is assumed the matrix inverses exist. Note that it is quite possible for a matrix inverse not to exist if one or the other of $\boldsymbol{\Omega}$ or $\boldsymbol{\sigma}$ is singular. For example the equivalent impedance of a thin rectangular slot is singular because there is perfect reflection when the electric field is aligned parallel to the slot. In this case $\boldsymbol{\Omega}$ exists but (strictly speaking) $\boldsymbol{\sigma}$ does not. The converse is true of a thin rectangular element.

4 Basis and shape functions

4.1 Introduction

This section is concerned with the calculation of the elements of the $\boldsymbol{C}$, $\overline{\boldsymbol{C}}$, $\boldsymbol{R}$ and $\overline{\boldsymbol{R}}$ matrices associated, respectively, with the basis functions and the impedance shape functions.

As outlined earlier, we will employ RWG [11] basis functions and piecewise constant shape functions for the impedance terms. Both are employed on a general triangular lattice as illustrated in figure 4-1. For the slotted formulation, the regions of non-perfectly conducting aperture are meshed using small triangles, where the electric fields on the aperture are the principal unknowns. For the element formulation, the regions of non-empty perfect or imperfectly conducting elements are meshed using small triangles, where the electric currents on the elements are the principal unknowns.

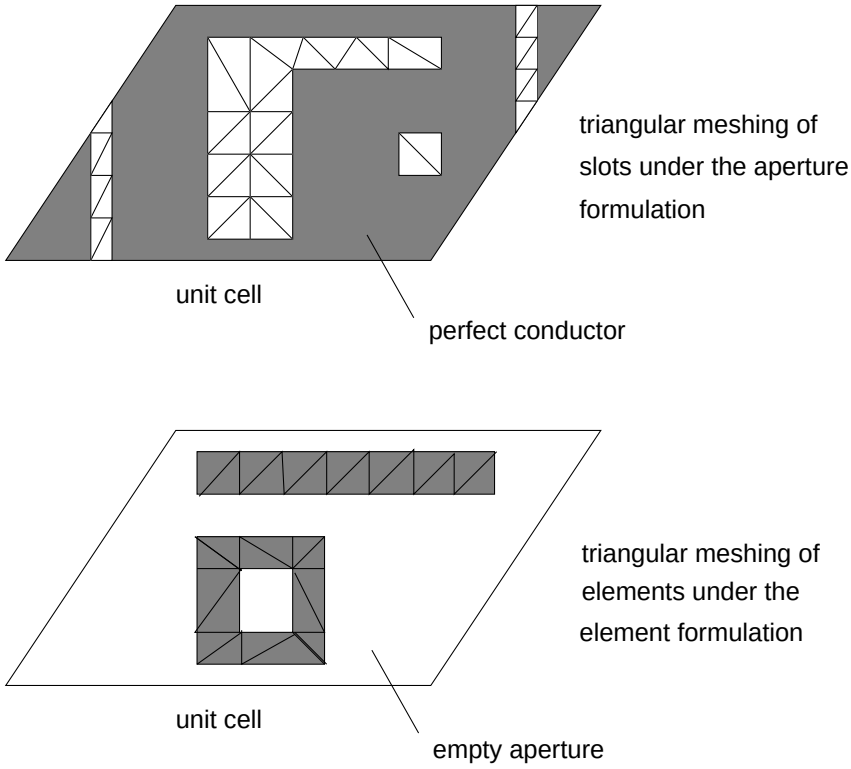

Figure 4-1: The triangular meshing of a slot or element defined FSS

QDAS assumes the nodal positions and connectivity describing the triangular mesh are fixed, independent of a definition of unit cell. It is thus up to the user to employ a sensibly defined global or local unit cell.

An RWG basis function [11] is a two dimensional generalisation of a one dimensional ramp function that linearly interpolates a vector field across triangle boundaries. A basis function

is associated with a contiguous triangle pair sharing a common side. In the modeling of electric currents, $\jmath(x,y)$ has a dominant current flow normal to the common side which is continuous across the two triangles and the current flow tangential to the common side is approximately zero. While not a perfect model, the RWG functions are commonly applied to electromagnetic boundary problems and are known to give a good compromise between accuracy and computational complexity. It is less common to use RWG to model electric fields, but we employ the principal of complementarity and model the electric field basis functions, $\Psi(x,y) = \hat{\underline{z}} \times \jmath(x,y)$. Note that this is equivalent to our previous definition of $\jmath(x,y) = \hat{\underline{n}} \times \Psi(x,y)$ assuming $\hat{\underline{n}} = -\hat{\underline{z}}$. Here, $\Psi(x,y)$ has a dominant component tangential to the common triangle side which is continuous. In this section we will designate $\underline{b}_m(x,y)$ as the m_{th} RWG function. Thus,

$$\begin{array}{ll} \underline{\jmath}_m(x,y) = \underline{b}_m(\underline{x}) & \text{for the element formulation} \\ \underline{\Psi}_m(x,y) = \hat{\underline{z}} \times \underline{b}_m(\underline{x}) & \text{for the aperture formulation} \end{array} \qquad \text{4-1}$$

It is important to note that in a periodic structure, the unit cell boundary is not a physical one. If a conducting element (or slot) straddles a boundary, the currents (fields) must be represented by basis functions that straddle the boundary. In practise, this is an issue of connectivity; the user designates such connections between nodes in one cell and the next using *multiplicity indices* associated with each node. This is described in section 4.8.

In our approach each triangle is ascribed a unique tensor-valued (four component) complex constant describing its conductivity (for slots) or resistivity (for elements). The conductivity or resistivity is *assumed* to be piecewise-constant on each triangle. This may represent a physically correct model of a particular structure or it may represent a piecewise-constant approximation to a continuously varying one. However, in either case it is important to note that the compatibility of such a representation with RWG basis functions is only well known for isotropic models. Strongly anisotropic models for conductivity or resistivity have not been validated (to our knowledge) in the literature with such basis functions. Some initial investigations of QDAS suggest that the accuracy may not be good in this case, possibly because the principal current (field) flows no longer remain perpendicular (tangential) to the common triangle sides. This is an area which requires more investigation.

4.2 The current basis functions and evaluation of the elements of $\overline{C}$

Suppose we consider a triangle pair as illustrated in figure 4-2 supporting a basis function. Every triangle sharing a common edge with another triangle supports a basis function so a single triangle can support a maximum of three half-basis functions. A single triangle, with no connecting triangles, will support no basis functions.

The electric current basis function $\underline{\jmath}(x,y) = \underline{b}(\underline{x})$, where $\underline{b}(\underline{x})$ is the RWG basis function associated with the triangle pair,

$$\underline{b}(\underline{x}) = \begin{cases} \dfrac{l_1}{2A^+}(\underline{x} - \underline{x}_{1+}) & \text{for } \underline{x} \in \text{top triangle } (A^+) \\ \\ \dfrac{l_1}{2A^-}(\underline{x}_{1-} - \underline{x}) & \text{for } \underline{x} \in \text{bottom triangle } (A^-) \end{cases} \qquad \text{4-2}$$

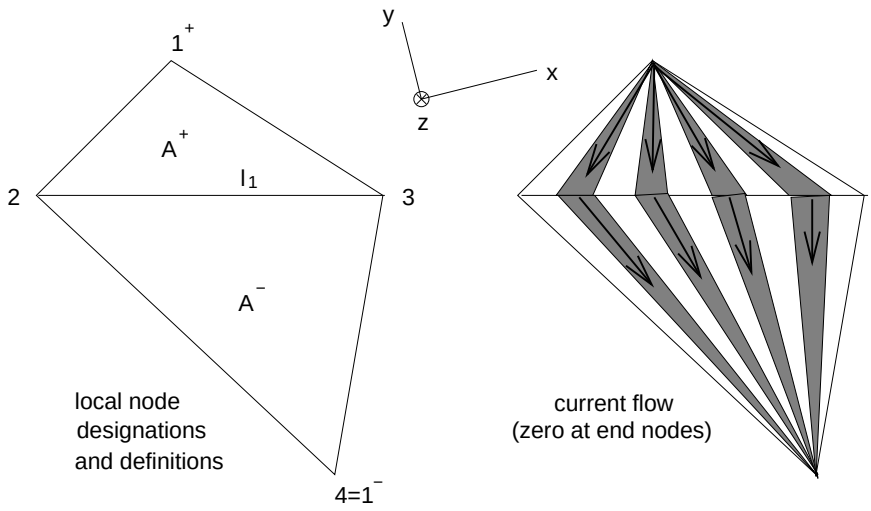

Figure 4-2: An RWG basis function associated with a triangle pair for electric current

Here, $\underline{x}_{1+}$ and $\underline{x}_{1-}$ are the coordinates of opposite nodes, A^+ and A^- are the areas of the top and bottom triangle and $\underline{x}_2 = (x_2, y_2)$ and $\underline{x}_3 = (x_3, y_3)$ are the coordinates of the nodes terminating the common side.

We need to evaluate elements of the $\overline{\boldsymbol{C}}$ matrix, of the form

$$\overline{c}_{pqr} = \iint_{\text{triangle pair}} \underline{\jmath}(\underline{x}).\underline{\phi}^{\star}_{pqr}(\underline{x})dxdy \qquad 4\text{-}3$$

for each of the l basis functions represented by $\underline{\jmath}(\underline{x})$ (the l suffix implicit). We use vector notation for the variables of integration, $\underline{\phi}^{\star}_{pqr}(\underline{x}) \equiv \underline{\phi}^{\star}_{pqr}(x, y)$. The domain of integration can be split into contributions from the top and bottom triangle which we will designate as Δ_T and Δ_B, respectively. Thus,

$$\overline{c}_{pqr} = \overline{c}_T + \overline{c}_B \qquad 4\text{-}4$$

where

$$\begin{aligned} \overline{c}_T &= \iint_{\Delta_T} \underline{\jmath}(\underline{x}).\underline{\phi}^{\star}_{pqr}(\underline{x})dxdy \\ \overline{c}_B &= \iint_{\Delta_B} \underline{\jmath}(\underline{x}).\underline{\phi}^{\star}_{pqr}(\underline{x})dxdy \end{aligned} \qquad 4\text{-}5$$

To perform the integrations, we use a standard transformation in to Barycentric coordinates. We first consider the top triangle as representative of any triangle with area A and coordinates $\underline{x}_1 = (x_1, y_1)$, $\underline{x}_2 = (x_2, y_2)$ and $\underline{x}_3 = (x_3, y_3)$ defining a Barycentric transformation,

$$\begin{aligned} \underline{x} &= \underline{x}_1 + \eta(\underline{x}_2 - \underline{x}_1) + \xi(\underline{x}_3 - \underline{x}_1) \\ &= \eta\underline{x}_2 + \xi\underline{x}_3 + (1 - \xi - \eta)\underline{x}_1 \end{aligned} \qquad 4\text{-}6$$

where η and ξ lie between zero and one over a right-angle triangle, as illustrated in figure 4-3.

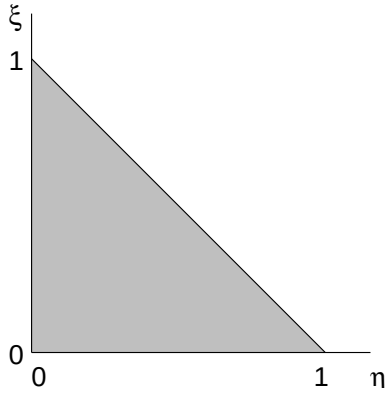

Figure 4-3: Domain of barycentric coordinate integration

Note that,

$$d\eta d\xi = \frac{dxdy}{2A} \tag{4-7}$$

Using the definition of $\underline{\phi}_{pqr}(\underline{x})$ given in equation (1-2) we write,

$$\underline{s}_{pqr} = \underline{s}^{\star}_{pqr} = s_{x,pqr}\hat{\underline{x}} + s_{y,pqr}\hat{\underline{y}} = \begin{cases} \frac{1}{\sqrt{d_x d_y}}\left(\frac{v_{pq}}{t_{pq}}\hat{\underline{x}} - \frac{u_{pq}}{t_{pq}}\hat{\underline{y}}\right) & \text{for } r = 1 \\ \frac{1}{\sqrt{d_x d_y}}\left(\frac{u_{pq}}{t_{pq}}\hat{\underline{x}} + \frac{v_{pq}}{t_{pq}}\hat{\underline{y}}\right) & \text{for } r = 2 \end{cases} \tag{4-8}$$

Let,

$$\begin{aligned} \delta_\eta &= u_{pq}(x_2 - x_1) + v_{pq}(y_2 - y_1) \\ \delta_\xi &= u_{pq}(x_3 - x_1) + v_{pq}(y_3 - y_1) \end{aligned} \tag{4-9}$$

with implied (p, q) dependence and

$$\begin{aligned} \gamma_\eta &= s_{x,pqr}(x_2 - x_1) + s_{y,pqr}(y_2 - y_1) \\ \gamma_\xi &= s_{x,pqr}(x_3 - x_1) + s_{y,pqr}(y_3 - y_1) \end{aligned} \tag{4-10}$$

with implied (p, q, r) dependence. In the new coordinates,

$$\underline{\phi}^{\star}_{pqr}(\underline{x}) = \underline{s}_{pqr} e^{j(u_{pq}x_1 + v_{pq}y_1)} \exp(j\eta\delta_\eta) \exp(j\xi\delta_\xi) \tag{4-11}$$

and it is straight forward to show that,

$$\overline{c}_T = l_1 e^{j(u_{pq}x_1 + v_{pq}y_1)} \int_0^1 d\eta \exp(j\eta\delta_\eta) \int_0^{(1-\eta)} d\xi (\eta\gamma_\eta + \xi\gamma_\xi) \exp(j\xi\delta_\xi) \tag{4-12}$$

This integral may be evaluated analytically using standard trigonometric functions, with regard to some special cases. First let us define the function,

$$P(\eta) = \int_0^{(1-\eta)} d\xi (\eta\gamma_\eta + \xi\gamma_\xi) \exp(j\xi\delta_\xi) \tag{4-13}$$

Provided $\delta_\xi \not\to 0$, the general integration by parts gives us the expression,

$$P(\eta) = \frac{-\gamma_\eta \eta}{j\delta_\xi} + \frac{\gamma_\xi}{(j\delta_\xi)^2} + \frac{e^{j\delta_\xi(1-\eta)}}{j\delta_\xi}\left\{(\gamma_\eta - \gamma_\xi)\eta + \gamma_\xi\left(1 - \frac{1}{j\delta_\xi}\right)\right\} \qquad 4\text{-}14$$

To perform the integral over $P(\eta)$, we will need some common integrals in a form useful for numerical implementation,

$$P_{I0}(\delta) = \int_0^1 e^{j\eta\delta} d\eta = \begin{cases} \frac{1}{j\delta}(e^{j\delta} - 1) & \text{for } \delta \neq 0 \\ \left(1 - \frac{\delta^2}{6}\right) + j\frac{\delta}{2}\left(1 - \frac{\delta^2}{12}\right) + O(\delta^4) & \text{for } \delta \to 0 \end{cases} \qquad 4\text{-}15$$

$$P_{I1}(\delta) = \int_0^1 \eta e^{j\eta\delta} d\eta = \begin{cases} \frac{e^{j\delta}}{j\delta} - \frac{P_{I0}(\delta)}{j\delta} & \text{for } \delta \neq 0 \\ \left(\frac{1}{2} - \frac{\delta^2}{8}\right) + j\frac{\delta}{3} + O(\delta^3) & \text{for } \delta \to 0 \end{cases} \qquad 4\text{-}16$$

For future use we will also form,

$$P_{I2}(\delta) = \int_0^1 \eta^2 e^{j\eta\delta} d\eta = \begin{cases} \frac{e^{j\delta}}{j\delta} - \frac{2P_{I1}(\delta)}{j\delta} & \text{for } \delta \neq 0 \\ \frac{1}{3} + j\frac{\delta}{4} + O(\delta^2) & \text{for } \delta \to 0 \end{cases} \qquad 4\text{-}17$$

$$P_{I3}(\delta) = \int_0^1 \eta^3 e^{j\eta\delta} d\eta = \begin{cases} \frac{e^{j\delta}}{j\delta} - \frac{3P_{I2}(\delta)}{j\delta} & \text{for } \delta \neq 0 \\ \frac{1}{4} + j\frac{\delta}{5} + O(\delta^2) & \text{for } \delta \to 0 \end{cases} \qquad 4\text{-}18$$

Thus, provided $\delta_\xi \neq 0$, we obtain,

$$\overline{c}_T = l_1 e^{j(u_{pq}x_1 + v_{pq}y_1)} \left\{ \begin{array}{l} -\frac{\gamma_\eta}{j\delta_\xi} P_{I1}(\delta_\eta) - \frac{\gamma_\xi}{\delta_\xi^2} P_{I0}(\delta_\eta) \\ +\frac{e^{j\delta_\xi}}{j\delta_\xi}(\gamma_\eta - \gamma_\xi) P_{I1}(\delta_\eta - \delta_\xi) + \frac{e^{j\delta_\xi}}{j\delta_\xi}\gamma_\xi\left(1 - \frac{1}{j\delta_\xi}\right) P_{I0}(\delta_\eta - \delta_\xi) \end{array} \right\}$$

for $\delta_\xi \neq 0$

4-19

In the limit as $\delta_\xi \to 0$ we need an alternative form for the above expression. Using the above limits to the standard integrals, to the orders given, it can be shown that,

$$\overline{c}_T = l_1 e^{j(u_{pq}x_1 + v_{pq}y_1)} \left\{ \begin{array}{l} j\delta_\xi\left(\frac{\gamma_\eta}{2} - \frac{\gamma_\xi}{3}\right) P_{I3}(\delta_\eta) + \left(-\gamma_\eta + \frac{\gamma_\xi}{2} + j\delta_\xi(-\gamma_\eta + \gamma_\xi)\right) P_{I2}(\delta_\eta) \\ +\left(\gamma_\eta - \gamma_\xi + j\delta_\xi(\gamma_\eta/2 - \gamma_\xi)\right) P_{I1}(\delta_\eta) + \gamma_\xi\left(\frac{1}{2} + j\frac{\delta_\xi}{3}\right) P_{I0}(\delta_\eta) \\ +O(\delta_\xi)^2 \end{array} \right\}$$

for $\delta_\xi \to 0$

4-20

Computationally we have found good accuracy may be achieved with a changeover between general (4-19) and limiting (4-20) expressions when $|\delta_\xi| \approx 0.0005$ using complex double precision arithmetic. A similar cross-over point is used in evaluating the integrals P_{I0}, P_{I1}, P_{I2} and P_{I3} (a value of 0.001 is currently employed).

The expression for $\overline{c}_B$ may be found by making the substitution $\underline{x}_1 \rightarrow \underline{x}_4$ (i.e. $\underline{x}_{1+} \rightarrow \underline{x}_{1-}$), together with $\overline{c}_B \rightarrow -\overline{c}_T$, because current flow is towards rather than away from the vertex.

Another point to note is that evaluation of $s_{x,pqr}$ and $s_{y,pqr}$ requires the terms u_{pq}/t_{pq} and v_{pq}/t_{pq}. These fractions are well behaved except when $t_{pq} = 0$ which occurs only when $p = q = 0$ and $\sin\theta_{in} = 0$. Under these special conditions, $u_{pq}/t_{pq} = \cos\phi_{in}$ and $v_{pq}/t_{pq} = \sin\phi_{in}$.

4.3 The field basis functions and evaluation of the elements of $\boldsymbol{C}$

In the aperture formulation, a triangle pair is used to represent an electric field distribution. The notation is similar to that employed for the electric current element formulation, as illustrated in figure 4-4 below.

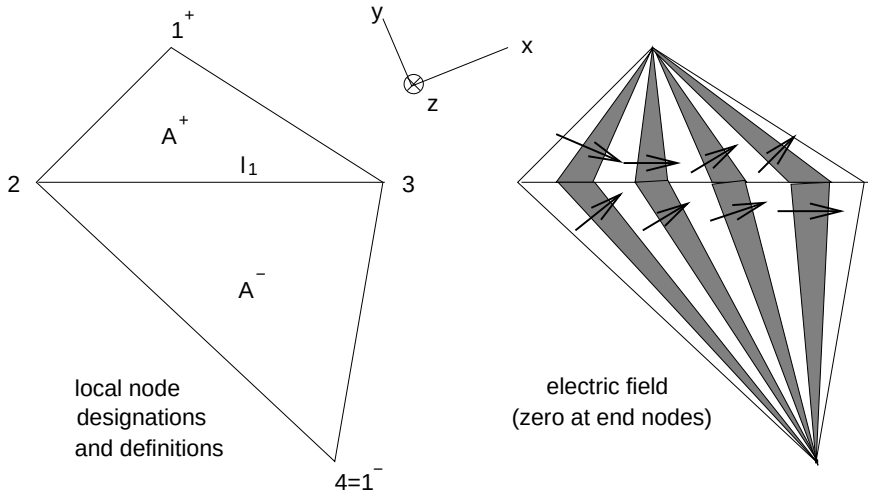

Figure 4-4: A rotated RWG basis function associated with a triangle pair for electric field

The electric field basis function is taken to be $\underline{\Psi}(\underline{x}) = \hat{\underline{z}} \times \underline{b}(\underline{x})$ for each triangle pair. Thus,

$$\underline{\Psi}(\underline{x}) = \begin{cases} \dfrac{l_1}{2A^+}\hat{\underline{z}} \times (\underline{x} - \underline{x}_{1+}) & \text{for } \underline{x} \in \text{top triangle } (A^+) \\ \dfrac{l_1}{2A^-}\hat{\underline{z}} \times (\underline{x}_{1-} - \underline{x}) & \text{for } \underline{x} \in \text{bottom triangle } (A^-) \end{cases} \qquad 4\text{-}21$$

and we need to evaluate the elements of the matrix $\boldsymbol{C}$,

$$c_{pqr} = c_T + c_B \qquad 4\text{-}22$$

(basis function l suffix implicit) where

$$\begin{aligned} c_T &= \iint_{\Delta_T} \underline{\Psi}(\underline{x}).\underline{\phi}^{\star}_{pqr}(\underline{x})dxdy \\ c_B &= \iint_{\Delta_B} \underline{\Psi}(\underline{x}).\underline{\phi}^{\star}_{pqr}(\underline{x})dxdy \end{aligned} \quad 4\text{-}23$$

The calculation proceeds exactly as in the element case, except with an alternative definition for γ_η and γ_ξ given in (4-10). Thus we now have $\overline{c}_T \rightarrow c_T$ and $\overline{c}_B \rightarrow c_B$, under the substitution,

$$\begin{aligned} \gamma_\eta &= -s_{x,pqr}(y_2 - y_1) + s_{y,pqr}(x_2 - x_1) \\ \gamma_\xi &= -s_{x,pqr}(y_3 - y_1) + s_{y,pqr}(x_3 - x_1) \end{aligned} \quad 4\text{-}24$$

It is also possible to show that,

$$\begin{aligned} \overline{c}_{pq1} &= c_{pq2} \\ \overline{c}_{pq2} &= -c_{pq1} \end{aligned} \quad 4\text{-}25$$

so that essentially the same numerical formulation for the inner products of basis functions can be applied to both slots and elements.

4.4 Evaluation of the terms of $\overline{R}$ and R for elements and slots

Under the element formulation we require to calculate the terms $\overline{R}_{ml}$ defined in (3-89),

$$\overline{R}_{ml} = \sum_{k=1}^{K} \iint_{El} [\underline{\underline{\Omega}}_k.\underline{j}_l(x', y')].\underline{j}^{\star}_m(x', y')p_k(x', y')dx'dy' \quad 4\text{-}26$$

Under the aperture formulation we require to calculate the terms R_{ml} defined in (3-29),

$$R_{ml} = \sum_{k=1}^{K} \iint_{Ap} [\underline{\underline{\sigma}}_k.\underline{\Psi}_l(x', y')].\underline{\Psi}^{\star}_m(x', y')p_k(x', y')dx'dy' \quad 4\text{-}27$$

In both cases we assume a shape function $p_k(x', y')$ which is piece-wise constant and, in particular, is piece-wise constant over each triangle,

$$p_k(x, y) = \begin{cases} 1 & \text{for } (x, y) \in \text{triangle } k \\ 0 & \text{otherwise} \end{cases} \quad 4\text{-}28$$

Some complexity arises because, whereas the integral is over the support of basis functions involving triangle pairs, the impedance supports are over individual triangles so we need to consider the various kinds of overlaps that can occur for different values of m and l.

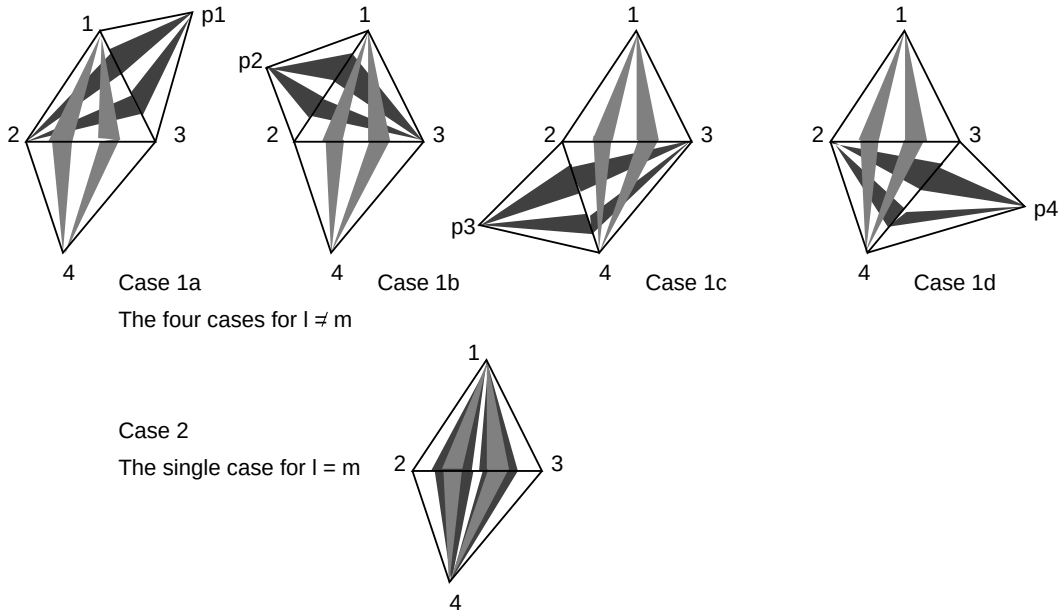

Figure 4-5: Impedance overlap configurations

Associated with the m_{th} basis function there are 4 possible cases (4 possible values of l) when $m \neq l$, which we label as cases 1a, 1b, 1c and 1d respectively. Then there is the case, case 2, when when $m = l$. These are illustrated schematically in figure 4-5 below. Cases 1a and 1b each involve an integration over the overlapped triangle specified by the local nodes 1, 2 and 3. Cases 1c and 1d each involve an integration over the overlapped triangle specified by the local nodes 4, 2 and 3. Case 2 involves an integration over both overlapped triangles.

Note that the matrices $\boldsymbol{R}$ ($\overline{\boldsymbol{R}}$), with elements R_{ml} ($\overline{R}_{ml}$) for $1 \leq m, l \leq M$ are sparse with at most 5 and at least 1 non-zero entry (the diagonal entry) in each row and column unless the resistance (element formulation) or conductance (aperture formulation) is exactly zero on both triangles of the m_{th} basis function. In the latter case all entries on the m_{th} row and column are zero.

Associated with a given pair of basis functions specified by $m \neq l$ (case 1) there is only a single value of k which contributes to the sum over k in (4-26) and (4-27). This is the k_{th} triangle common to both basis functions. When $m = l$ (case 2) there are exactly two values of k in the sum over k which contribute to the sum. These are the two triangles that make up the basis function.

4.4.1 The case for current elements

Suppose we consider the top triangle (cases 1a, 1b and one half of case 2) of area A, with sides of length l_1, l_2 and l_3 opposite local nodes 1, 2 and 3. Each contributing term to the sum in the expression for $\overline{R}_{ml}$ takes one of three possible forms. We will consider the element

case first. Dropping the k suffix, associated with the top triangle, these are designated by,

$$O_{1i} = \frac{l_1 l_i}{4A^2} \iint_{\Delta} [\underline{\underline{\Omega}}.(\underline{x} - \underline{x}_1)].(\underline{x} - \underline{x}_i) dxdy \qquad 4\text{-}29$$

where Δ represents the domain of the top triangle. Applying the Barycentric transformation (4-6), it may be shown that,

$$O_{1i} = \frac{l_1 l_i}{2A} \int_0^1 d\eta \int_0^{1-\eta} (\beta_\eta \eta + \beta_\xi \xi + \beta_{\eta\xi} \eta\xi + \beta_{\eta\eta} \eta^2 + \beta_{\xi\xi} \xi^2) d\xi \qquad 4\text{-}30$$

where

$$\begin{gathered}
\beta_\eta = \Omega_{11}(x_2 - x_1)(x_1 - x_i) + \Omega_{12}(y_2 - y_1)(x_1 - x_i) + \Omega_{21}(x_2 - x_1)(y_1 - y_i) \\
+\Omega_{22}(y_2 - y_1)(y_1 - y_i) \\
\\
\beta_\xi = \Omega_{11}(x_3 - x_1)(x_1 - x_i) + \Omega_{12}(y_3 - y_1)(x_1 - x_i) + \Omega_{21}(x_3 - x_1)(y_1 - y_i) \\
+\Omega_{22}(y_3 - y_1)(y_1 - y_i) \\
\\
\beta_{\eta\xi} = 2\Omega_{11}(x_2 - x_1)(x_3 - x_1) + (\Omega_{12} + \Omega_{21})[(y_2 - y_1)(x_3 - x_1) + (y_3 - y_1)(x_2 - x_1)] \\
+2\Omega_{22}(y_2 - y_1)(y_3 - y_1) \\
\\
\beta_{\eta\eta} = \Omega_{11}(x_2 - x_1)^2 + (\Omega_{12} + \Omega_{21})(y_2 - y_1)(x_2 - x_1) + \Omega_{22}(y_2 - y_1)^2 \\
\\
\beta_{\xi\xi} = \Omega_{11}(x_3 - x_1)^2 + (\Omega_{12} + \Omega_{21})(y_3 - y_1)(x_3 - x_1) + \Omega_{22}(y_3 - y_1)^2
\end{gathered} \qquad 4\text{-}31$$

and where Ω_{ij} represent the i, j entries of the matrix $\underline{\underline{\Omega}}$ in the global (x, y) coordinate system. Ω_{11} represents the x-component of induced voltage by a unit x-directed current, Ω_{12} represents the x-component of induced voltage by a unit y-directed current, Ω_{21} represents the y-component of induced voltage by a unit x-directed current and Ω_{22} represents the y-component of induced voltage by a unit y-directed current.

The expression (4-30) is simple to evaluate and takes the form,

$$O_{1i} = \frac{l_1 l_i}{12A} \left(\beta_\eta + \beta_\xi + \frac{1}{2} \left[\frac{\beta_{\eta\xi}}{2} + \beta_{\eta\eta} + \beta_{\xi\xi} \right] \right) \qquad 4\text{-}32$$

For the present, we assume that overlap triangles are both top triangles for each of the two basis functions, or both bottom triangles. There is a sign issue if this is not the case, which we describe presently.

$\overline{R}_{ml}$, for $m \neq l$, is represented by one O_{1i} term. If the overlap occurs on the top triangle, then $\overline{R}_{ml} = O_{1i}$ with $i = 2$ corresponding to case 1b and $i = 3$ corresponding to case 1a. If the overlap occurs on the bottom triangle then $\underline{x}_1$ should be replaced by $\underline{x}_4$ with A representing the area of the bottom triangle. With this substitution, $\overline{R}_{ml} = O_{1i}$ with $i = 2$ corresponding to case 1c and $i = 3$ to case 1d. When $m = l$, $\overline{R}_{ml}$ is represented by the sum over two terms. These are the terms O_{11} for the top and bottom triangle.

4.4.2 The case for apertures

The aperture case is similar to the element one described above. In this case R_{ml} are represented by a sum over terms of the form,

$$O_{1i} = \frac{l_1 l_i}{4A^2} \iint_{\Delta} [\underline{\underline{\sigma}}. \{\hat{\underline{z}} \times (\underline{x} - \underline{x}_1)\}]. \{\hat{\underline{z}} \times (\underline{x} - \underline{x}_i)\}\, dxdy \qquad 4\text{-}33$$

with notation, as before, appropriate to the top triangle. The analysis is similar and it can be shown that the result for R_{ml} is identical to that for $\overline{R}_{ml}$ under the transformation,

$$\begin{aligned} \Omega_{22} &\rightarrow \sigma_{11} \\ \Omega_{21} &\rightarrow -\sigma_{12} \\ \Omega_{12} &\rightarrow -\sigma_{21} \\ \Omega_{11} &\rightarrow \sigma_{22} \end{aligned} \qquad 4\text{-}34$$

where σ_{ij} are the elements of $\underline{\underline{\sigma}}$, defined such that σ_{11} represents the x-component of induced current by a unit x-directed voltage, σ_{12} represents the x-component of induced current by a unit y-directed voltage, σ_{21} represents the y-component of induced current by a unit x-directed voltage and σ_{22} represents the y-component of induced current by a unit y-directed voltage.

4.4.3 Sign issues and basis function orientation

Care must be taken in determining the sign of the basis functions when there are non-zero terms to R_{ml} or $\overline{R}_{ml}$. When R_{ml} and $\overline{R}_{ml}$ are zero (i.e. the FSS are composed of perfect conductors), the sign of the basis functions can be arbitrary without consequence. However, the addition of the resistive terms requires a consistency.

Referring to figures 4-2 or 4-4, a basis function defined using local nodes 1, 2, 3 and 4 is invariant under a node numbering change between nodes 2 and 3. However, interchange of node numbers 1 and 4 reverses the direction of current flow for currents or field direction for electric field. This is because current is always defined flowing from node 1 to node 4 and electric field defined flowing anti-clockwise about node 1 and clockwise about node 4. In a numerical scheme, the ordering of nodes can be arbitrary and hence also the sign of the basis function.

This means that a triangle common to two basis functions may be a top triangle with respect to one and a bottom triangle with respect to another. This is illustrated in figure 4-6 with reference to local node ordering in three configurations. The figure shows four equilateral triangles making up a larger equilateral triangle represented by three basis functions which are labeled by Ψ_1, Ψ_2 and Ψ_3. Because Ψ_3 is top/bottom switched with respect to the other two, there is no 120 degrees rotational invariance without a sign change.

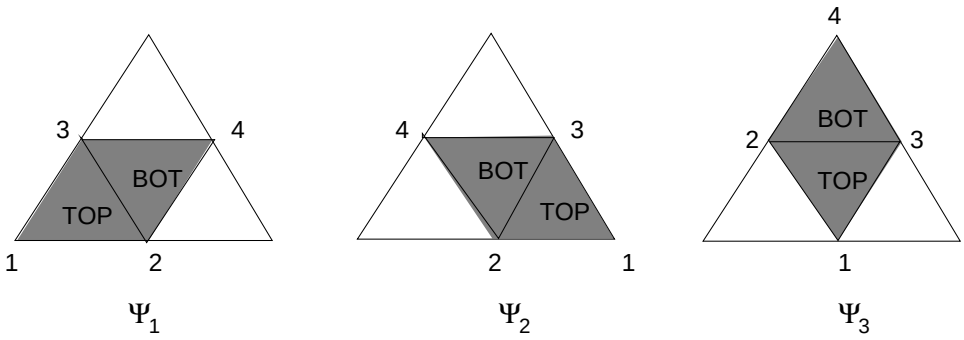

Figure 4-6: An overlap triangle defined as both 'top' and 'bottom'

There is, in general, no easy way to control top/bottom ordering. However, the resistance integrals O_{1i} assume an overlay of currents (fields) on a single triangle which is defined as top for both basis functions. The result is the same if both are defined as bottom. However, there is a sign change if one is top and the other bottom which is yet to be accounted for. Consequently, there is a requirement to examine the local node ordering of the basis function overlap triangles to determine whether they are defined as top or bottom. To achieve the correct values for R_{lm} and $\overline{R}_{ml}$, we thus find the values as determined in the two previous sub-sections and multiply by a sign factor; -1 if overlaps are top/bottom (or bottom/top) and $+1$ if overlaps are top/top or bottom/bottom.

4.5 Efficiency savings using triangles of equal size and shape

Sections 4.2 and 4.3 describe the formulation and evaluation of the elements of the matrices $\overline{\boldsymbol{C}}$ and $\boldsymbol{C}$. Although the formulation allows for arbitrary triangles, not restricted to a regular lattice, the construction of all elements $(p, q, r) \in \mathcal{T}$ can be computationally expensive. However, it is possible to construct *most* triangles of most geometrical structures to be of equal size and shape. This allows the use of translational symmetry to significantly reduce the computational effort.

Suppose that a triangle pair is defined by the local nodes 1, 2, 3 and 4 with nodal coordinates, $\underline{x}_1$, $\underline{x}_2$, $\underline{x}_3$ and $\underline{x}_4$, respectively. Suppose that another displaced triangle pair exists with the same local nodes ordered in the same way with coordinates $\underline{x}'_1$, $\underline{x}'_2$, $\underline{x}'_3$ and $\underline{x}'_4$. Let $c_{pqr}(\underline{x}_1, \underline{x}_2, \underline{x}_3, \underline{x}_4)$ be an element of the matrix $\boldsymbol{C}$ showing the explicit dependence on coordinates of the l_{th} basis function. Translational invariance implies that,

$$\underline{x}'_1 - \underline{x}_1 = \underline{x}'_2 - \underline{x}_2 = \underline{x}'_3 - \underline{x}_3 = \underline{x}'_4 - \underline{x}_4 \qquad 4\text{-}35$$

It is then straight forward to show that,

$$c_{pqr}(\underline{x}'_1, \underline{x}'_2, \underline{x}'_3, \underline{x}'_4) = c_{pqr}(\underline{x}_1, \underline{x}_2, \underline{x}_3, \underline{x}_4) \exp(j\underline{k}_{pq}.[\underline{x}'_1 - \underline{x}_1]) \qquad 4\text{-}36$$

where

$$\underline{k}_{pq} = u_{pq}\hat{\underline{x}} + v_{pq}\hat{\underline{y}} \qquad 4\text{-}37$$

and u_{pq} and v_{pq} are the Floquet wave number components defined in (1-1) with respect to the local unit cell.

The same result holds for the elements of the matrix $\overline{\boldsymbol{C}}$. To exploit this symmetry, and the use of (4-36) to compute shifted elements, requires a method of identifying the shape equivalence of triangle pairs. QDAS is designed to recognise a set of triangle pair primitives such that all other triangle pairs are translated copies of the given set. Given that the number of basis functions is relatively small (usually significantly less than 1000) a simple $O(N^2)$ search algorithm can be implemented to test for the translational equivalence of triangle pairs based on a threshold on the coordinate differences. The tolerance can be based on the the maximum spectral resolution defined by P and Q.

It is necessary to test against all possible configurations of local nodes. Equation (4-35) assumes the same ordering of local nodes which does not occur in an arbitrary configuration of triangles. There are four ways in which nodes can be uniquely assigned, as illustrated in figure 4-7. We need to compare all cases against the template ordering (shown as case 1 in

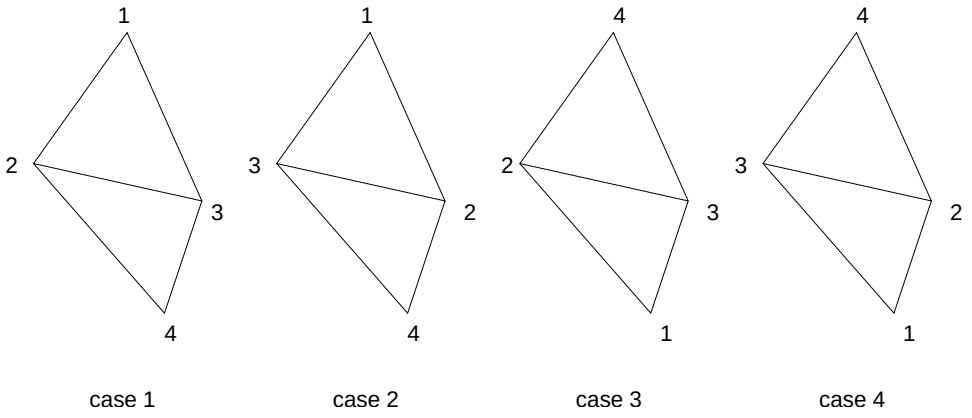

Figure 4-7: Local node arrangements on a triangle pair

the figure). To this end, let the four coordinates of the j_{th} triangle pair be designated as $\underline{x}_1(j)$, $\underline{x}_2(j)$, $\underline{x}_3(j)$ and $\underline{x}_4(j)$, ordered arbitrarily. Define,

$$\left.\begin{array}{l}\underline{\Delta x}_1(i,j)=\underline{x}_1(j)-\underline{x}_1(i)\\ \underline{\Delta x}_2(i,j)=\underline{x}_2(j)-\underline{x}_2(i)\\ \underline{\Delta x}_3(i,j)=\underline{x}_3(j)-\underline{x}_3(i)\\ \underline{\Delta x}_4(i,j)=\underline{x}_4(j)-\underline{x}_4(i)\end{array}\right\}\ \text{case 1} \qquad \left.\begin{array}{l}\underline{\Delta x}_1(i,j)=\underline{x}_1(j)-\underline{x}_1(i)\\ \underline{\Delta x}_2(i,j)=\underline{x}_3(j)-\underline{x}_2(i)\\ \underline{\Delta x}_3(i,j)=\underline{x}_2(j)-\underline{x}_3(i)\\ \underline{\Delta x}_4(i,j)=\underline{x}_4(j)-\underline{x}_4(i)\end{array}\right\}\ \text{case 2}$$

$$\left.\begin{array}{l}\underline{\Delta x}_1(i,j)=\underline{x}_4(j)-\underline{x}_1(i)\\ \underline{\Delta x}_2(i,j)=\underline{x}_2(j)-\underline{x}_2(i)\\ \underline{\Delta x}_3(i,j)=\underline{x}_3(j)-\underline{x}_3(i)\\ \underline{\Delta x}_4(i,j)=\underline{x}_1(j)-\underline{x}_4(i)\end{array}\right\}\ \text{case 3} \qquad \left.\begin{array}{l}\underline{\Delta x}_1(i,j)=\underline{x}_4(j)-\underline{x}_1(i)\\ \underline{\Delta x}_2(i,j)=\underline{x}_3(j)-\underline{x}_2(i)\\ \underline{\Delta x}_3(i,j)=\underline{x}_2(j)-\underline{x}_3(i)\\ \underline{\Delta x}_4(i,j)=\underline{x}_1(j)-\underline{x}_4(i)\end{array}\right\}\ \text{case 4} \qquad \text{4-38}$$

For each of the four cases compute $|\underline{\Delta x}_1(i,j)-\underline{\Delta x}_4(i,j)|$, $|\underline{\Delta x}_2(i,j)-\underline{\Delta x}_4(i,j)|$ and $|\underline{\Delta x}_3(i,j)-\underline{\Delta x}_4(i,j)|$, where $|.|$ is any computationally convenient vector norm (e.g. the 1-norm). If all

three norms are sufficiently small (i.e. $< \varepsilon$) for one (and only one) of the four cases, the triangle pairs i and j may be assumed to be translational copies.

The measure of smallness, ε, can be based on the values of P and Q that determine the spectral resolution of the unit cell. For example,

$$\varepsilon = \frac{1}{C \max(u_{max}, v_{max})} \qquad 4\text{-}39$$

where C is an arbitrary positive number $C \gg 1$ (we assume $C = 10.0$) and u_{max} and v_{max} are the maximum values for u_{pq} and v_{pq},

$$\begin{aligned} u_{max} &= k_0 + \frac{2\pi P}{d_x} \\ v_{max} &= k_0 + \frac{2\pi Q}{d_y} + \frac{2\pi P \cot\alpha}{d_x} \end{aligned} \qquad 4\text{-}40$$

Finally, it is worth noting that other symmetries may also be exploited. For example if the lattice is N-fold rotationally symmetric ($N = 2, 3, 4$ or 6) then N-fold rotational symmetries on triangles can be exploited. However, although common, such symmetry is not general and we do not currently exploit it within QDAS.

4.6 A note on convergence of the $\boldsymbol{Y}$ matrix and the set $\mathcal{T}$

If the set of modes $\mathcal{T}$ is infinite, i.e. both $P \to \infty$ and $Q \to \infty$, then the $\boldsymbol{Y}$ matrix defined in (3-31) or (3-91) are the exact interaction matrices between basis functions, analogous to the impedance matrix in a finite boundary element or moment method problem.

From a formal mathematical perspective, the convergence of terms in the $\boldsymbol{Y}$ matrix is generally slow as P and Q are increased. What, then, are the consequences of the truncation error? Fortunately, it seems that *provided each term in the matrix is computed over the same set* $\mathcal{T}$, the effect on predictions of transmission and reflection coefficients is acceptably small for moderately large values of P and Q. While we attempt no mathematical justification, our interpretation is that the finiteness of P and Q may be regarded as imposing a modification of the basis functions on the infinite $\mathcal{T}$ space. Since the RWG basis functions, on an infinite $\mathcal{T}$ space, are only able to approximate the current and field distributions there may be very little to be gained by significant increases in P and Q without a similar increase in the number (and reduction in size) of the basis functions. Physically, the effect of finite P and Q is to "blur" the basis functions over the unit cell. An example of optimum choice of P and Q for a given number of basis functions has been studied in [13].

There is a theoretical possibility, for a given finite set of basis functions, that values for P and Q which are too large may *reduce* accuracy for particular FSS geometries. Physically, the "blurred" basis function set may provide a more accurate field distribution than a less blurred one if the less blurred one does not provide a good representation. However, such effects are

likely to be problem dependent and we have little reported evidence for their existence. If present, then there will be finite values of P and Q, for a given selection of basis functions, which achieve maximum accuracy; a feature of relative convergence. However, studies on simple structures, such as rectangular patches, do not appear to demonstrate such effects [14].

The main advantage, should there be one, in an infinite mode set $\mathcal{T}$ is the fact that any inaccuracy in solution can be traced to the basis functions alone. Convergence studies may then be undertaken with less uncertainty in the cause of possible errors. However, to do this requires convergence acceleration methods. Unfortunately, there is no simple or general analytic form to the terms c_{pqr} taken as a function of p, q, r for multi-layer composites. Numerical acceleration methods assume the existence of certain analytic properties of this functional behaviour, even if the functions themselves are either unknown or too complex to be useful. The required properties associated with a given acceleration scheme have, to our knowledge, not been demonstrated for general FSS composites. References exist, e.g. [12], which demonstrate acceleration methods for single interface FSS but we have been unsuccessful in obtaining convergence using such methods with a more complex multi-layer structure. This problem would seem to remain open.

We have examined another feature of the problem. Following the theory of finite moment method analysis using boundary elements it is known that the self-terms in the impedance matrix are large and important in contributing to overall accuracy. While such matrices are usually not diagonally dominant, it is good practice to spend effort in accurate evaluation of these terms. By analogy, we conducted an experiment whereby the self-terms of the $\boldsymbol{Y}$ matrix were computed with twice the values of P and Q used for the non-diagonal terms. Interestingly, this results in a significant *reduction* in the accuracy of the predicted reflection and transmission coefficients, compared to the case where all terms are computed on the same (smaller) $\mathcal{T}$ set. Further work is required to explain this effect, although it is consistent with the previous remarks. Currently, we have found no robust method which significantly reduces the computational effort in the summation over Floquet modes.

4.7 Specification of nodes and triangles

QDAS assumes that the triangles describing an FSS are specified by the user in terms of nodes. Each node is given a unique integer identifier so that a triangle requires three such integers, all different, in order to define it. In fact, further identification is also required for reasons outlined in the next section. Each node is defined by a pair of (x, y) real valued coordinates and referenced by the identification integer. Each triangle is also referenced by a unique sequential integer identifier. Because the number of basis functions is relatively small (e.g. usually $\ll 1000$) it is efficient to use a relatively simple $O(N^2)$ search algorith to automatically colate triangles in terms of triangle pairs sharing a common side. Each triangle pair is specified by four local nodes which are grouped so that nodes 2 and 3 define the common side. Other than this, the ordering of the nodes is assumed arbitrary.

It is possible to badly define nodes and triangles, e.g. with overlapping triangles, triangles defined by non-unique nodes, etc. Some warnings and error messages will be given should this occur, but not all eventualities are catered for. In fact, there may be special reasons when overlapping triangles are *required*. It is recommended that the user take advantage of the DRAWFSS command, which will show the triangle pairs created by the programme. While not fool-proof, most geometry problems can be spotted here.

4.8 Basis functions spanning unit cells

In general, a triangle from one unit cell may share a common edge with a triangle from an adjoining cell. Of course, the position of a unit cell boundary is arbitrary but there are many common FSS structures where such junctions must occur no matter how the cells are defined. Uninterupted grids are an example of such.

There are several ways to account for triangle pairs spanning cell boundaries. We adopt the concept of *multiplicity indices* associated with each node. Although each triangle requires three nodal identification integers to define it, these numbers are not sufficient to describe triangles that span unit cells. In general, each triangle is uniquely defined by three groups of three integers. Each integer group is defined by the node identification integer and two multiplicity integers which define the unit cell the node "lives in". Figure 4-8 shows a number of contiguous unit cells surrounding the principal unit cell. Figure 4-9 shows a triangle spanning a unit cell boundary and the associated triangle pair basis function.

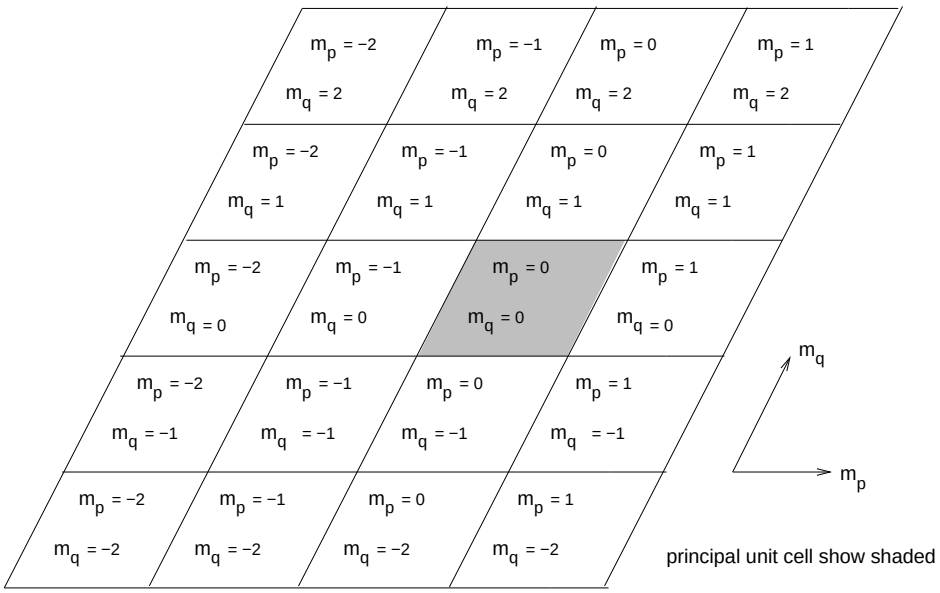

Figure 4-8: Multiplicity indices for contiguous unit cells

We adopt the convention that the multiplicity integers (m_p, m_q), associated with the node m, are zero when a node resides in the principal unit cell. Such a node is termed a *principal*

node. This convention must be adopted within QDAS for the correct identification of extra triangles. The integer m_p indexes the unit cell in the $\underline{\hat{x}}$ direction. The integer m_q indexes the unit cell in the other (skew) direction at angle α to the x-axis. Thus a connected node in a unit cell just to the right of the principal cell would be designated by the multiplicity integers $(1, 0)$ if its coordinates (those defined by the user) were in the principal cell. One just to the left by $(-1, 0)$. One just above (along the skew axis) by $(0, 1)$, etc. For example figure 4-9 shows all triangles with black nodes defined with $m_p = m_q = 0$. The spanning triangles employ $m_p = 1, m_q = 0$ for the white nodes. One new triangle pair is created with the nodes $7, 1, 2$ and 3. Note that node 4 is a principal node since its coordinates are assumed to be defined ouside the principal cell at the position of the indicated black dot.

If a node lies exactly on a boundary of the principal cell we should choose m_p and m_q to be zero unless the node is repeated on the opposite boundary in which case one of the indices of the repeated node would take the value ± 1, depending on its relative position according to the previous rules. At a corner, the repeated node would take non-zero vales for both m_p and m_q.

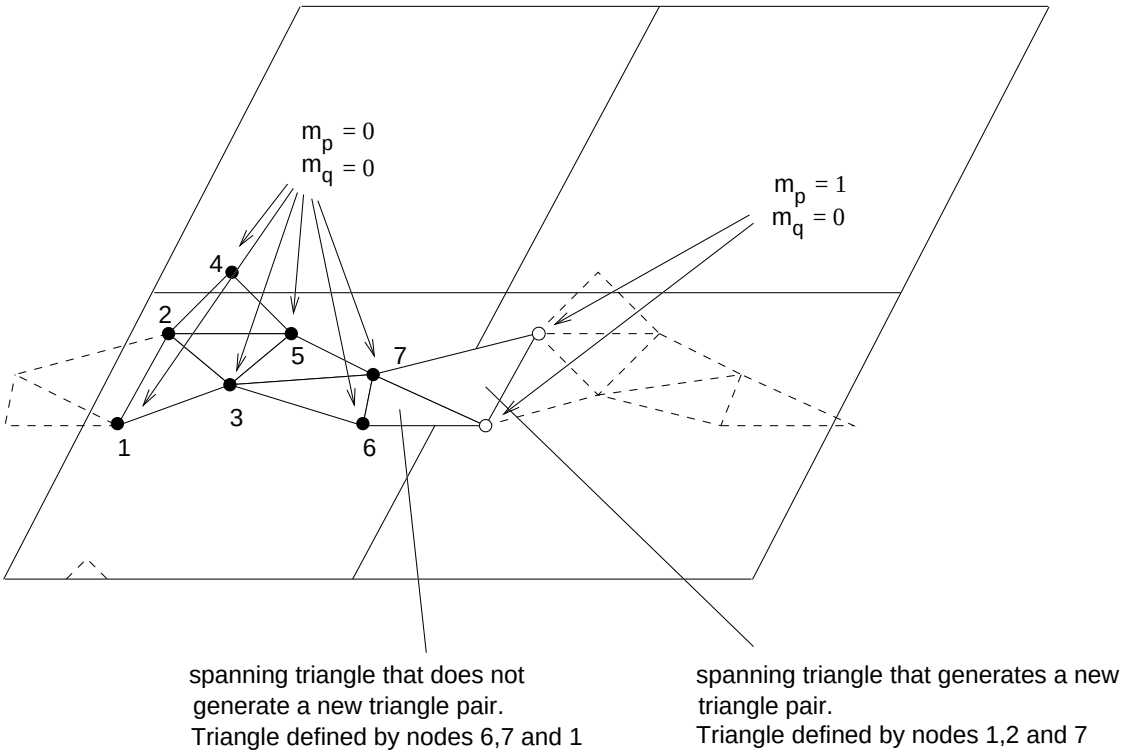

Figure 4-9: A structure with triangles spanning a unit cell boundary

For most structures we only need the multiplicity pairs $(0, 0)$, $(1, 0)$, $(0, 1)$ and $(1, 1)$. However, QDAS permits any integer pairs to investigate the use of basis functions spanning many unit cells. All multiplicity indices are referenced with respect to the local unit cell of the given FSS.

Once the triangles are defined, QDAS will automatically generate any triangle pairs that exist and the four coordinates that define them. If (X_m, Y_m) are the coordinates of the m_{th} node, as defined in the node list, then the coordinates used in constructing the triangle pairs, (x_m, y_m), are given by,

$$\begin{aligned} x_m &= X_m + m_p d_x + m_q d_y \cot\alpha \\ y_m &= Y_m + m_q d_y \end{aligned} \qquad \text{4-41}$$

Note that when triangles span unit cell boundaries, new triangles may need to be created automatically or, if this is not possible, manually by the user. For example, in figure 4-9, a new triangle is required which is a translated copy of the triangle with nodes $1, 2, 3$ in the cell to the right of the principal unit cell. This requires a triangle with a "promoted" vertex node (node 3 in figure 4-9).

The general location of additional triangle pairs and their coordinates should account for arbitrary multiplicity numbers and nodal coordinates. Special cases, such as where only one node is defined in the node list, should be permitted. However, a completely general algorith is not possible because of possible construction ambiguities. In QDAS it is assumed that a new triangle is created if and only if,

1. A triangle is defined with two of its three nodes within the same cell and outside of the principal unit cell.
2. The third of its three nodes lies in the principal unit cell.
3. All three nodes defining the triangle it will connect to lie in the principal unit cell.

If any of these conditions are not met, the user will have to manually define new triangles; the example with a single node per unit cell would fall in to this category. However, this should rarely prove necessary and if it does the manual definition of triangles is straight forward. QDAS will flag a warning if condition 1 is not met, but not (currently) conditions 2 and 3. As in the previous section, we would recommend the use of the DRAWFSS command where principal and non-principal nodes are displayed differently.

Suppose a triangle is specified by the nodal triplets, (m_3, m_{p3}, m_{q3}), (m_1, m_{p1}, m_{q1}) and (m_2, m_{p2}, m_{q2}) where (m_1, m_{p1}, m_{q1}) and (m_2, m_{p2}, m_{q2}) refer to the two nodes outside the principal cell with $m_{p1} = m_{p2}$ and $m_{q1} = m_{q2}$. If a triangle exists in the principal cell with nodal triplets, $(m_1, 0, 0)$, $(m_2, 0, 0)$ and $(m_0, 0, 0)$ then the new triangle, automatically created, is specified by the triplets (m_1, m_{p1}, m_{q1}), (m_2, m_{p1}, m_{q1}) and (m_0, m_{p1}, m_{q1}).

5 References

1 *A.J.Mackay.* 'User guide for QDAS, Q-par Dichroic Array Software' Q-par Angus report Q-par/FSS/TRFSS1/1.3, April 2003.

2 *E.L.Pelton, B.A.Munk.* 'A streamlined metallic radome' IEEE Trans Anten and Prop., AP-22, 1974, pp799-803

3 *B.A.Munk.* 'Frequency Selective Surfaces. Theory and design.' Wiley interscience publications, 2000.

4 *C.C.Chen.* 'Transmission through a conducting screen perforated periodically with apertures' IEEE Trans MTT-18, September 1979, pp627-632.

5 *T.Cwik, R,Mittra.* 'The cascade connection of planar periodic surfaces and lossy dielectric layers to form an arbitrary periodic screen' IEEE Trans Anten and Prop., AP-35, no. 12, December 1987, pp1397-1405.

6 *L.D.Landau, E.M.Lifshitz, L.P.Pitaevskii.* 'Electrodynamics of continuous media', second edition, Butterworth Heinemann Press, 1993.

7 *J.Pendry.* 'Electromagnetic materials enter the negative age', physics world, September 2001, pp47-51

8 *A.J.Mackay, J.G.Gallagher.* 'On a new class of frequency selective surfaces for aspect-stable high Q band pass filters', RSRE Memorandum 4321, DERA Malvern, St Andrews Road, Great Malvern, WORCS, UK. July 1989

9 *A.J.Mackay, J.G.Gallagher.* 'Frequency Selective Structure' RSRE patent application no. 9018262 (originally UK Classified), first filed September 1990.

10 *A.J.Mackay, J.G.Gallagher.* 'A well conditioned formulation for the analysis of multilayered frequency selective surfaces using a cascaded matrix approach', RSRE Memorandum 4289, DERA Malvern, St Andrews Road, Great Malvern, WORCS, UK. May 1989.

11 *S.M.Rao, D.R.Wilton, A.W.Glisson.* 'Electromagnetic scattering by surfaces of arbitrary shape' IEEE Trans Anten and Prop., vol AP-30, May 1982, pp 409-418.

12 *S.Singh et al.* 'Accelerating the convergence of series representing the free space periodic Greens function' IEEE Trans Anten and Prop., Vol 38, No 12, December 1990, pp1958-1990.

13 *N.V.Shuley.* 'Relative convergence for moment-method solutions of integral equations of the first kind as applied to dichroic problems' Electronics Letters, Vol 21, No. 3, January 1985, pp95-97.

14 *K.J.Webb, R. Mittra.* 'Numerical convergence in dichroic problems' Microwave and optical technology letters, Vol 1, No. 9, November 1988, pp317-320.